Nederlandse Geografische Studies

124

frans mulder

assessment of landslide hazard

NETHERLANDS GEOGRAPHICAL STUDIES

nederlandse geografische studies / netherlands geographical studies

ISSN 0169-4839

nederlandse geografische studies 124

assessment of landslide hazard

frans mulder

amsterdam/utrecht, 1991

koninklijk nederlands aardrijkskundig genootschap/
faculteit ruimtelijke wetenschappen universiteit utrecht

CIP-GEGEVENS KONINKLIJKE BIBLIOTHEEK, DEN HAAG

Mulder, Frans

Assessment of landslide hazard / Frans Mulder. — Amsterdam : Koninklijk Nederlands Aardrijkskundig Genootschap ; Utrecht : Faculteit Ruimtelijke Wetenschappen Universiteit Utrecht. — Ill. — (Nederlandse geografische studies, ISSN 0169-4839 ; 124)
Ook verschenen als proefschrift Utrecht, 1991. — Met lit. opg. — Met samenvatting in het Nederlands.
ISBN 90-6809-134-4
Trefw.: aardverschuivingen ; Franse Alpen ; onderzoek / aardverschuivingen ; risico-bepalingen.

ISBN 90-6266-083-5 (Thesis)
ISBN 90-6809-134-4 (NGS)

Printed in the Netherlands by Elinkwijk b.v., Utrecht.

CONTENTS 5

TABLES

FIGURES

VOORWOORD

Een proefschrift, hoewel een persoonlijk werkstuk, komt niet tot stand zonder de hulp en medewerking van derden. Vanaf het begin van het onderzoek in november 1984, hebben een groot aantal mensen op enige manier meegewerkt.
Ten eerste dank aan alle studenten, die in hun 2de jaars veldwerk in de Franse Alpen met engelengeduld en misschien met teveel fantasie de formulieren hebben ingevuld.
Veel dank ben ik verschuldigd aan de studenten, die hun 3de jaars veldwerk in de Franse Alpen hebben uitgevoerd. Ze hebben niet alleen veel van de gegevens verzameld onder barre omstandigheden, maar ze hebben het verblijf in Frankrijk voor mij dragelijk gemaakt. Ik zal nooit de barbecues, de zondagse wandelingen of de flessen 'Mont Ventoux' vergeten. Dank dus: Chris van de Meene, Peter Buster, Cor Luyten, Jeroen Oosterweeghel, Everhard van Veen, Hans Schutjes, Alex de Jong, Gerard Hazeu, Hans van Ammers, Frank van Lamoen, Martin Schellekens, Michael de Vos, Bart Kessels, Margriet Hartman, Pauline Brombacher, Fred Brouwer en Ronuald te Molder.
Mijn werk in Utrecht werd veraangenaamd door de zeer regelmatige kreet 'nog een bakkie (koffie)', Niek, Ivo, Pieter, Will en Wilfried nog mijn dank.
Verder wil ik de staf van het Fysisch Geografisch Laboratorium, C. Klawer, T. Tiemissen, J. van Barneveld en W. Haak noemen, die steeds klaar stond met raad en daad, wanneer er weer een hulpkreet vanuit Frankrijk binnenkwam.
De heren H. Rieff, F. van der Horst en G. van Omme voor het verzorgen van keurige tekeningen.
The assistance of mr Murra and mr Deymier of the CEMAGREF, Grenoble France, is greatly acknowledged. The CEMAGREF provided the equipment to drill the holes for the open standpipes in the landslide next to 'La maison Le Treou'.
De vakgroep Fysische Geografie van de Rijksuniversiteit Groningen verdient meer dan een woord van dank voor de mogelijkheden, die ze mij heeft geboden om het onderzoek af te kunnen ronden. In het bijzonder wordt Prof. dr. A.W.L. Veen bedankt voor de tijd en energie, die hij in dit proefschrift heeft gestoken. Verder wordt Drs. J. Delvigne hartelijk bedankt voor alle taalcorrecties.
Iemand anders die zich druk heeft gemaakt om het aantal taalfouten in dit proefschrift te doen verminderen, is m'n broer Jan Mulder. Veel van het correctie werk is gedaan door Marise Mulder-Timmers. Gelukkig kan je in tijden van nood nog een beroep op je familie doen. Dit heeft mij in de laatste weken op de been gehouden.
Veel dank ben ik ook verschuldigd aan mijn promotor Prof. dr. J.H.J. Terwindt. Zijn vele kritische opmerkingen bij eerdere versies hebben veel bij gedragen aan de leesbaarheid en de inhoud van dit proefschrift.
Tenslotte wil ik bedanken mijn co-promotor Dr. T.J.W van Asch, de drijvende kracht achter het werk. Theo is iemand, wiens enthousiasme en kennis nooit ophoudt. Het onderzoek sprak hem zo aan, dat hij zelfs zover ging dat familieleden mee gingen helpen (Thijs nog bedankt).
Mijn oude studiegenoten, Bert van der Ploeg en Wilfried Ivens, ik zal onze studietijd nooit vergeten. Het viel me zwaar mijn eerste onderzoeksstappen zonder jullie.

Groningen, maart 1991.

1 INTRODUCTION

1.1 Background of the study

Mass movement is the major denudational process in steeply sloping terrains. It is a natural and common feature. - Mass movement is the downslope movement *en masse* of soil and rock material under the influence of gravity. Mass erosion and mass wasting are synonymous terms. Mass movement is popularly known as 'landslide', although strictly speaking landslide or slide refers to a particular type of mass movement. A landslide is a mass movement, in which movement occurs along a specific surface (Gray and Leisner, 1982). -
Field observations indicate that human activity influences the initiation and frequency of mass movement. For example mass movements occur more often in the first few years following the cutting of forests (Swanston, 1969; Burroughs and Thomas, 1977). On the other hand, mass movements also affect human activity by reducing the productivity of forests and arable lands and supply large quantities of debris to rivers (Sidle et al., 1985). The latter may endanger water quality and fish habitats downstream. Individual mass movements are usually not as spectacular as other natural hazards, like earthquakes and major floods. However, mass movements are more widespread. The total financial loss, due to mass movements, is estimated to account for over one billion dollars per year for the USA alone (Gray and Leisner, 1982), exceed that of other geological hazards.
The need for methods, to assess and evaluate the landslide hazard in an area is therefore evident.

1.2 Landslide hazard analysis

Landslide hazard is defined by Varnes (1984) as the probability of occurrence of landslides within a specific period of time (temporal hazard) and within a given area (spatial hazard). Temporal landslide hazard is mainly determined by climatological and meteorological factors, while landscape factors primarily determine the spatial hazards.
The aims of landslide hazard analysis are to asses the landslide hazard in a region and to subdivide the region into land units with different actual and/or potential landslide hazard.
Statistical and soil mechanical approaches dominate landslide hazard studies. Which approach is used, depends on the scale level and the accuracy needed. At regional scale, statistical methods usually are appropriate; at local scale higher accuracies are needed, which ask for a soil mechanical approach (Mulder and Van Asch, 1987; Ward et al., 1981).
At the statistical approach a variety of methods and techniques have been proposed. All methods are based on the same conceptual model (Carrara, 1983). This model implies the identification and mapping of a set of terrain parameters, which directly or indirectly control the landslide hazard of an area. In addition, it involves the

estimation of the relative contribution of these parameters in generating mass movements.This estimation may be based, either on personal judgement or on statistical techniques (Carrara, 1983). The basic assumption is that future slope failure will be more likely to occur under those circumstances which in the past have led to slope failure. A landslide hazard map is finally obtained by superimposing maps of the individual parameters, according to their assigned weight (Aniya, 1985).
In a soil mechanical approach the estimation of landslide hazard is based on the laws of physics and causality. Application of the principles of soil mechanics has advantages over the statistical approach, as it may give better predictions on the effects of changes in land use. However, the high costs involved in this method,have, until now, hampered a full exploration of its merits. It is the purpose of the present study to contribute to this exploration.

1.2.1 The soil mechanical approach

Basic principles

Every soil mass in a sloping area is subject to a shear stress, due to the gravitational force. If the resistance to movement, defined by the shear strength of the soil, is at any moment larger than the shear stress, the soil mass is stable. If the shear stress becomes larger than the shear strength, the soil will slump or slide down to a level where the strength is again larger than the shear stress.
At the moment of failure, the shear stress mobilizes the available shear strength of the soil. At stable slopes, the actually mobilized shear strength is less than the available shear strength. In this respect it is conventional to introduce a factor of safety, F, defined by (Craig, 1987):

$$F = \frac{\text{shear strength available}}{\text{shear strength mobilized}} \qquad (1.1)$$

The available shear strength of the soil is given by the Coulomb Strength Law.
This law states that the shear stress, needed for failure θ, increases linearly with the applied stress, normal to the failure surface σ_n.
The Coulomb Strength Law is:

$$\tau = c + (\sigma_n - u) \tan \phi \quad \text{or} \quad \tau = c + \sigma_n' \tan \phi \qquad (1.2)$$

where :

σ_n	=	$\gamma \cdot z$ = normal stress	(kPa)
γ	=	unit weight	(kPa/m)
z	=	depth	(m)
τ	=	shear strength	(kPa)
c	=	cohesion	(kPa)
σ_n'	=	effective normal stress	(kPa)

σ_n	=	total normal stress	(kPa)
u	=	pore pressure	(kPa)
ϕ	=	angle of internal friction	(°)

Five primary factors are pertinent for failure: unit weight, cohesion, angle of internal friction, slope angle and pore pressure.

Effects of vegetation

Vegetation may influence the shear strength of the soil, as illustrated by its potential effect on some of the primary factors, pertinent to failure.
Cohesion of the soil may increase, due to root reinforcement. Reported magnitudes of this effect range from 2 to 25 kPa (Burroughs and Thomas, 1977; Ziemer, 1981; Riestenberg and Sovonick-Dunford, 1983).
Normal stresses at the failure surface may increase, due to a surcharge of weight by the vegetation biomass. Gray and Megahan (1981) show a range of 0 to 10 kPa for extra normal stresses due to vegetation. An extra stress of 5 kPa is comparable to the stress exerted by a soil layer of 25 cm and a bulk density of 2 g/cm^3; apparently this vegetation effect has a minor importance to deeper seated failure surfaces.
Pore pressures of the soil may be affected, due to hydrological effects of vegetation: evapotranspiration losses influence the depths of the groundwater table, which in its turn determines pore pressure.

The assessment of landslide hazard

The assessment of landslide hazard involves the use of analytical or numerical methods. Such methods are commonly formulated on the assumption of limit equilibrium. The limit equilibrium method of analysis postulates, that a slope fails, if a rigid soil mass starts to slide over a failure surface. The basic assumption is, that the overall slope and each part of it are in static equilibrium at the moment of failure. Such an analysis explicitly takes into account the primary factors, pertinent to failure, and is based on the safety factor (equation 1.1). Translation of a safety factor into a landslide hazard is not easy. In the deterministic safety factor concept, the actual landslide hazard of a slope with a certain safety factor is assessed on the basis of past experiences with slopes with a comparable safety factor. This concept can be criticized: the choice of a landslide hazard depends on personal judgement and is therefore subjective and often arbitrary (Read and Harr, 1988). Furthermore, the translation of a safety factor in a landslide hazard is not linear in any of the limit equilibrium models. For example, a slope with a safety factor of 2.6, is not twice as reliable as one with a safety factor of 1.3 (Read and Harr, 1988). In addition, different assumptions in different limit equilibrium methods result in incomparable safety factors.
An alternative to the deterministic safety factor concept is a probabilistic safety factor concept where the landslide hazard is expressed in terms of the probability of a safety

factor less than unity (VanMarcke, 1977), or as the probability that a safety margin (i.e. the difference between the shear strength and the shear stress) less than zero (Chowdhury and A-Grivas, 1982). The probability of failure may be estimated, if in addition to the safety factor, its variance is known. A variance of the safety factor can be calculated, using the uncertainties, associated with data, employed in limit equilibrium methods (Read and Harr, 1988).
The probabilistic safety factor concept is still subjective, but the translation of a safety factor into a landslide hazard is standardized. The subjectivity of the concept is caused by the need to choose a probability density function of the safety factor.
Because the probabilistic safety factor concept is a relatively recent development, its possibilities until now have not been fully explored and rarely been tested.

1.2.2 The statistical approach to landslide hazard analysis

On regional scale levels, landslide hazard analyses are dominated by statistical methods. These methods explore the relations between landscape factors and the occurrence of mass movements. Detailed study of the geological, soil, hydrological, geomorphological and vegetation characteristics of the failed mass and the parent slope, is required to identify and assign rates or weights to the landscape factors that contribute in generating mass movements in an area.
The assessment of the degree of hazard may be based on the qualitative evaluation of the landscape factors within a certain area. Good examples are the ZERMOS maps made in France (Antoine, 1977). Other designers of hazard zonation maps assess the degree of hazard in a more quantitative way by a numerical rating system: the degree of hazard is determined by the total score of the values,assigned to the factors which contribute to instability (Kienholz, 1978). The difficulty of these rating systems is the weighting of the different factors. This weighting can be done more accurately by computer assisted statistical (multivariate) analysis (Reger, 1979; Carrara, 1983). The significant factors, contributing to instability, are weighted according to their statistical significance. Discriminant analysis is often used for this purpose. The factors used in a discriminant function, yield a discriminant score, which can be related to a degree of stability (Neuland, 1976; Carrara, 1983).
The statistical methods require an elaborate assembling of data. The weight of the factors is only valid for the specific study area.
A statistical approach is only suitable for large regions. For smaller regions the range of the data will generally not be wide enough to give statistically and physically meaningful results.

1.3 Aim of research

The general aim of this study is to extend the probabilistic soil mechanical approach to landslide hazard analysis.
The central objective is to test this approach on a local scale (chapters 2, 3 and 5).
Special attention is given to the mechanical effects of roots on the shear strength of a soil (chapter 4).
The final objective is to test both a statistical and a probabilistic soil mechanical approach for a landslide hazard analysis on regional scales (chapter 6).

1.4 Study area.

General description

The study area is situated in the basin of Barcelonnette in the Southern French Alps (figure 1.1). It is an area of about 15 km wide and 25 km long, with an elevation from 1000 to nearly 3000 m above sea level.
It is a geological window in the allochthonous Flysch à Helminthoides Nappes. Within these nappes, the autochthonous dark marl (terres noires) of early Malm (Oxfordien) age crops out over considerable areas. The nappes consists of relatively erosion resistant sand- and limestone.

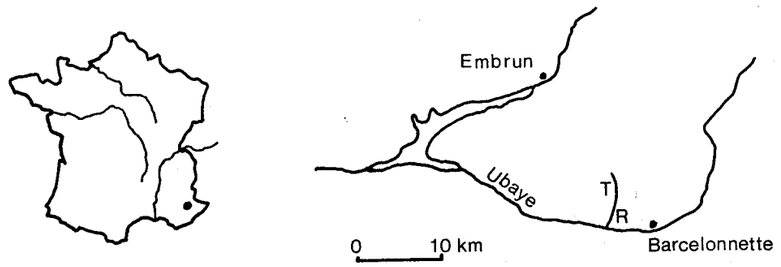

study plot : T = Le Treou R = Riou Bourdou

Figure 1.1 Location of the study area

The Ubaye River traverses the basin of Barcelonnette from the East to the West. During the Wurm glaciation the Ubaye valley has been covered with ice, up to altitudes of approximately 2000 m. A large part of the area is now covered by glacial deposits. The presence of ground moraine on top of impervious marl (terres noires), in combination with the relief and hydrological factors, is responsible for the vulnerability to mass movements.
The climate is sub-mediterranean. The mean annual precipitation is 752 mm (1926-1980). The most arid month is July with 47.5 mm (1926-1980). During winter precipitation is mainly in the form of snow. Due to the East-West orientation of the valley, there is a distinct difference in evaporation, temperature and duration of the snow cover between the north-facing slopes,and those, facing south. The south facing slopes have the highest temperatures and evaporation, and the shortest snow cover period.
During the 18th and 19th century the developing industries caused a growing need for timber. The logging of trees resulted in the deforestation of large areas. In the same period a part of the rural population migrated to the cities. The study area was no exception to this development. The logged or abandoned agricultural areas were very prone to erosion. Action was taken to stop the erosion. A reforestation program started in the Ubaye Valley, as in other parts of the French Alps, at the turn of the century. *Pinus sylvestris* is dominant in the lower regions, *Larix decidua* is commonly found in the higher regions.
In the Barcelonnette basin two plots were selected for field observations and sampling.

Riou Bourdou --- Plot 1

Plot 1 is situated east of the Riou Bourdou, a small tributary of the Ubaye (see figure 1.1, R). The elevation is about 1300 m. The exposure is south-west. The plot is located at the site of a mass movement, which shows signs of recent activity. The elevation difference between the toe and upper scarp is about 65 m. The total length is 170 m, the width varies between 30 and 45 m. The mass movement surface comprises a large number (about 100) of small (about 2-5 m), and about five larger (10-50 m) moving elements. This results in a fissured surface. The mass movement site is characterized by a lower elevation and an smaller slope angle than the surrounding stable area.
The landslide material consists of weathered terres noires mixed with morainic material. This colluvium consists of about 60-80 % silt, 10-35 % clay and 0-10 % sand. The texture of 16 soil samples, taken all over the plot at different depths, are shown in figure 1.2.

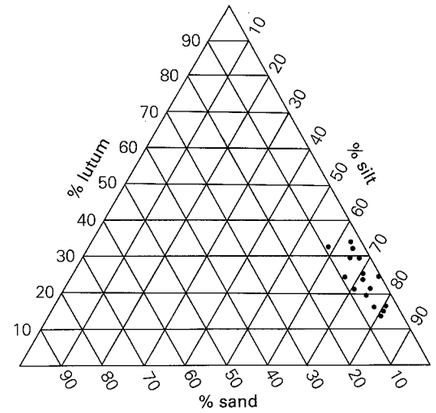

Figure 1.2 Texture diagram for 16 soil samples from study plot "Riou Bourdou"

Atterberg limits show a plasticity index, varying from 5 to 10 %. The peak strength of the material measured with tri-axial tests, shows a cohesion of 12.44 kPa and an angle of internal friction ϕ_{peak} = 24.7°. The residual values for the cohesion and the angle of internal friction ϕ_c were 0.6 kPa and 25.6° respectively (van Asch et al., 1989). The soil is slightly overconsolidated. Dry bulk density ranges from 1.2 to 2.3 g/cm^3 with a mean of 1.73 g/cm^3. Wet bulk density ranges from 1.5 to 2.6 with a mean of 2.08 g/cm^3.
Terres noires have a dark grey clayey matrix, with larger pieces of chalk. The clay material is made up of chlorites and illites.
The contact between the colluvium and the 'solid' terres noires is about 6-10 m below the surface (J. Caris, pers. comm.).
In dry conditions the colluvium is able to absorb a large amount of water. The terres noires are quite solid, when dry; in wet conditions they soften considerably.
On the plot the maximum groundwater levels, reached in early spring, are at about 0.3 m below the surface. In autumn the groundwater level drops to more than 3 m below the surface. On the stable areas surrounding the landslide groundwater levels never reach within 3 m of the surface. There were no signs of surface runoff.
The vegetation is mainly *Pinus sylvestris* with excessive undergrowth of grass and small scrubs.

La Maison Forestiere Le Treou --- Plot 2

Plot 2 is situated 20 m west of the house 'La Maison Forestiere Le Treou' at an elevation of about 1450 m (figure 1.1, T). The width is about 25 m and length 73 m. The elevation difference between scarp and toe is 31 m. The exposition of the plot is

south. The plot is also located at the site of a mass movement, which shows signs of recent activity. Its toe is level with a forest road. An enlargement of this road in 1987 caused an increased activity of the mass movement.
The mass movement has developed in very coarse morainic material, with stones up to 2 m in diameter. This has prohibited the determination of geotechnical parameters. The boundary between the morainic material and the underlying 'solid' terres noires is about 5 - 6 m below the surface.
On the landslide the maximum groundwater levels are at about 0.5 m below the surface and are reached in early spring. In autumn the groundwater level drops to more than 3 m below the surface. On the stable areas surrounding the landslide the groundwater levels never reach within 3 m of the surface.
Vegetation is very sparse on this slide and consists mainly of grasses and shrubs.

2 SOIL MECHANICAL METHODS TO ASSESS LANDSLIDE HAZARD ON A LOCAL SCALE

2.1 Introduction

In current practice, the assessment of the landslide hazard by soil mechanical methods, like limit equilibrium analysis, is based on the deterministic safety factor concept (see paragraph 1.2.1). The application of the deterministic safety factor concept is difficult for several reasons:
- the translation of the safety factor into a landslide hazard is not clear and depends on the personal judgement, which makes it subjective and arbitrary (Read and Harr, 1988).
- the translation of a safety factor into a landslide hazard is not linear and depends on the method of analysis.
- deterministic limit equilibrium analyses are often used to determine the safety factor. Generally in such analyses, the candidate failure surface is divided into a number of slices. It is assumed that the individual safety factors of each slice are equal. However, numerous stress-deformation studies on the basis of the finite element method have shown that the safety factors of individual slices may be quite different (Chowdhury and A-Grivas, 1982). Chowdhury and A-Grivas quote a study of Bishop, where local failure occurred even though the calculated overall safety factor was as high as 1.8. Such a failure occurs if the peak strength of a soil is reached at some points on the (potential) failure surface, before this happens at other points. In that case the average mobilized strength will be somewhat less than the peak strength around the failure surface. The calculated overall safety factor, based on the peak strength of a soil, will overestimate the safety of a slope. The effect is very prone in materials that exhibit a clear difference between peak and residual strength, like clay.
- the Coulomb failure theory is not suitable in conjunction with a nonlinear increase in shear strength with depth (or normal load). Such a nonlinear increase with depth is often found in shallow landslides (Terwilliger and Waldron, 1990).
- the position of the failure surface is to a large extend unknown, even in areas with previous sliding.
- the safety factor obtained is single valued and does not account for the inherent variability of vegetation, soil or rock properties or their interaction. The true value of the stability controlling factors or soil parameters is never known, but can be estimated from a number of measurements. Measurements are subject to error and introduce a variance in the expected value of the soil parameters or controlling factors. These uncertainties introduce a variance in the safety factor. This variance offers an alternative for the deterministic safety factor concept: a probabilistic safety factor concept. Based on the variance of the soil strength parameters, it is possible to define the landslide hazard of an area as the *probability* of a safety factor below unity.
In this chapter the probabilistic safety factor concept is incorporated in a limit equilibrium analysis. The incorporation consists of the following steps: (1) the basic equations of a limit equilibrium analysis satisfying all equilibrium conditions and using the method of slices will be derived (paragraph 2.2.1), (2) derivation of the

equations of the variance of the safety factor as function of the primary factors (paragraph 2.2.2.1) and (3) estimation of the probability of failure if the safety factor and its variance are known (paragraph 2.2.2.3). Finally the developed probabilistic methods are applied to a test profile in order to reveal the validity of the assumptions implied in the various methods (paragraph 2.4).

2.2 Limit Equilibrium Analysis in two dimensions - Method of Slices

In a limit equilibrium analysis, it is postulated that a slope fails, if a rigid soil mass starts to slide over a failure surface. The basic assumption of a limit equilibrium analysis is that the overall slope and each part of it, are in static equilibrium at the moment of failure. Such analyses take explicitly into account the primary factors: unit weight, cohesion, angle of internal friction, slope angle and pore pressure and is based on the safety factor (equation 1.1). A rigid body is in static equilibrium if all forces and moments applied to it, are in balance. In two dimensions the equations of equilibrium may be written as (Meriam and Kraige, 1987) :

$$\Sigma F_x = 0 \quad \text{and} \quad \Sigma F_y = 0 \quad \text{and} \quad \Sigma M_o = 0 \qquad (2.1)$$

The first two equations assure the vertical and the horizontal force balance. The third equation represents the zero sum of moments of all forces about any point, on or off the body.
In order to establish the safety factor of a slide, the forces on the failure surface have to be determined. The method of slices achieves this by dividing the 'failed' soil mass into a number of slices. The forces acting on a slice are shown in figure 2.1.
The forces are (Craig, 1987):
- the total weight of the slice, $W=\gamma \cdot b \cdot h$ (γ_{sat} where needed).
- the total normal force on the base, $N=\sigma \cdot L$. In general this force has two components, an effective force $N'=\sigma' \cdot L$ and the boundary force, $U=u \cdot L$, where u is the pore water pressure at the base center and σ' is effective normal pressure acting at the base center.
- the mobilized shear force on the base, S.
- the shear force on the sides, T.
- the total normal force on the sides, E.

The forces T and E are commonly known as the interslice forces. Any external force is neglected.
Boundary conditions and relations between the forces, which help to solve the problem of estimating the safety factor, are:
- an equilibrium of forces exists for each slice and for the slide as a whole.
- an equilibrium of moments exists for each slice and for the slide as whole.
- a relation between mobilized shear force and the total normal force at the base of the slice, i.e. the maximum mobilized shear strength in terms of a safety factor.
- the sum of change in interslice force over the slice is zero for the whole slide. ($\Sigma dT = \Sigma dE = 0$; Terzaghi and Peck, 1968).

Every force (W, S, N, T, E) is defined by 3 variables: the line of action, the direction and its magnitude. The forces shown in figure 2.1 are known only in direction except for the weight, W, which has a known line of action, magnitude and direction and the vertical force T, which has a known direction and line of action.

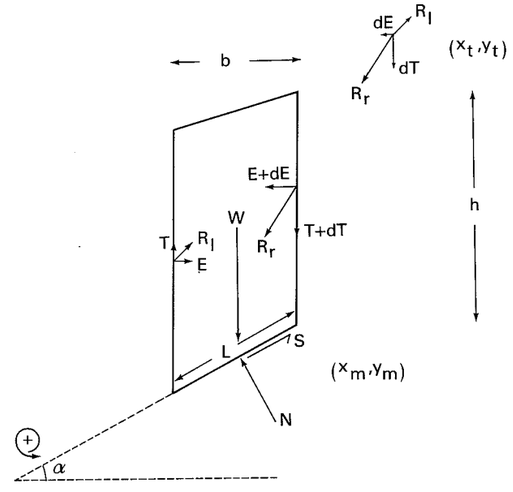

α	=	angle of base of the slice with horizontal	(°)
W	=	total weight of the slice, $W=\gamma \cdot b \cdot h$ (γ_{sat} if needed)	(kN/m)
γ	=	unit weight	(kPa/m)
N	=	total normal force on the base, $N=\sigma \cdot L$	(N)
S	=	mobilized shear force on the base	(N)
T	=	shear force on the sides	(N)
E	=	total normal force on the sides	(N)
R	=	resultant of the interslice force	(N)
(x_m,y_m)	=	midpoint of the base	
h	=	height of the slide	(m)
L	=	base length of the slice	(m)
b	=	width of the slide	(m)

Figure 2.1 Forces acting on a slice of soil

This leaves as known variables in the n equations describing the safety factor:
- the safety factor of each slice (n unknowns variables)
- the normal effective force at the base of each slice (n unknown variables)
- the position of the lines of action of the effective normal force (n unknown variables)
- the shear force on the base of each slice (n unknown variables)
- the position on the base of the shear force line of action on the slice (n unknown variables)
- the interslice shear forces (n-1 unknown variables)
- the interslice effective normal forces (n-1 unknown variables)
- the position of the interslice normal force line of action (n-1 unknown variables).

In total 8n-3 unknown variables have to be estimated before the safety factor of the whole slide is known. One should remember that n slices only have n-1 sides where the interslice forces are active. There are 3n equations describing the static conditions available and n equations relating the safety factor, the shear force and the normal force at the base of the slice to each other. This leaves us with 4n-3 unknown variables. The estimation of the safety factor is indeterminate.
Assumptions are made to overcome this indetermination. This implies that non of the methods of slices is yielding the 'correct' value of the safety factor. The approximation of the safety factor by the different methods depends on the accuracy of the different assumptions made. The assumptions in most cases imply that not all boundary conditions needed for an equilibrium of forces and moments of each slice and of whole slide are assured. For example the assumption by Fellenius (1927, 1936 in Nash, 1987) that the resultant of all forces acting on the vertical side of a slice, has no component normal to the failure surface, implies no horizontal or vertical force equilibrium per slice or of the slide as a whole (Nieuwenhuis, 1983). The assumption by Bishop (1955) of a horizontal line of action of the resultant of interslice forces, implies that in general the sum of all interslice forces is not equal to zero, i.e there is no equilibrium of horizontal forces for the whole slide.
Commonly applied assumptions of the slice methods that satisfy all equilibrium conditions are (Morgenstern-Price, 1965; Spencer, 1967):
(1) the normal force, N, acts at the center of the base of each slice (n assumptions). The normal force is due to the weight of a slice. The weight of a slice, W, is a gravitational force distributed over the volume of the slice and may be taken as a concentrated force acting through the center of gravity (Meriam and Kraige, 1987). This implies for small slices a line of action passing through the center of the slice base.
(2) the line of action of the shear forces passes through the center of the slice base (n assumptions). For small slices the base may be approximated by a straight line.
(3) the safety factor is constant along the failure surface (n-1 assumptions).
(4) the ratio of the vertical-horizontal component of the interslice forces is known along the failure surface (Spencer, 1967; Morgenstern-Price, 1965) or the position of the line of action of the interslice normal forces is known (Janbu, 1954) (n-1 assumptions).
These assumptions make estimation of the safety factor redundant, i.e. there are more equations than unknown variables. Because the analysis is redundant it is not possible

to ensure that all equilibrium conditions are satisfied in a physically acceptable manner (Lambe and Whitman, 1969). The magnitude of error which is introduced is difficult to asses. In order to avoid the redundant condition, a method of slices will be formulated using the resultant of the interslice forces (see 2.2.1).

2.2.1 A deterministic general limit equilibrium analysis (DLEA) using the resultant of interslice force per slice

The slices are assumed to be rigid bodies. The forces acting on the slice are shown in figure 2.1. The use of the vertical and horizontal component of the resultant of the interslice forces, dT resp. dE, leads to the following reasoning, a slope divided in n slices has 8 n unknown variables: W is known in direction, line of action and magnitude per slice. The forces N, S, dE and dT have an unknown line of action and magnitude, but are known in direction.
Assume :
(1) the normal force, N, acts at the center of the base of each slice (n assumptions).
(2) the shear force, S, acts at the center of the base of each slice (n assumptions).
(3) the safety factor is constant along the failure surface (n-1 assumptions).
The 3n-1 assumptions together with the 3n equations of the static equilibrium and the n relations between S, N and F leaves 8n-(3n-1)- 3n-n = n+1 unknown variables.
The estimation of the safety factor is unspecified.
Assume (4) a function describing the ratio between the vertical and horizontal component of the interslice forces along the failure surface (n assumptions). The remaining equation is derived from the boundary condition that the sum of change in interslice force over the slice is zero for the whole slide (Σ dT = Σ dE =0; Terzaghi and Peck, 1968). The method has just as many unknown as known variables and is no longer redundant.
The equilibrium condition of the slide determines that the resultant of all forces acting on the slide and each part has to be zero and the sum of the moments of all forces about any point O on or off the body equals zero (see equation 2.1). This condition and the earlier mentioned assumptions lead to two expressions with two unknown variables, the safety factor and the ratio between the vertical and horizontal component of the interslice forces.

Force equilibrium equation

The horizontal and vertical force balance of a typical slice of unit width, as depicted in figure 2.1, gives:

vertical: $W + dT = N \cos \alpha + S \sin \alpha$ (2.2)
horizontal: $dE = S \cos \alpha - N \sin \alpha$ (2.3)

The relation between total normal force, N, mobilized shear strength, S, and the safety factor, F, is based on the Coulomb failure criterion and is given by (Nash, 1987):

$$S = \frac{cL + (N-uL)\tan\phi}{F} \qquad (2.4)$$

c = cohesion (kPa)
S = shear strength (kN/m)
N = total normal force (kN/m)
u = pore pressure (kPa)
ϕ = angle of internal friction (°)
L = base length of the slice (m)

The factor of safety is not significantly affected by the choice of the function describing the relation between the interslice forces (Craig, 1987). Therefore, it is assumed that the ratio between dT and dE is constant along the failure surface.

$$\lambda = \frac{dT}{dE} = constant \qquad (2.5)$$

Combination of equations 2.2 - 2.5 together with $1=b/\cos\alpha$ yields an equation based on an equilibrium of forces:

$$dT = \frac{W(\tan\phi - F\tan\alpha) + (c - u\tan\phi)(\frac{b}{\cos^2\alpha})}{(\frac{1}{\lambda})(F + \tan\alpha\tan\phi) - (\tan\phi - F\tan\alpha)} \qquad (2.6)$$

where:
b = width of the slice (m)

The conditions for equilibrium of the entire sliding mass gives (Terzaghi and Peck, 1968), with omitting the index, i, of each slice:

$$\sum dT = \sum \frac{W(\tan\phi - F\tan\alpha) + (c - u\tan\phi)(\frac{b}{\cos^2\alpha})}{(\frac{1}{\lambda})(F + \tan\alpha\tan\phi) - (\tan\phi - F\tan\alpha)} = 0 \qquad (2.7)$$

Moment equilibrium equation

Before the moment equilibrium equation is derived, the application point of the resultant of the interslice forces needs to be known.
The resultant of interslice forces at both sides of a slice is constructed using the principle of transmissibility. This principle states that a force may be applied at any point on its given line of action without altering the resultant effects of the force external to the rigid body on which it acts (Meriam and Kraige, 1987).
If the interslice forces acting at the left or right side of the slice are not equal to each other, their lines of action will intersect (see fig 2.1). Assume the intersection is at (x_t,y_t). The force working at this point is the resultant of the interslice force over the slice. The point of the application of the remaining forces (S, N, W) is at the midpoint of the base of the slice (x_m,y_m; see assumptions).
If the slice has a balance of forces, the resultant of the interslice forces acting at (x_t,y_t) is opposite but equal to the resultant of the forces acting at (x_m,y_m). If the two forces don't have the same line of action, the moment is known as a couple. The moment of a couple has the same magnitude for all moment centers and is the product of the perpendicular distance between the two lines of action of the forces and the magnitude of the forces.
The moment of the slice is zero due to the equilibrium condition. The forces themselves are unequal to zero. Therefore, the two forces have the same line of action, which passes through the base of the slice (x_m,y_m).
Because the slide is in equilibrium, the moments of each slice and of the slide as a whole can be taken about any point without changing the result. The moment equilibrium per slice, with turning point at (0,0) can be written as:

$$-dTx_m + dEy_m + F_y x_m - F_x y_m = 0 \qquad (2.8a)$$

where F_y and F_x are respectively the vertical and the horizontal component of all forces other than the interslice forces. This results in the following expression of the moment equilibrium equation for the whole slide, omitting the index i for each slice:

$$-\Sigma\, dTx_m + \Sigma\, dEy_m + \Sigma\, F_y x_m - \Sigma\, F_x y_m = 0 \qquad (2.8b)$$

where x_m and y_m are the coordinates of the midpoint of the base of the slide.
The result of a couple does not change if it is replaced by another couple in the same plane and with the same moment. Thus, it is possible to construct a resultant of all forces acting on the different slices as if they are acting at (0,0), i.e.:

$$-\Sigma\, dT + \Sigma\, dE + \Sigma\, F_y - \Sigma\, F_x = 0. \qquad (2.8c)$$

Because $\Sigma\, dT = 0$ and $\Sigma\, dE = 0$ (see assumptions), equation 2.8c changes to:

$$\Sigma\, F_y - \Sigma\, F_x = 0. \qquad (2.8d)$$

The action of a force does not change if (1) the force is transferred parallel to its line of action and if (2) at the same time a couple is introduced with a moment equal to the moment of the original force to its new point of action. If the resultant of the forces in the x-direction (ΣF_x) and the resultant in the y-direction (ΣF_y) are moved to the midpoint of each slice (x_m,y_m), we get the following expression of the moment of the slide as whole, with the turning point (0,0):

$$\Sigma F_y x_m - \Sigma F_x y_m = 0 \qquad (2.8e)$$

The constant ratio between dT and dE, and combining equation 2.8b and 2.8e, gives:

$$-\Sigma dTx_m + \Sigma dEy_m = -\Sigma dTx_m + \lambda \Sigma dTy_m = 0 \qquad \text{or}$$

$$\lambda = \frac{\sum dTx_m}{\sum dTy_m} \qquad (2.9)$$

The iteration scheme to estimate the safety factor and the ratio, λ, for the whole slide is as follows: First ratio, λ, is assumed. The safety factor is calculated using equation 2.7. The calculated safety factor is used together with equation 2.6 and 2.9 to give a new estimation of the ratio, λ. The new ratio, λ, is used to calculate a new F with equation 2.7. The iteration loop is continued until the changes in F and the ratio, λ, are less than a given tolerance.

2.2.2 Probabilistic limit equilibrium methods

In this paragraph equations will be derived, relating the mean and variance of the safety factor to variables used in a deterministic limit equilibrium analysis.
Furthermore, it will be shown that if the mean and variance of the safety factor are determined and a probability distribution for the safety factor is assumed, it is possible to calculate the probability of a safety factor below unity, i.e. the landslide hazard (paragraph 2.2.2.3).
The relations between safety factor, its variance and the probability of failure provides an alternative for one of the assumptions which were made to overcome the indetermination in estimating the safety factor (paragraph 2.2.1).
Three alternative assumptions will be considered, resulting in two new methods for landslide hazard assessment. The alternatives are of equal merit. Which of the alternatives is taken depends on the functionality of the assumptions. For example the assumption of a constant safety factor is doubtful if the failure surface passes through layers with different strength characteristics.
The alternative assumptions are:
(1) the safety factor is constant for each slice along the failure surface. The use of this assumption makes it possible to calculate the variance of the safety factor and the probability of failure for each slice (paragraph 2.2.2.1).

(2) the probability of failure is constant for each slice. The use of this assumption makes it possible to calculate the safety factor and its variance for each slice (paragraph 2.2.2.3).
(3) the variance of the safety factor is constant for each slice. The use of this assumption makes it possible to calculate the safety factor and probability of failure for each slice (paragraph 2.2.2.4).
Common to each of the alternatives are the assumptions:
- the normal force, N, and the mobilized shear force, S, act at the center of the base of each slice.
- the ratio between the vertical and the horizontal component of the interslice forces is constant.
The influence of the assumptions on the landslide hazard will be clarified in paragraph 2.4.
Both the Fellenius method and the DLEA method (paragraph 2.2.1) are extended with a variance equation. The Fellenius method appeared to provide the fastest way to get an impression of the probability of failure and the variance along the critical failure surface.
Recalling from probability theory (Grimmett and Stirzaker, 1982; Mood et al, 1974):
Theorem 1, the sum of two independent random variables x and y
where a_1, a_2, a_3 are constants, is given by:

mean : $M[a_1 \cdot x + a_2 \cdot y + a_3] = a_1 \cdot M[x] + a_2 \cdot M[y] + a_3$
variance : $V[a_1 \cdot x + a_2 \cdot y + a_3] = a_1^2 \cdot V[x] + a_2^2 \cdot V[y]$

Theorem 2, the product of two independent random variables x and y is given by

mean : $M[x \cdot y] = M[x] \cdot M[y]$
variance : $V[x \cdot y] = M[x]^2 \cdot V[y] + M[y]^2 \cdot V[x] + V[x] \cdot V[y]$

M[.] = mean
V[.] = variance

2.2.2.1 General limit equilibrium analysis (GLEA)

Assume the safety factor, F, is a random variable and a function of other stochastic variables, with a finite mean, M[F] and a variance of V[F].
Rewriting equation 2.6, an equation to describe the safety factor of each slice is obtained. The use of Theorem 1 and 2 results in an equation describing the mean of the safety factor (equation 2.10) and the variance of the safety factor (equation 2.11).
The strength parameters cohesion and angle of internal friction are assumed to be independent (see 3.3.4).
Other assumptions are: b_1 is independent of $\tan\phi$ and b_2 is independent of u, $\tan\phi$ and c.

$$M[F] = M[b_1]\cdot M[\tan\phi] - M[b_2]\cdot M[u]\cdot M[\tan\phi] + M[b_2]\cdot M[c] \quad (2.10)$$

where:

$$b1 = \frac{W + dT - \lambda dT \tan\alpha}{\lambda dT + (W + dT)\tan\alpha} \qquad b2 = \frac{\frac{dx}{\cos^2\alpha}}{\lambda dT + (W + dT)\tan\alpha}$$

W	=	weight of slice	(kN/m)
dx	=	width of slice	(m)
α	=	angle of failure surface	(°)
dT	=	vertical component of the resultant of the interslice forces	(kN)
dE	=	horizontal component of the resultant of the interslice forces	(kN)

Using equation 2.10 and Theorem 1 and 2, the variance equation can be written as:

$$V[F] = VP + VQ + VR \quad (2.11)$$

$$VP = M[b_1]^2\cdot V[\tan\phi] + M[\tan\phi]\cdot V[b_1] + V[\tan\phi]\cdot V[b_1]$$

$$VQ = M[c]^2\cdot V[b_2] + M[b_2]^2\cdot V[c] + V[c]\cdot V[b_2]$$

$$VR = (M[b_2]^2\cdot V[\tan\phi] + M[\tan\phi]^2\cdot V[b_2] + V[\tan\phi]\cdot V[b_2])(M[u]^2 + V[u]) + M[b_2]^2\cdot M[\tan\phi]^2\cdot V[u]$$

c	=	cohesion	(kPa)
u	=	pore pressure	(kPa)
ϕ	=	angle of internal friction	(°)

Equation 2.11 shows that the variance of the safety factor is a function of the mean and variances of pore water pressure, u, tan(ϕ), cohesion and the variables b_1 and b_2. $V[b_1]$ and $V[b_2]$ are the variances of the variables b_1 and b_2. These variances are due to errors in the estimation of the bulk density, location of the failure surface, the ratio, λ, dT and dE. Because there is no simple exact formula for the mean and variance of the quotient of the independent random variables in terms of the mean and variance of these two variables the variances of b_1 and b_2 are assumed. It will be assumed that the coefficient of variation of b_1 and b_2 are constant. The coefficient of variation is the ratio between the standard deviation and the mean value of a variable.

2.2.2.2 Probabilistic Fellenius analysis

The Fellenius or ordinary method of slices assumes that the forces acting on the sides of any slice have, a zero resultant in the direction normal to the failure surface for the slice (Lambe and Whitman, 1969). The safety factor of each slice in a Fellenius analysis can be expressed as (Nash, 1987):

$$F = \frac{cL + (W\cos\alpha - uL)\tan\phi}{W\sin\alpha} \quad (2.12)$$

where:

c	=	cohesion	(kPa)
u	=	pore pressure	(kPa)
ϕ	=	angle of internal friction	(°)
L	=	base length of the slice	(m)
W	=	weight of slice	(kN/m)
α	=	angle of failure surface	(°)

This method is redundant and it is in general not satisfying the conditions of a static equilibrium. In some problems the safety factor obtained with this method, may be only 10 to 15 % below the range of equally correct answers, where as in other problems the error may be as much as 60 % (Whitman and Baily, 1967). Comparison of the results of the Fellenius method with simplified Bishop, Janbu and GLEA methods reveals that erroneous answers are obtained if the angle of the failure arc is very small over a part of the failure surface.
Rewriting equation 2.12 and using Theorem 1 and 2:

$$M[F] = M[b_1]\cdot M[\tan\phi] - M[b_2]\cdot M[u]\cdot M[\tan\phi] + M[b_2]\cdot M[c] \quad (2.13)$$

$b_1 = 1/\tan\alpha \qquad b_2 = 1/(W\cdot\sin\alpha\cdot\cos\alpha)$

Using equation 2.13 and Theorem 1 and 2, the variance equation can be written as:

$$V[F] = VP + VQ + VR \quad (2.14)$$

$$VP = M[b_1]^2\cdot V[\tan\phi] + M[\tan\phi]\cdot V[b_1] + V[\tan\phi]\cdot V[b_1]$$

$$VQ = M[c]^2\cdot V[b_2] + M[b_2]^2\cdot V[c] + V[c]\cdot V[b_2]$$

$$VR = (M[b_2]^2\cdot V[\tan\phi] + M[\tan\phi]^2\cdot V[b_2] + V[\tan\phi]\cdot V[b_2])(M[u]^2 + V[u]) + M[b_2]^2\cdot M[\tan\phi]^2\cdot V[u]$$

2.2.2.3 A method assuming a constant probability of failure along the failure surface (PROBCON)

Probability of failure

The variable F is defined by the equations 2.10 and 2.11 or 2.13 and 2.14 as a random function of the stochastic variables cohesion, angle of internal friction, pore

water pressure and two variables b_1, b_2 which are a function of the weight and geometry of the slice and in case of the GLEA model also of the interslice forces. The probability of failure (P_f) for each slice is the probability of having a safety factor smaller than 1 ($F<1$):

$$P_f = P[F<1] \tag{2.15}$$

P[.] = probability.

If the probability density function (PDF) of F is known then equation 2.15 can be written as:

$$P_f = \int PDF(F)\, dF \tag{2.16}$$

Figure 2.2 depicts an example of a probability density function for the safety factor of an infinite slope model (see paragraph 6.3). The probability of failure is equal to the hatched area. A probability density function, which resembles closely the shape of figure 2.2 is a lognormal distribution. The lognormal distribution describes the behavior of many random variables in the range of 0 - ∞. This is theoretically also the range of the safety factor, because the shear strength required for stability is in the range of 0 - ∞ (equation 1.1).

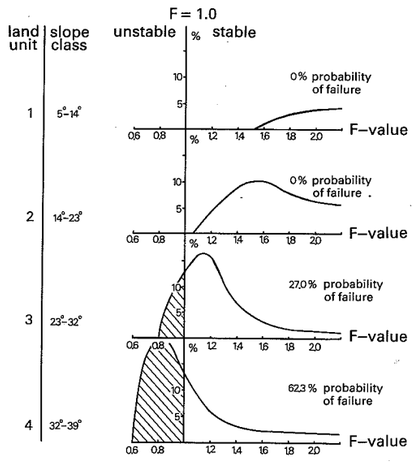

Figure 2.2 The distribution of the safety factors for four slope classes

The lognormal distribution is obtained by transforming a normal distribution. If $x=\ln F$ and x is normally distributed, then F has a lognormal distribution given by (Harr, 1977; Mood et al, 1974):

$$PDF(F) = \frac{1}{\sigma_x\sqrt{2\pi}} e^{\left[\frac{-1}{2}\frac{(\ln F - m_x)^2}{\sigma_x^2}\right]} \tag{2.17}$$

$$m_x = \textit{the mean value of } x = \ln(M[F]) - \frac{\sigma_x^2}{2}$$

$$\sigma_x^2 = \textit{the variance of } x = \ln\left(\frac{V[F]}{M[F]^2} + 1\right)$$

$$P[F<1] = \int_{-\infty}^{\ln 1=0} \frac{1}{\sigma_x\sqrt{2\pi}} e^{\left[\frac{-1}{2}\frac{(-m_x)^2}{\sigma_x^2}\right]} \tag{2.18}$$

or

$$P[F<1] = \int_{-\infty}^{R} \frac{1}{\sqrt{2\pi}} e^{\frac{R^2}{2}} \qquad \wedge \qquad R = \frac{-m_x}{\sigma_x} \tag{2.19}$$

R is normally distributed with a mean zero and a variance of unity.

Equation 2.18 gives the probability that the safety factor is less than unity, under the assumption that the probability density function of the safety factor is lognormal.

Derivation of the PROBCON method

A method for assessment of the landslide hazard assuming a constant probability of failure along the failure surface, was introduced by Read and Harr (1988). According to Read and Harr the justification for this assumption is found in the thermodynamic theory. They state: the principle of maximum entropy demonstrates that the least biased estimate of the landslide hazard would present a constant probability of failure of a slice along the failure surface.

The probability of failure is expressed in the parameter, R (equation 2.19), i.e. if R is a constant along the failure surface, the probability is also constant. R is a function of the variance and mean of the safety factor.

$$R = \frac{\ln\left(\frac{V[F]}{M[F]^2}+1\right)}{2} - \ln(M[F]) \Bigg/ \sqrt{\ln\left(\frac{V[F]}{M[F]^2}+1\right)}$$

If the ratio, λ, or R is known or assumed, both the variance and the mean of the safety factor are complicated functions of one unknown variable, dT (equation 2.10 and 2.11).

$$M[F]=M[b_1]\cdot M[\tan\phi]-M[b_2]\cdot M[u]\cdot M[\tan\phi]+M[b_2]\cdot M[c] \qquad (2.10)$$

$$V[F]= \quad VP + VQ + VR \qquad (2.11)$$

where:

$$VP = M[b_1]^2V[\tan\phi]+M[\tan\phi]V[b_1]+V[\tan\phi]V[b_1]$$

$$VQ = M[c]^2V[b_2]+M[b_2]^2V[c]+V[c]V[b_2]$$

$$VR = (M[b_2]^2V[\tan\phi]+M[\tan\phi]^2V[b_2]+V[\tan\phi]V[b_2])(M[u]^2+V[u]) + M[b_2]^2M[\tan\phi]^2V[u]$$

$$b1 = \frac{W+dT-\lambda dT\tan\alpha}{\lambda dT+(W+dT)\tan\alpha} \qquad b2 = \frac{\frac{dx}{\cos^2\alpha}}{\lambda dT+(W+dt)\tan\alpha}$$

W	=	weight of slice	(kN/m)
dx	=	width of slice	(m)
α	=	angle of failure surface	(°)
dT	=	vertical component of resultant of the interslice forces	(kN)
dE	=	λdT = horizontal component of resultant of the interslice forces	(kN)

The boundary condition, Σ dT =0, is used to solve the problem of finding the constant probability of failure along the failure surface.
This resulted in the following iteration scheme: At first the ratio, λ, is assumed. Then R is changed until Σ dT=0. This value of R and the assumed ratio, λ, are used to calculate dTx_m and dTy_m, the vertical and horizontal moment of a slice. Equation 2.9 gives a new estimation for the ratio, λ. This new ratio, λ, is used to calculate a new

R for which Σ dT =0. This iteration loop is continued until the changes in R and the ratio, λ, are less than a given tolerance.

2.2.2.4 A method assuming a constant variance of the safety factor along a failure surface (VARCON)

A constant variance of the safety factor of the slices along a failure surface is based on the concept of a variance of the safety factor, which is independent of the mean of the safety factor.
The variance of the safety factor is a function of the stochastic variables; weight, cohesion, angle of internal friction, pore water pressure, bulk density and the location of the failure surface and is given in equation 2.11.
If the ratio, λ, or the variance of the safety factor is known or assumed the mean of the safety factor is a complicated function of one unknown variable, dT.

$$V[F] = VP + VQ + VR \qquad (2.11)$$

where:

$$VP = M[b_1]^2V[\tan\phi]+M[\tan\phi]V[b_1]+V[\tan\phi]V[b_1]$$

$$VQ = M[c]^2V[b_2]+M[b_2]^2V[c]+V[c]V[b_2]$$

$$VR = (M[b_2]^2V[\tan\phi]+M[\tan\phi]^2V[b_2]+V[\tan\phi]V[b_2])(M[u]^2+V[u]) + M[b_2]^2M[\tan\phi]^2V[u]$$

W	=	weight of slice	(kN/m)
dx	=	width of slice	(m)
α	=	angle of failure surface	(°)
dT	=	vertical component of resultant of the interslice forces	(kN)
dE	=	λ·dT = horizontal component of resultant of the interslice forces	(kN)

The boundary condition, Σ dT =0, is used the solve the problem of finding a constant variance along the failure surface.
This resulted in the following iteration scheme: At first the ratio, λ, is assumed. Then variance is changed until Σ dT=0. This value of the variance and the assumed ratio, λ, are used to calculate dTx_m and dTy_m, the vertical and horizontal moment of a slice. Equation 2.9 gives a new estimation for the ratio, λ. This new ratio, λ, is used to calculate a new R for which Σ dT =0. This iteration loop is continued until the changes in variance and the ratio, λ, are less than a given tolerance.

2.3 A computer program for the assessment of landslide hazard on a local scale

The probabilistic limit equilibrium methods of GLEA, PROBCON, VARCON and the extended Fellenius method were programmed. The computer program uses an automatic slice subdivision of the slide. The best combination of calculation speed and accuracy is obtained in this way. The number of slices used depends on the accuracy with which the safety factor and the other parameters, like the ratio, λ, need to be known; it is function of the geometry and stratigraphy of the landslide under consideration.
Recognizing that summation equations may be written as an integral, a whole family of powerful algorithms for numerical integration is available. The program uses the computer code of the Romberg integration algorithm as it is given by Press et al. (1986). This integration algorithm uses the least number of function evaluations to reach a given accuracy (Press et al, 1986).
The problem of finding the safety factor for which equation 2.7 equals zero, was solved using the 'van Wijngaarden-Dekker-Brent' root finding algorithm (Press et al., 1986). This algorithm was preferred to the well known Newton-Raphson algorithm for the following reasons: it uses only function evaluations and does not require an evaluation of the derivative of equation 2.7 with respect to safety factor, F.
In the next paragraph the computer program was used to discuss the advantages and pitfalls of the different methods developed in this chapter.

2.4 The assumptions of the probabilistic limit equilibrium methods; their validity and implications

The probabilistic limit equilibrium methods as developed in paragraph 2.2.2 are applied to a test profile in order to reveal the validity and the implications for the stress situation in the sliding soil mass, of the assumptions implied in the various methods. The test profile was selected from Fredlund and Krahn (1977). Fredlund and Krahn (1977) use the specific profile to compare various deterministic methods for slope stability analyses.
The slope profile is outlined in figure 2.3. Its is a simple 2:1 slope of 12 meter high. The slope consists of three layers, labelled 1, 2, and 3 and has a groundwater level labelled GW.
Two different conditions of the slope, will be discussed:

case 1 All three layers have the same strength parameters, $\phi = 20°$, c=28.73 kPa, bulk density = 1.92 g/cm^3. The center of the circle representing the failure surface is at Mx = 12.19 m, My = 27.42 m, the radius of the circle is 24.38 m, the scarp is at 34.80 m and the toe is at 0.39 m.

case 2 Conditions like as *case 1*, the failure surface may be represented by a circle of case 1 except that it never reaches layer 3. Instead it follows the thin horizontal layer 2. This thin horizontal layer is at residual strength with $\phi = 10°$, c=0 kPa, bulk density = 1.92 g/cm^3. The failure surface follows this weak layer (2).

Lee et al. (1983) give some coefficients of variation of the angle of friction, ϕ, and cohesion, c. A mean value of the coefficient of variation for ϕ is 0.1 and for the cohesion 0.25. Therefore, the standard deviation of cohesion is assumed to be 7 kPa and for the angle of internal friction to be 2°.
The residual strength of layer 2 and a coefficient of variation of 0.25 would give a standard deviation of zero for the cohesion. This is thought to be unrealistic, because it would imply that there is no variation in the cohesion along the failure surface. Therefore, it is assumed that the standard deviations remain unaffected by the fact that a soil is at peak or at residual shear strength.

Table 2.1 Assumptions of the different probabilistic limit equilibrium analyses to overcome indetermination

	Method			
Assumption	GLEA	PROBCON	VARCON	Fellenius
Normal forces act at the center of the base of a slice	Yes	Yes	Yes	Yes
Shear forces act at the center of the base of the slice	Yes	Yes	Yes	Yes
Safety factor is constant along the failure surface	Yes	No	No	No
Variance of safety factor is constant along the failure surface	No	No	Yes	No
Probability of failure is constant along the failure surface	No	Yes	No	No
Interslice forces	constant ratio (λ)	constant ratio (λ)	constant ratio (λ)	no vertical component of the resultant to the failure surface
Static limit equilibrium	force moment	force moment	force moment	moment

2.4.1 Assumptions implied in the probabilistic limit equilibrium methods

Before the probabilistic limit equilibrium methods can be applied, some assumptions need to be made and the boundary conditions defined. These are listed below.
- As shown in paragraph 2.2 the limit equilibrium methods need assumptions to overcome the indetermination of the equations originating from the static equilibrium

condition and the boundary conditions. The assumptions for the various methods to overcome the indetermination are listed in table 2.1.- The variance of the safety factors is defined by equation 2.11 for the methods satisfying static equilibrium (GLEA, PROBCON and VARCON) and by equation 2.14 for the Fellenius method. Variables used in these equations are the pore water pressure, u, and the variables b_1 and b_2. There is no exact formula for the variance of b_1 and b_2 based on the mean and variance of bulk density, the location of the failure surface and the interslice forces. Therefore, it is assumed that the coefficient of variation of u, b_1 and b_2 remains constant along the failure surface. The coefficient of variation is the ratio between the standard deviation and the mean value of a variable. No data was available to assess its magnitude for the variable b_1 and b_2. Therefore, it is assumed that $SD[b_1]/b_1 = SD[b_2]/b_2 = 0.1$ and the $SD[u]/u = 0.1$, where SD[.] = standard deviation. The assumed value of 0.1 is within the range of coefficients of variation of various geotechnical parameters mentioned in Lee et al. (1983). For the Fellenius method the assumption indicates a standard deviation of $0.1 \cdot \tan\alpha$ for b_1. If the mean angle of the failure arc, α, is about 30°, b_1 has a standard deviation of about 2°.

- The pore water pressures acting on the failure surface are assumed to be the result of a groundwater water level at a certain depth below the surface and a groundwater flow parallel to the slope.
- The lognormal distribution is used to calculate the probability of failure. This lognormal distribution for the safety factor is used, because it fits the obtained experimental distribution of the safety factors in a Monte Carlo simulation (see chapter 6 and paragraph 2.2.2.3).

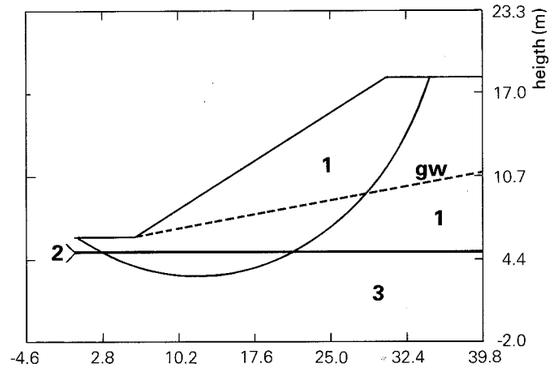

Figure 2.3 Morphometry for *case 1*

2.4.2 Validity and implications of the assumptions

An analysis is physically realistic, if static equilibrium and boundary conditions along the failure surface are satisfied and if the implied state of stress within the soil mass is physically realistic (Morgenstern-Price, 1965). The latter is physically unrealistic if a state of tension exists within a landslide over considerable length of the failure surface or if the shear strength of the slope material is exceeded somewhere within the soil mass (Morgenstern-Price, 1965; Nash, 1987).

The internal shear stress was used to check if the failure criterion of the Coulomb strength law had been exceeded. The vertical internal shear stress, T_{stress}, is obtained by dividing the vertical interslice shear force, T, by the height of the slice. Failure will occur if the shear stress is larger than the shear strength. The shear strength on the side of the slice is equal to $c + Es \cdot \tan\phi = c + \lambda \cdot T_{stress} \cdot \tan\phi$, where T_{stress} = vertical shear stress along the sides of the slice, λ is the constant ratio between the vertical and horizontal component of the interslice forces and Es is the stress normal to the side of a slice. Equation 2.7 is used to calculate the distribution of the vertical interslice shear force, T, along the failure surface.

For *case 1* under the assumption of T=0 at the toe the distribution of the vertical interslice shear forces (T) is shown in figure 2.4 using the VARCON method. Identical plots were obtained for the GLEA and PROBCON methods: however the maximum values were different. The maximum values for the vertical shear force, T, were 101.2 kN (PROBCON), 146.5 kN (GLEA) and 188.5 kN (VARCON). The maximum values for the T_{stress} were 61.2 kPa (PROBCON), 57.5 kPa (GLEA) and 31.8 kPa (VARCON).

For *case 1* the distribution along the failure surface of the vertical shear stress on the sides of a slice is given in figure 2.4. Remembering that the cohesion of the soil material is 28.75 kPa, figure 2.4 shows that the shear strength of the soil is exceeded at the toe of the landslide. Only the first two or three slices in the toe area give vertical shear stresses exceeding the shear strength of the soil. This is probably caused by the calculation accuracy. The slices at the toe are of a very small height. A small error in the height or the vertical shear force introduces a large error in the estimation of the shear stress. It may be concluded that the overall stress situation of the analysis is physically realistic with a possible exception of the toe area. A similar conclusion could be drawn for the GLEA and PROBCON.

In *case 2* the various methods show considerable differences in the distributions of the vertical interslice shear force, T. The VARCON method showed a identical shaped distribution to the GLEA method (figure 2.5). However, the magnitude of the interslice forces was very different in the methods. While the VARCON method gave a vertical interslice shear force, T, with a maximum of 220 kN, GLEA indicated a maximum vertical interslice shear force, T, of 3 kN. Both stress situations are physically realistic, because no tension exists along the failure surface and the shear strength of the soil is not exceeded.

The sharp dips in the line at an x-coordinate of 2.8 metre and 21 metre are due to the change in strength parameters, as the failure surface enters/leaves the weak horizontal layer (2).

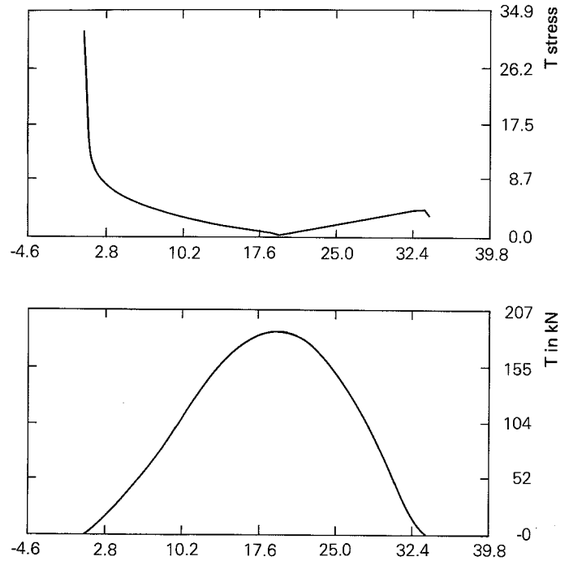

x - coordinate *test profile* (m)
scarp at 34.50 m and toe at 0.39 m

Figure 2.4 The distribution of the vertical interslice shear force, T, along the failure surface for *case 1* using the VARCON method

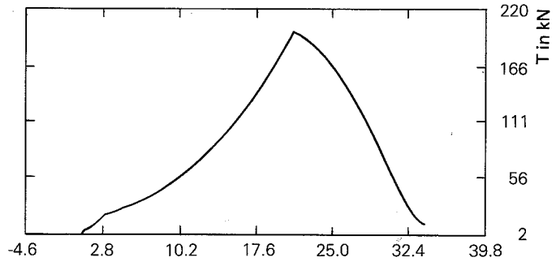

x - coordinate *test profile* (m)
scarp at 34.50 m and toe at 0.39 m

Figure 2.5a The distribution of the vertical interslice force, T, along the failure surface for *case 2* using the VARCON method

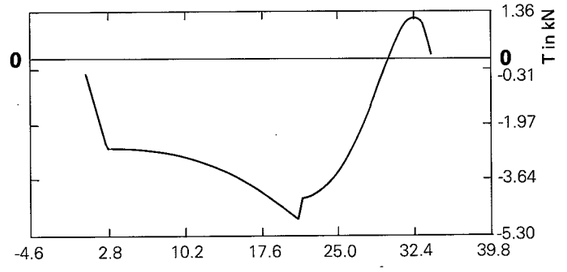

x - coordinate *test profile* (m)
scarp at 34.50 m and toe at 0.39 m

Figure 2.5b The distribution of the vertical interslice force, T, along the failure surface for *case 2* using the PROBCON method

The PROBCON method shows almost no interslice forces and the vertical shear force, T, is slightly negative over a large part of the failure surface (figure 2.5 b). It seems that for this method the implied stress situation is questionable, because tension exists along a major part of the failure surface.
For all methods the vertical shear stress, is smaller than the cohesion of the soil. So nowhere in the sliding mass the shear strength of the soil is exceeded.
Great differences exist between the various methods in values of ratio λ (table 2.2) and in the distributions of vertical interslice shear force, T, along the failure surface. This shows that implied stress situations along and within the sliding soil mass varies considerable between the methods: an indication that the results of either of the methods should be interpreted carefully.

Table 2.2 Comparison of the overall values of the safety factor, variance of the safety factor and probability of failure of the test profile under different conditions along the failure surface

Methods	safety factor	variance of the safety factor	standard deviation of the safety factor	probability of failure	ratio λ
Case 1					
GLEA	1.845	0.140	0.374	0.050	0.242
PROBCON	1.819	0.171	0.413	0.041	0.191
VARCON	1.997	0.145	0.381	0.102	0.317
Fellenius	1.711	0.608	0.780	0.338	--
Case 2					
GLEA	1.226	4.044	2.011	0.485	0.119
PROBCON	1.983	126.24	11.23	0.417	-0.024[ss]
VARCON	1.278	0.147	0.383	0.546	0.325

λ = constant ratio between vertical and horizontal component of the interslice forces
[ss] implied stress situation physical unrealistic

The overall values represent the mean of the parameters of all individual slices

The largest overall probability is given by the extended Fellenius method. The overall probability of failure is the mean of the probability to fail of every slice. In the methods satisfying all equilibrium conditions, the VARCON method gives the highest estimate of the overall probability.
The probability of failure along the failure surface for *case 1* is shown in figure 2.6. The Fellenius method indicates the highest probability of failure near the scarp (figure 2.6 a). This leads to the tentative conclusion that if failure occurs, it will start in the upper part. Failure of a slice in the upper part, may give rise (1) an extra stress at the adjacent slice in the direction of the toe and (2) the slice upwards of the failed slice is loosing its support. Both effects may cause one or both adjacent slices to fail.
Figure 2.6b (GLEA) and 2.6c (VARCON) both indicate that the highest probability of failure is in the center of the failure surface. If failure occurs, it will start somewhere half way between the scarp and the toe of the landslide.
The differences in the probability of failure along the failure surface in the Fellenius method and GLEA, PROBCON and VARCON methods may be explained by the different assumptions concerning the ratio, λ, between the vertical and horizontal component of the interslice forces.
In *case 2* the Fellenius method was omitted, because of the large extend of the failure surface with an angle of zero.
Figure 2.6d (GLEA) and 2.6e (VARCON) display the distribution of the probability along the failure surface. Both show that the probability of failure for the weaker

zone, between 2.8 m and 21 m, is much higher. The highest probability of failure is in the weaker zone at the lower end of the slope.
Although the mean probability to fail does not differ much per method - 0.546 for the VARCON method and 0.485 for the GLEA method-, the VARCON method has a larger range in its estimation of the probability of failure as shown in their maximum probability to fail, 0.958 for VARCON method and 0.739 for the GLEA method.

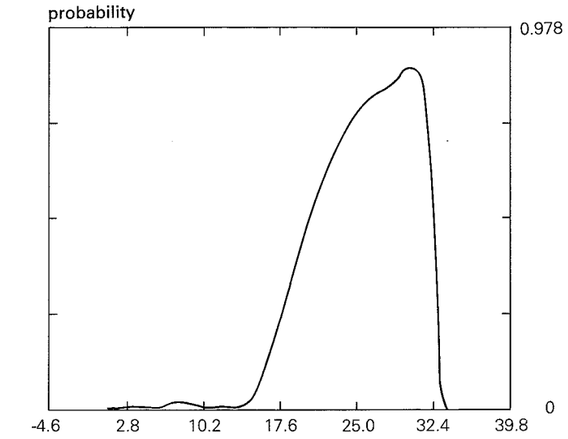

Figure 2.6a The probability of failure along the failure surface for *case 1* using the Fellenius method.

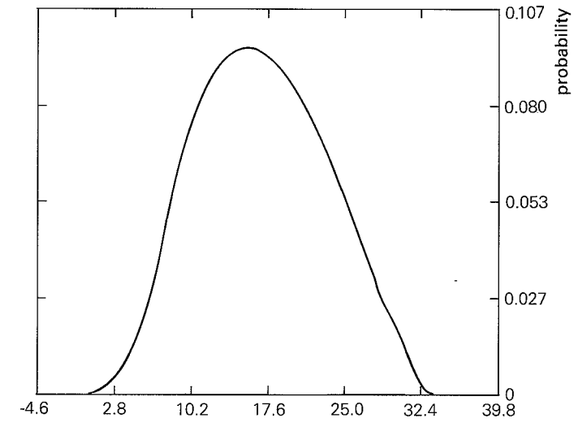

Figure 2.6b The probability of failure along the failure surface for *case 1* using the GLEA method.

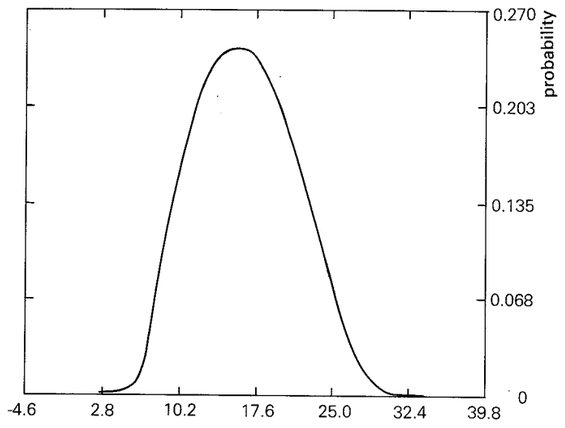

x - coordinate *test profile* (m)
scarp at 34.50 m and toe at 0.39 m

Figure 2.6c The probability of failure along the failure surface for *case 1* using the VARCON method

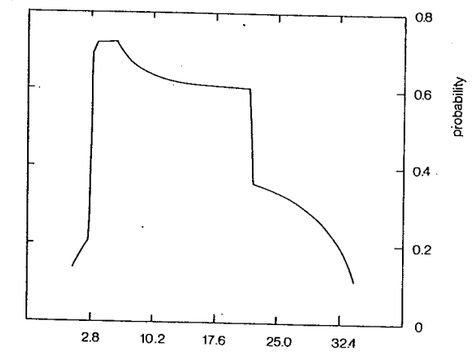

x - coordinate *test profile* (m)
scarp at 34.50 m and toe at 0.39 m

Figure 2.6d The probability of failure along the failure surface for *case 2* using the GLEA method.

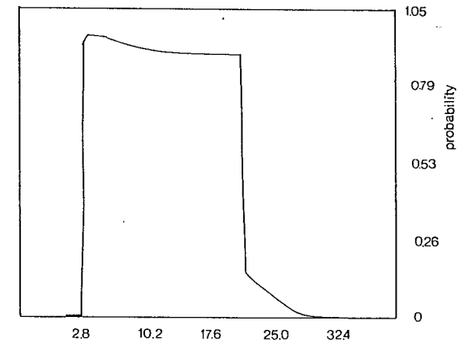

x - coordinate *test profile* (m)
scarp at 34.50 m and toe at 0.39 m

Figure 2.6e The probability of failure along the failure surface for *case 2* using the VARCON method

The overall values of the safety factors of slices along the failure surface remain within 15 % of each other for the various methods, except for the PROBCON method in case of failure surface cutting a heterogeneous material profile (*case 2*, table 2.2). The overall values represent the mean of the safety factors of all individual slices of the landslide. The reason for the extremely high safety factor of the PROBCON method may be explained by the fact that the PROBCON method implies an physically questionable stress distribution under the conditions of a heterogenous profile.
The overall value of safety factor estimated with VARCON method is always higher as the overall value factor of safety based on the GLEA method.
For *case 1* the overall values of safety factors according to the various methods do not differ much (table 2.2). However, the distributions of the safety factor along the failure surface do differ strongly (figure 2.7).
The safety factor, F, of equation 2.10 may be divided in:
(1) a part due to the effective normal stress, FP = $(M[b_1]\text{-}M[b_2]\cdot M[u])\cdot M[\tan\phi]$
(2) a part due to the cohesion, FQ = $M[b_2]\cdot M[c]$
(3) a reduction of the safety factor due to the water pressure at the failure surface, FR = $M[b_2]\cdot M[u]$.

It should be noted that the safety factor, F, equals the sum of FP and FQ.
The safety factor of GLEA is shown figure 2.7b. The safety factor is made up equally of FQ (cohesion) and FP (normal stress), where the contribution of the cohesion is the largest towards the edges of the failure surface.

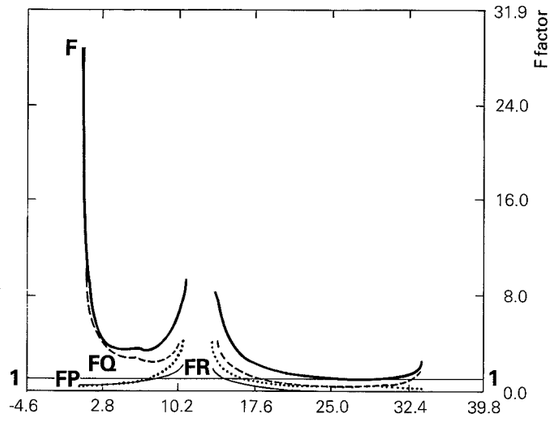

x - coordinate *test profile* (m)
scarp at 34.50 m and toe at 0.39 m

Figure 2.7a The distribution of the safety factors along the failure surface for *case 1* using the Fellenius method (The calculation of the safety factor was omitted between 10.4 and 12.2 m, because the angle of the failure surface was less than 2°)

The distribution of the safety factors along the failure surface according to the PROBCON method is shown in figure 2.7c. This method implies higher safety factors in the center and decreasing safety factors toward the edges of the failure surface. The distribution of the safety factor along the failure surface according to the VARCON method is shown in figure 2.7d. This figure gives an opposite impression of figure 2.7c. The safety factor is small in the center and increases towards the edges. While the PROBCON method indicates that the overall safety factor of the slope is determined to a large extent by the safety factors of the slices in the center of the failure zone, the VARCON method indicates the opposite: an overall safety factor of the slope, which is to a large extent determined by the safety factors of the slices at the fringes of the failure surface. An interpretation of the results could lead to a different assessment of the influences of an excavation at the toe of the slope on the stability of the slope. The PROBCON method would suggests that such an excavation is not of a large influence, because the overall safety factor is for a large extent determined by the safety factors at the center of the failure surface. The VARCON method suggests the opposite.

For *case 2* the analysis based on the Fellenius method was omitted due to the large impact of a failure surface with an angle of zero on the safety factor. This causes the safety factor, F, to go to infinity (see equation 2.12). The results for the other methods are shown in figure 2.8a-c. The differences between the methods are much larger than for *case 1*, figure 2.7a-d.
Both the assumption of a constant safety factor along the failure surface, the GLEA method, and the assumption of a constant probability of failure along the failure surface, the PROBCON method, seems to be unrealistic in case of a failure surface crossing layers of different strength: the calculations show that the safety factors will be equal or higher for the weaker layers than those of the stronger parts along the failure surface. In *case 2* the failure surface follows the weaker layer between 2.8 m and 21 m. The safety factors are higher (PROBCON) or equal (GLEA) for the weaker layer than for the stronger layer as shown in figure 2.8. The VARCON method gives a distribution of the safety factor as could be expected: safety factors below unity for the weak zone (figure 2.8c). Thus the VARCON method seems the appropriate method to use if a stability analysis is performed of a slope with heterogenous material, either in bedding or by changes in the material strength.

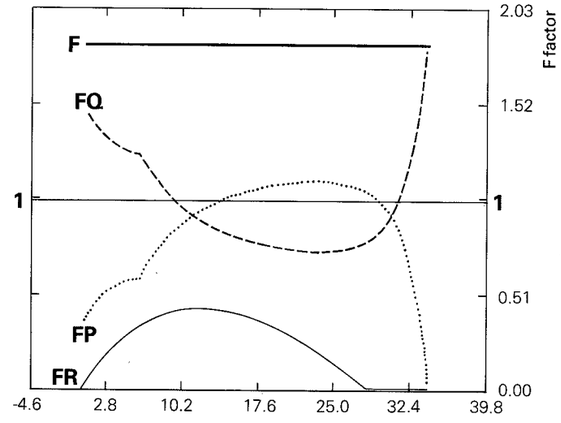

x - coordinate *test profile* (m)
scarp at 34.50 m and toe at 0.39 m

Figure 2.7b The distribution of the safety factors along the failure surface for *case 1* using the GLEA method

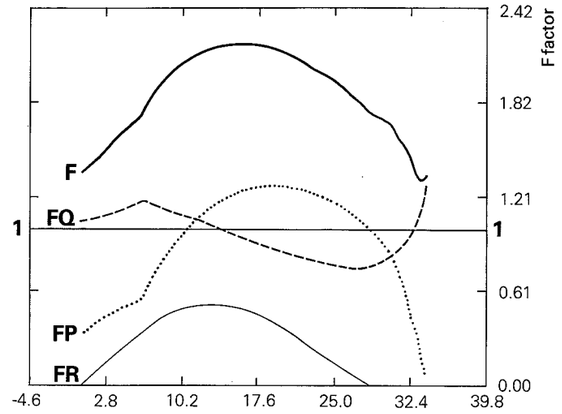

x - coordinate *test profile* (m)
scarp at 34.50 m and toe at 0.39 m

Figure 2.7c The distribution of the safety factors along the failure surface for *case 1* using the PROBCON method

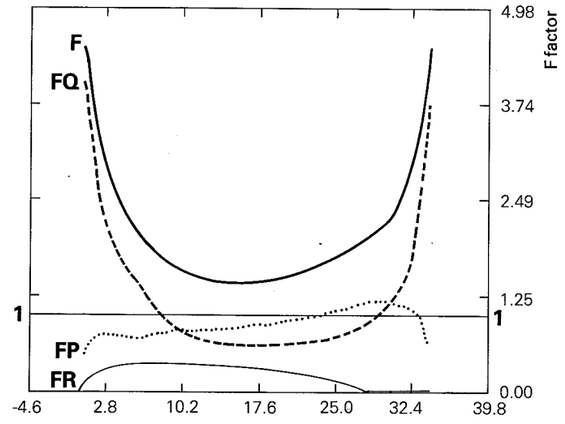

x - coordinate *test profile* (m)
scarp at 34.50 m and toe at 0.39 m

Figure 2.7d The distribution of the safety factors along the failure surface for *case 1* using the VARCON method

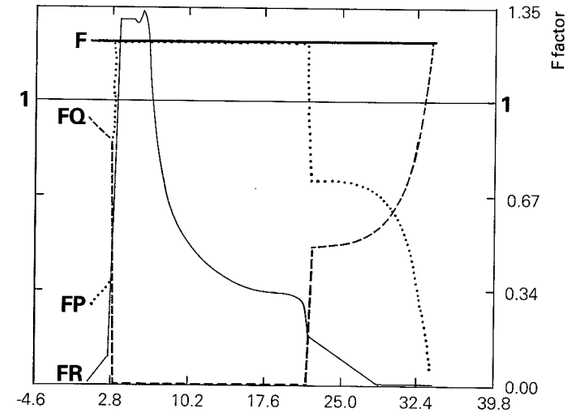

x - coordinate *test profile* (m)
scarp at 34.50 m and toe at 0.39 m

Figure 2.8a The distribution of the safety factors along the failure surface for *case 2* using the GLEA method

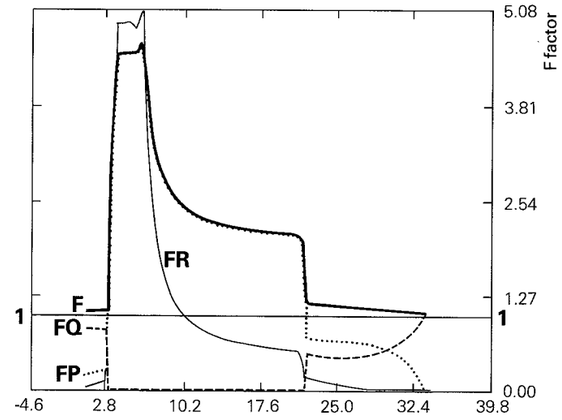

x - coordinate *test profile* (m)
scarp at 34.50 m and toe at 0.39 m

Figure 2.8b The distribution of the safety factors along the failure surface for *case 2* using the PROBCON method

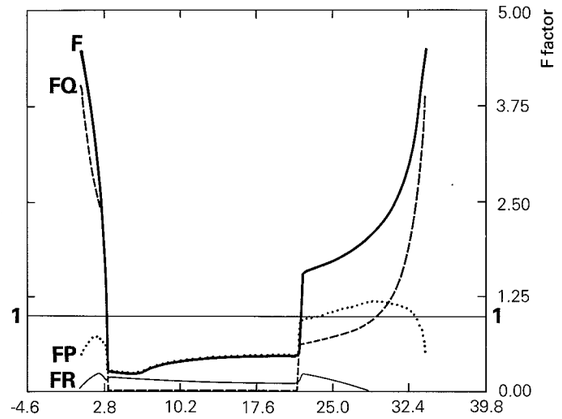

x - coordinate *test profile* (m)
scarp at 34.50 m and toe at 0.39 m

Figure 2.8c The distribution of the safety factors along the failure surface for *case 2* using the VARCON method

The variances of the safety factors of the VARCON method are nearly independent of the conditions of a slope as shown by table 2.2. The GLEA method has very large overall variances compared with the VARCON method in case of a failure surface following a weak layer (2) (*case 2*, table 2.2).
For the sake of clarity, in the figures the standard deviations instead of the variances are given. The standard deviation of the safety factor, S, may be divided into:
(1) a part due to the effective normal stress, SP,
(2) a part due to the cohesion, SQ,
(3) a part due to the water pressure at the failure surface, SR.
For *case 1* the distributions of the standard deviations estimated by PROBCON and GLEA methods are similar, only the standard deviations of the GLEA method are smaller (figure 2.9a and b). The standard deviations are due to the normal stress, SP, for 90-95 % (figure 2.9a and b). The Fellenius method gives incomparable results (figure 2.9c). This is probably due to the differences in the handling of the interslice forces between the Fellenius method and the other probabilistic methods. The ratio, λ, between the vertical, T, and horizontal component, E, of the interslice forces is not a constant in the Fellenius method.

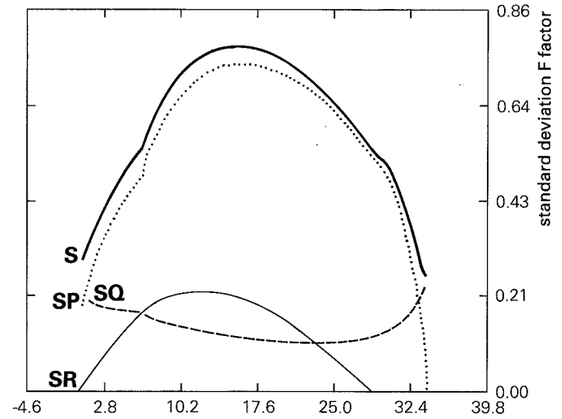

x - coordinate *test profile* (m)
scarp at 34.50 m and toe at 0.39 m

Figure 2.9a The distribution of the standard deviation of the safety factors along the failure surface for *case 1* using the GLEA method.

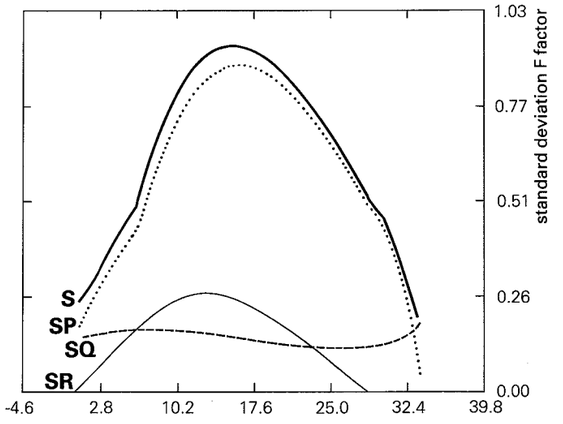

x - coordinate *test profile* (m)
Scarp at 35.80 m and toe at 0.39 m

Figure 2.9b The distribution of the standard deviation of the safety factors along the failure surface for *case 1* using the PROBCON method

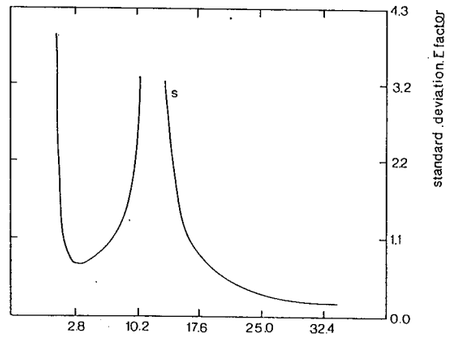

Figure 2.9c The distribution of the standard deviation of the safety factors along the failure surface for *case 1* using the Fellenius method.

2.5 Concluding remarks concerning the various methods

As pointed out in paragraph 2.1, the application of the deterministic safety factor concept to landslide hazard analysis is difficult due to several problems. Among the problems are:
- the translation of the safety factor into a landslide hazard.
- the assumption of a constant safety factor for all individual slices, while numerous stress-deformation studies on basis of finite element method have shown that the safety factor may be quite different (Chowdhury and A-Grivas, 1982).
- the safety factor is single valued and does not account for the inherent variability of vegetation, soil or rock properties.

A probabilistic safety facor concept may account for the variations of the stress and strength along the failure surface. This concept makes it possible to calculate the mean and variance of the safety factor of each slice on basis of the mean and variances of the primary factors. The mean and variance of the safety factor may be used together with an assumed probability distribution to give a probability of failure. The obtained probability of failure is a linear measure for the landslide hazard.

The probabilistic concept provides alternatives to the assumption of a constant safety factor along the failure surface. Two alternatives were formulated:
(1) a method based on the assumption of a constant probability of failure along the failure surface (PROBCON)
(2) a method based on the assumption of a constant variance along the failure surface (VARCON).

The probabilistic concept may provide more details about the stress situation in a landslide. However, comparing the different probabilistic methods (GLEA, Fellenius, PROBCON and VARCON) it appears that there are considerable differences in the outcomes of the distribution of the safety factors, standard deviation and the ratio λ. This indicates that the four methods incorporate different stress distributions along the failure surface. This implies that probably neither of the methods describes the actual stress situation and that the interpretation of the results should be done with some caution.

The variance of the safety factor seems to be primarily influenced by the normal stress at the failure surface. The normal stress is a function of location of the failure surface, the internal forces and bulk density. Furthermore, the variances of the safety factor calculated by the VARCON method are nearly independent of the conditions of a slope.

The results of the probabilistic Fellenius method are quite different to the other probabilistic methods. This indicates that the way the interslice forces are incorporated in the method influences the results considerable.

The assumptions of a constant probability of failure along the failure surface (PROBCON) or a constant safety factor along the failure surface (GLEA, Fellenius) are questionable in case of heterogeneous profiles and sometimes result in physically unrealistic stress situations in the sliding soil mass.

The VARCON method seems to be the appropriate method to use if the landslide hazard has to be estimated of a slope with heterogenous material, either in bedding or by changes in the material strength.

3 THE VARIABILITY OF STRENGTH PARAMETERS USED IN METHODS TO ASSESS LANDSLIDE HAZARD ON A LOCAL SCALE

3.1 Introduction

The variability of strength parameters plays an important role in the assessment of landslide hazard by means of probabilistic limit equilibrium methods (see chapter 2). The actual probability of failure, which might be a measure for landslide hazard, is a function of the safety factor and of its variance. The probability of failure can be determined for each point in a grid system, if the mean and variance of the safety factor are known or can be estimated at that point. The mean and variance of the safety factor is depending on measurement errors and spatial variations in the strength parameters (see par. 1.2.1).
Measurements are subject to error. Several sources of errors can be distinguished: (a) random errors creating variance of unpredictable or unknown nature; these errors are assumed to be normally distributed with a zero mean; (b) systematic errors occurring as a result of: (1) samples not being representative for the area under consideration, (2) sample properties being altered in the process of sampling and transport, (3) inaccurate tests, and (4) calculation errors.
The total variance is the result of the accumulation of all different sources of errors. Spatial variation in strength parameters is another factor to take account of. The value of a continuous spatial parameter can be expressed as the sum of three major components. These are: (1) a structural component associated with a constant mean or with a constant trend, (2) spatially related variation in the variance, and (3) a random noise or residual error term (Burrough, 1986).

3.2 Field sampling and laboratory methods to assess shear strength

Field sampling of cores for laboratory tests on shear strength, was performed in the colluvium of plot 1, Riou Bourdou (Fig. 1.4).
The sampling depth varied between 10 and 450 cm. Sampling was performed using a thin walled sampler (inner diameter 66 mm, outer diameter 67 mm, length about 400 mm), which was driven into the soil with a hammer. Visible disturbance of the samples due to the sampling was restricted to the outer 2 mm.
Sampling was executed following an unbalanced nested sampling technique. The number of samples taken on each scale level was roughly the same. This provides an economic way of estimating the scale and pattern of variation of continuous spatial variables (Oliver and Webster, 1986).
If a spatially related variation in the variance of strength parameters exists, it yields a way to reduce the number of observations needed to estimate the mean and variance of the parameters. One may expect that the parameters at places next to each other have the same values, while these may differ over larger distances. Any observation carries some information about its neighborhood. When a region is sampled at

random, some of the observations inevitably will be close. The duplication of information is minimized by locating the sampling points as far from each other as possible (McBratney and Webster, 1983). The maximum distance, where information duplication occurs can be estimated using a semivariogram. A semivariogram is a plot of the semivariance versus lag or distance. It displays how the semivariance changes with sample spacing. The semivariance ($\gamma(h)$) is a measure of the variance of the estimation of $x(z+h)$ by $x(z)$.
Ideally the semivariance increases with increasing sampling distance h until it reaches a maximum value (the sill). This maximum value approximates the total variance of the sample population (Journal and Huybregts, 1978). The lag or distance necessary to reach the maximum value is known as the range (see figure 3.1). It is often observed that if the lag approaches zero, the curve of the semivariance does not pass through the origin, but crosses the y-axis at a positive value, the nugget.

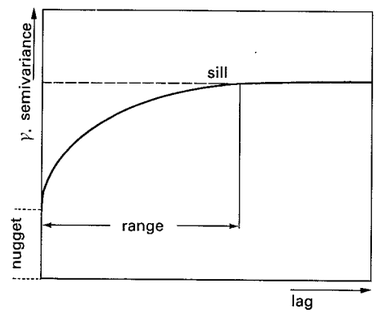

Figure 3.1 Idealized semivariogram

Different laboratory tests were used to determine the shear strength of the samples. Consolidated drained direct shear tests were performed on 131 core samples. All cores, each with a diameter of 66 mm and a length of 400 mm, were saturated by submersion in water for one to two weeks. To fit in a standard direct shear box, the saturated cores were divided into 4 sub-samples with a height of 25 mm and diameter of 60 mm. The tests were run at a deformation rate of 10 mm/hr at a normal load between 5 and 55 kPa. This resulted in 402 different combinations of normal stress and shear strength.
Consolidated drained tri-axial tests (multi-stage) were used to estimate the peak strength of the colluvium material. In total 7 core samples of 400 mm height and 66 mm diameter were utilized in the test. The cores were taken closely spaced at plot 1, Riou Bourdou, at a depth between 100-150 cm. The 7 cores were divided in 2-3 sub-samples, giving 19 different combinations of σ_1 and σ_3 at failure. The tri-axial tests are run at a 0.25 mm/hr deformation rate on cylindrical shaped samples (66 mm diameter by 135 mm long). Consolidation pressures varied from 20 to 200 kPa, with

a standard back pressure of 300 kPa. A complete description of the tests is given in Hazeu (1988).
Unconfined compression tests were used to test the relationship between peak shear strength and root content. A total of 64 tests were performed on saturated samples with a height of 120 mm and a diameter of 66 mm. The tests were run at a 2 mm/min deformation rate on the cylindrical shaped samples. A complete description of the test are given in Brombacher and Hartman (1989).

3.3 Estimation of peak shear strength

3.3.1 Approximation of the failure envelope

The failure envelope is the line connecting the different combinations of the shear stress and normal stress, where failure just occurs. The shear stress needed to obtain failure at a certain normal stress is also called shear strength. The failure envelope is approximated by a straight line in the Coulomb failure theory (equation 1.2). The parameters describing the linear relationship between shear stress and normal stress at failure, are the cohesion (intercept with the y-axis) and the angle of internal friction ($\tan(\phi)$ = slope of the straight line). These parameters may be obtained by a linear regression analysis.

$$\tau = c + \sigma_n' \tan \phi \qquad (1.2)$$

τ = shear stress (kPa)
σ_n' = effective normal stress (kPa)

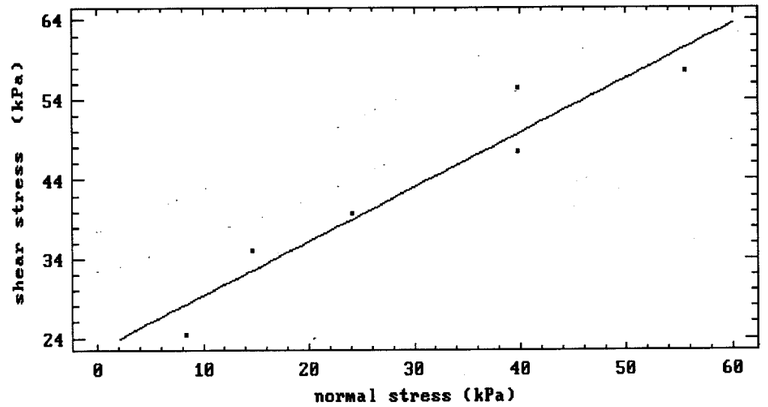

Figure 3.2a Plot of the shear strength (kPa) versus normal stress (kPa) of sample 522. Linear regression r^2=0.917

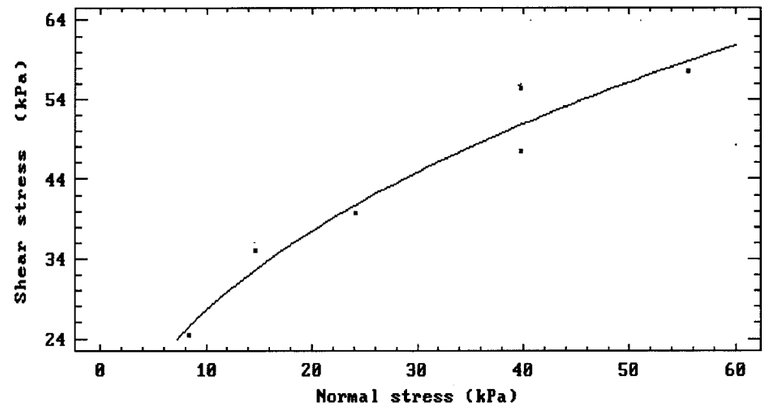

Figure 3.2b Plot of the shear strength (kPa) versus normal stress (kPa) of sample 522. Power regression (r^2= 0.974)

It is commonly observed that the failure envelope has a curved character at smaller normal stresses, while at higher normal stresses the envelope is almost a straight line (Hawkins, 1988; see fig 3.2). The departure of the failure envelope of a straight line is often attributed to increasing interlocking of the particles with decreasing normal stresses (Nieuwenhuis, 1983) or to the presence of fissures due to sampling (Craig, 1987).
If no attention is given to the curvature at smaller normal stresses, the estimation of the stability or landslide hazard of a shallow landslide may be in error. However, for calculation purposes it is desirable to replace this curved envelope with a straight line. This is done by providing a best fit line over the stress range of interest as shown by Kenny (1984). Thus different strength parameters will be obtained, depending on the stresses involved. Note that the linear relationship may give a non-zero cohesion parameter, even though the actual failure envelope passes through the origin. Because the linear regression on the lower stress range, is based on less combinations of shear stress and normal stress, the already considerable variance of the cohesion and tan(ϕ) will be further increased. In order to reduce the variance of the parameters describing the failure envelope, it is proposed to fit a curved line on the different combinations of shear stress, τ, and normal stress σ_n, where failure just occurs (equation 3.1). This is a power regression, where P_1 and P_2 are regression constants.

$$\tau = P_1 \sigma_n^{P_2} \quad \vee \quad \ln(\tau) = \ln(P_1) + P_2 \ln(\sigma_n) \tag{3.1}$$

P_1 = modified 'cohesion'
P_2 = modified 'tanϕ'

3.3.2 Spatial variation of shear strength

If a slope starts to fail, it is important to know the dimensions of the area involved. VanMarcke (1977) has developed a model for the estimation of the width of a landslide, provided the depth of the failure surface is known and assuming that shear strength has a specific spatially related variance. If such a spatially related variance exists, VanMarcks' model may be used to estimate the width of the landslide. So it is worthwhile to study spatial dependence.
Core samples from plot 1, Riou Bourdou, were used to estimate the spatial dependence of the variance.
The parameters of the linear fit (cohesion, angle of internal friction) and of the power fit (P_1 and P_2) have an estimation error. Not all combinations of shear stress and normal stress are perfectly situated on the failure envelope (figure 3.2). The shear strength at a normal stress of 55 kPa (Shear 55) was studied as well, because the estimation error of the parameters may be large compared with other sources of error and therefore may cover up (a part of) the spatial variation of the variance.

Spatial dependence of the mean values

The spatial dependence of the mean value or trend of shear strength parameters is studied using a multi-variate analysis. The multi-variate analysis is used to obtain a linear relation between geographical coordinates and the strength parameters. For the analysis only those parameters were used, which refer to samples taken at a depth of 100-150 cm. In this way the variance due to a possible variation with depth of the parameters was reduced. The results are listed in table 3.1.
If the slope of the linear regression is not significantly different from zero, the shown increase is not significant. This slight increase was tested for significance using a Student-t test. On the 0.975 significance level (n=100) the t-value has to be larger than 1.984 to be significant on that level.

Table 3.1 Results of a trend analysis for the strength parameters

	intercept	X	t-value	Y	t-value	r^2(%)
cohesion (kPa)	0.702	$-2.02\cdot10^{-2}$	-1.46	$-2.55\cdot10^{-2}$	-1.04	3.82
tan(ϕ) (°)	0.772	$6.63\cdot10^{-4}$	1.16	$-9.23\cdot10^{-4}$	-0.91	0.00
P_1	6.848	$-0.90\cdot10^{-4}$	-0.91	$-2.05\cdot10^{-3}$	-1.16	1.73
P_2	0.543	$2.52\cdot10^{-4}$	0.98	$1.15\cdot10^{-4}$	0.25	0.00
Shear 55 (kPa)	61.17	$-3.51\cdot10^{-2}$	-0.97	$-1.68\cdot10^{-2}$	-0.23	2.00

Table 3.1 reveals that non of the fitted trend surfaces are significant. Therefore, it is concluded that there is no trend in the mean values of the strength parameters on plot 1.

The strength data are also tested for a difference in the mean values between sample cores taken at the stable area or at the landslide of plot 1. The results are listed in table 3.2.

Table 3.2 Comparison between the mean values estimated on the stable areas and the landslide of plot 1.

		stable		landslide		hypothesis
number of		21		75		
observations		mean	variance	mean	variance	
cohesion	(kPa)	17.55	55.61	17.28	42.61	accept
tan(ϕ)	(°)	0.67	0.03	0.77	0.06	accept
P_1		6.56	0.63	1.85	0.18	accept
P_2		0.52	0.01	0.54	0.01	accept
Shear 55	(kPa)	54.87	140.3	60.17	210.0	accept

The mean values of the different parameters are tested for a significant difference at 0.95 level using a Student-t test. The H0 hypothesis is that the differences between the means are equal to zero. As shown in table 3.2, for all parameters the H0 hypothesis has to be accepted. This indicates that there is no difference in the mean values of strength parameters obtained from samples taken at the stable area or at the landslide of plot 1.

Spatial dependence of the variance

The spatial dependence of the variance of shear strength parameters is studied using a semivariogram over a maximum lag of 50 meters and a step size of 1 m. For the semivariogram only those parameters were used, which refer to samples taken at a depth of 100-150 cm. In this way the variance due to a possible variation with depth of the parameters was reduced.

Table 3.3 Parameters estimations of the semivariograms (n=49)

	intercept	slope	t-value	r^2(%)
cohesion (kPa)	40.86	0.0267	0.184	0.07
tan(ϕ) (°)	0.051	$3.9 \cdot 10^{-4}$	1.775	6.16
P1	0.602	$6.3 \cdot 10^{-4}$	0.650	0.87
P2	0.009	$9.0 \cdot 10^{-5}$	1.819	6.45
Shear 55 (kPa)	177.2	0.777	0.758	1.18

The results of linear regression between semivariance of the different parameters and the distance are shown in table 3.3. All five semivariograms show a slight increase of

the semivariance with distance. If the slope of the linear regression is not significantly different from zero, the shown increase is not significant. This slight increase was tested for significance using a Student-t test. On the 0.975 significance level (n=49) the t-value has to be larger than 2.01 to be significant on that level.
Table 3.3 reveals that non of the slopes are significantly different from zero at the 0.975 level. A zero slope of the regression line indicates no spatial dependence. The semivariogram displays a pure nugget effect. In those situations the best estimate of a value of a parameter is the usual mean, computed from all sample points without taking spatial dependence into account (Burrough, 1986). A pure nugget effect is indicative of a parameter that is highly variable over distances less than the sampling interval.

The above presented analysis indicates that neither the mean value nor the variance of the strength parameters is spatially related. Thus, VanMarcke's model (1977) to estimate the width of a landslide, is not appropriate for the study area.

3.3.3 Variation with depth of the shear strength parameters

Roots increase the apparent cohesion of a soil and have no influence on the angle of internal friction (Waldron (1977), Wu et al (1979), Gray and Leisner (1980), Ziemer (1981) and Greenway (1987)). Thus it may be expected that there is a difference in cohesion between the rooting zone and the subsoil.
The root zone, which was defined as the soil layer containing 80 % of the roots, was observed to be between 40-60 cm. The maximum rooting depth was more than 250 cm.
Table 3.4 shows that P_1 is the only strength parameter related to the depth at the 0.975 significance level.
In order to analyze if there is a difference in the strength parameters of the root zone and the subsoil, the sample cores were divided in two groups. In table 3.5 the results of a comparison between the mean values are shown.
None of the mean values of the root zone and the subsoil differed significantly from each other at the 0.975 level, except for the shear stress needed to obtain failure at a normal stress of 55 kPa (Shear 55).

Table 3.4 Relation between strength parameters and depth

		intercept	slope	t-value	r^2 (%)	n
tan(ϕ)	(°)	0.654	$4.1 \cdot 10^{-4}$	1.22	1.17	131
cohesion	(kPa)	14.99	$1.5\ 10^{-2}$	1.64	1.18	131
P_1		5.307	$1.1\ 10^{-3}$	1.98	2.26	131
P_2		0.587	$-2.6\ 10^{-4}$	-1.38	1.44	131
Shear 55	(kPa)	52.19	$2.2\ 10^{-2}$	1.01	1.02	100

The slope differs significantly from zero, if t-value > 1.978, n=131 at the 0.975 level
The slope differs significantly from zero, if t-value > 1.984, n=100 at the 0.975 level

Table 3.5 Comparison of the mean values of the strength parameters of the root zone and the deeper layer.

	root zone		subsoil		hypothesis
number of observations	15		121		
	mean	variance	mean	variance	
cohesion (kPa)	12.66	31.68	16.71	62.50	accept
tan(ϕ) (°)	0.630	0.035	0.724	0.074	accept
P_1	1.809	0.604	5.657	1.317	accept
P_2	0.551	0.095	0.550	0.026	accept
Shear 55 (kPa)	43.80	91.12	56.42	228.2	reject

The magnitude of root reinforcement of soils in the study area has been analyzed by comparing shear strengths established by unconfined compression tests on samples with different root contents. The data showed no relationship ($r^2 = 0.03$) between root content and peak or residual shear strength (Fig. 3.3). There was a relation with dry bulk density ($r^2 = 0.34$).

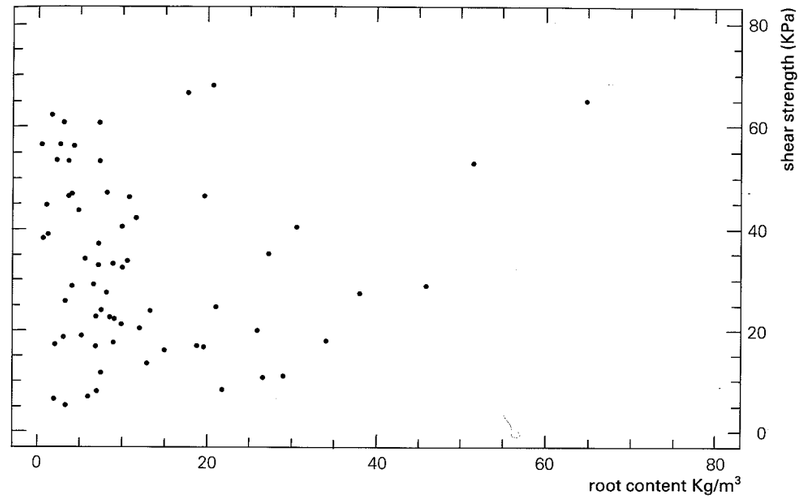

Figure 3.3 The relation between root content and peak shear strength

3.3.4 Correlations between the parameters describing the shear strength

In paragraph 3.2.2 an equation of the safety factor variance was derived using two statistical theorems, which assumed independence of the cohesion and tanϕ. This independence is tested by calculating the correlation between the cohesion and the angle of internal friction.
It appears that cohesion and tan(ϕ) are independent variables (r = -.0578; n=131). A similar conclusion was derived by Lumb (1970). He suggested that the slight negative correlation sometimes observed (Lumb, 1970; McGuffy et al, 1981; Read and Harr, 1988) was caused by insufficient low strain rates during testing. It appears that this is not the case in our data.
The parameters P_1 and P_2 of equation 3.1 are strongly correlated (r=-0.8035), suggesting that it is possible to describe the failure envelope with only one parameter.

Table 3.6 Correlations (r) between the strength parameters (n=131).

	cohesion	tan(ϕ)	P_1	P_2
cohesion	1	-0.0578	0.7879	-0.4417
tan(ϕ)		1	-0.1278	0.5882
P1			1	-0.8035
P2				1

3.3.5 The shear strength of the colluvium

Because the shear strength data showed no spatial dependency, all combinations of the shear and normal stress were used to establish the mean and the variance of the cohesion, angle of internal friction and the parameters P_1 and P_2 of equation 3.1. The results of a linear regression on the 402 combinations of shear and normal stress are shown in figure 3.4 (r=0.683). The plot shows a considerable variation. A multivariate analysis revealed that 7 % of the total variance is due to variations in the bulk density of a sample. In figure 3.5 the fitting of the power regression (equation 3.1) is shown (r=0.734). The linear regression indicates a cohesion of 20.02 kPa and a tanϕ of 0.773. The power regression indicates a P_1 of 7.43 and a P_2 of 0.516.

The failure envelopes based on direct shear tests are better approximated with a power model ($y = P_1 x^{P2}$, where y = shear strength, x = normal stress), than with the straight line as prescribed by the Mohr-Coulomb failure theory. The results of the linear regression, estimating c and tan(ϕ), and power regression, estimating P_1 and P_2, on 131 core samples are given in table 3.7.

Table 3.7 Statistical parameters of all direct shear tests (n=131)

	tan(ϕ)	ϕ	cohesion	P_1	P_2
mean	0.7118	35.44	13.55	5.75	0.545
median	0.6644	33.60	16.10	6.29	0.532
variance	0.0680	3.83	49.17	1.24	0.020
stand. err	0.0220	1.26	0.62	0.05	0.013

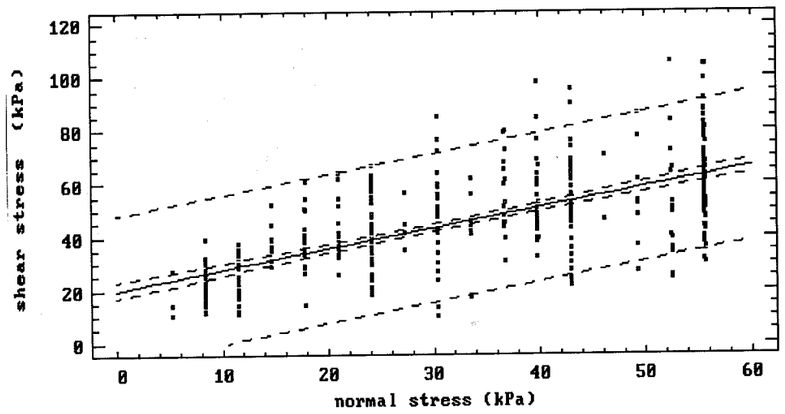

Figure 3.4 A linear regression on 402 combinations of shear stress and normal stress obtained in consolidated drained direct shear tests.

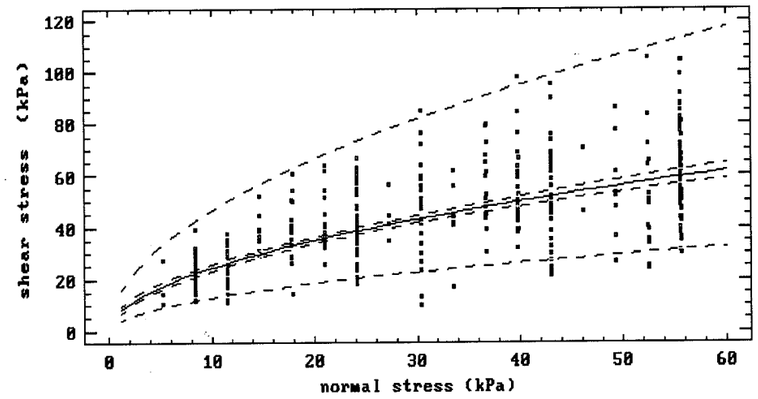

Figure 3.5 A power regression on 402 combinations of shear stress and normal stress obtained in consolidated drained direct shear tests.

The peak shear strength of the colluvium was also estimated using consolidated drained tri-axial tests (multi-stage). The results are listed in table 3.8.
Because the cores used for the tri-axial testing were closely spaced and the number of samples is small, no attempt was made to establish any spatial variation in mean or variance of the samples.
Comparison of the results of the direct shear test (Table 3.7) and the tri-axial test (Table 3.8) reveals higher estimates of the mean and smaller variances for cohesion and tan(ϕ) in a direct shear test. This is probably due to factors inherent to a direct shear test, the failure surface has to follow a prescribed path, while in a tri-axial test it may develop in the weakest part of a sample.

Table 3.8 Results of 19 consolidated drained tri-axial tests (multi-stage) for the determination of the peak strength

variable	estimate	standard error	variance
cohesion (kPa)	12.44	3.58	243.51
tan(ϕ) (°)	0.460	0.019	$6.8 \cdot 10^{-3}$

$r^2 = 0.972$
standard error of estimate = 0.081

3.4 Conclusions

The variability of the strength parameters, like cohesion and angle of internal friction were estimated on 131 core samples taken at plot 1, Riou Bourdou. The variances of the cohesion and the angle of internal friction in the data set are large, but well within the range of coefficients of variation up to 80%, as mentioned by Lee et al (1983) . The following conclusions may be drawn from the data:

- the absence of a spatial variation in the data on cohesion and the angle of internal friction, implies that the mean of the total data set is the best estimate of these parameters;
- the existence of a pure nugget effect in the data shows that the strength of a soil sample is due to processes and interactions on a scale much smaller than the sample size;
- the failure envelopes based on the direct shear tests are better approximated with a power model ($y = P_1 x^{P2}$, where y = shear strength, x = normal stress), than with a straight line as prescribed by the Coulomb failure theory;
- the parameters cohesion and angle of internal friction are independent parameters as shown by their correlation, $r = -0.0578$. Apparently, the assumption of independence as assumed in derivation of the variance equation of a safety factor in paragraph 2.2.2.1 is correct.
- the modified cohesion, P_1, and modified '$\tan\phi$', P_2, are strongly correlated ($r = -0.8035$), suggesting that it is possible to describe the failure envelope with only one parameter. Despite the reduction with one parameter, the resulting probabilistic limit equilibrium models were far more complicated than the conventional methods based on a straight line approximation.
- for core samples taken in the root zone and those from the subsoil no significant difference in the values of the means of the strength parameters could be found. This is in agreement with the results of unconfined compression tests where no relation between the root content and the root reinforcement could be established. Apparently the roots do not contribute to the shear strength of the soil. However, literature indicates opposite results: e.g. Ziemer (1981) and O'Loughlin (1972), both using large direct shear boxes for testing on peak strength, found correlations between root content and shear strength of $r^2 = 0.79$, respectively $r^2 = 0.56$. Reported magnitudes of root reinforcement range between 2 to 25 kPa (Burroughs and Thomas, 1977; Ziemer, 1981; Riestenberg and Sovonick-Dunford, 1983). These contradictory results have stimulated an investigation into the mechanical effects of roots of the shear strength of a soil (Chapter 4).

4 THE MECHANICAL EFFECTS OF ROOTS ON THE VARIATION IN SHEAR STRENGTH

4.1 Introduction

The mechanical effects of roots on soil strength are not very well understood. Experimental data are scarce and sometimes conflicting (see par. 3.4). This conclusion has initiated a further study of root effects.

Generally, research on the mechanical effects of roots on the strength of a soil was stimulated after the successful stabilization of slopes by metal strips or sheets of synthetic fabric. The research especially focussed on the magnitude of the stabilizing effects of a reinforcement by roots. Less attention was given to a more theoretical approach, which tries to explain the nature of root reinforcement of a soil.

An assessment of the effect of roots on the shear strength of a soil may be acquired by comparing identical soils either with or free of roots. Commonly used methods to measure the strength are the direct shear tests (in situ and on samples; Burroughs and Thomas, 1977; Ziemer, 1981; Waldron, 1977; Chapter 3) and unconfined compression shear tests (chapter 3). Another method is a back analysis of a failed vegetated soil mass (Riestenberg and Sovonick-Dunford, 1983). A back analysis uses a limit equilibrium model to estimate the extra strength needed to obtain a safety factor of 1. This extra strength is thought to be due to the presence of the roots. The used strength parameters are often those of a root free subsoil, which are not necessarily identical to those from the root zone. The higher biological activity in the root zone may change the strength characteristics. In addition most measurements of the angle of internal friction and cohesion are performed on saturated samples. A root zone tends to be unsaturated. It has been shown (Anderson and Pope, 1984; Fredlund, 1987) that soil suction has a considerable influence on the strength of a soil.

The just mentioned methods have their limitations. There is a difficulty in finding samples having the same soil properties, but different densities of roots. In addition the accuracy of the determination of the strength parameters (chapter 3) is not very great. As a result of these circumstances, there is a substantial variability in outcomes, which makes the comparison between the strength of rooted to non-rooted soils not very reliable. Quite often the variability is not acknowledged. This leads to expulsion of the data or statements like: "there was no rather than a negative reinforcement" (Terwilliger and Waldron, 1990).

Another limitation is the sample size. The sample size is often too small to represent the structure and root pattern of the soil adequately. The sample size itself influences the measured strength of a soil. The shear strength values of small undisturbed soil samples appeared to be an order of magnitude larger than the measured strength of larger samples (Terwilliger and Waldron, 1990; Schultz, 1957). Furthermore, a soil matrix with larger elements like roots, stones and soil aggregates may show a far larger soil strength in small cores than in large cores (Terwilliger and Waldron, 1990; Schultz, 1957).

Because of these limitations, theoretical approaches were undertaken to assess the magnitude of root reinforcement of the shear strength of soils. Theoretical models for

the root reinforcement of a soil are proposed by Wu et al. (1979), Gray and Ohashi (1983) and Waldron and Dakessian (1981). The models differ in their assumptions and are based on the concept of reinforced earth. This concept was developed by Vidal (1969). Vidal states: "A fibre (root) reinforced soil may be analyzed as if it was a composite material in which fibers of relatively high tensile strength are embedded in a matrix of lower tensile strength. The additional strength of such a reinforced soil is a result of frictional forces developing between the soil and the fibers".

4.2 Modelling of soil reinforcement by roots

A model for the reinforcement of the soil by will be derived and validated in this and the following paragraphs. The model is based on the following concept of the processes involved (see fig 4.1). Due to a displacement along a shear zone, a root, which crosses the shear zone, will elongate. This elongation generates a stress inside the root. This root stress gives rise to additional stresses in the shear zone. The root stress is transferred to the soil by a friction stress at the root-soil contact. In this it differs from the concept used by Waldron (1977), Wu et al. (1979), Gray and Ohashi (1983) and Waldron and Dakessian (1981). They assume that the root stress is due to stresses in the soil and these stresses are transferred to the root by friction at the root-soil contact. The friction stress at the root-soil contact causes the anchorage of a root in the soil. This is the concept of reinforced earth as proposed by Vidal (1969). The total force, that can be applied to a root is limited either by breaking of the root, or slipping of the root through the soil.
The derivation of a model for reinforcement of a soil by roots comprises the following steps: (1) estimation of the forces acting on the shear zone due to the presence of roots, (2) estimation of the root reinforcement of the soil assuming no restriction on the stresses applicable to roots, and (3) inclusion of limitations on the stresses applicable to roots.
Consider a shear zone intersecting a root zone (figure 4.1). After failing of the soil mass along a-b, the forces on and inside a root are due to displacements of soil material parallel and perpendicular to the root surface and the bending resistance of a root. If a root is small and flexible, it has been shown that the force and the resulting moment, M, due to bending is negligible (Wu, 1984; Jones, 1985).

Due to the displacements, a root force, F_r, develops inside the roots. An equation for this force is:

$$F_r = \sigma_a A_r \qquad (4.1)$$

A_r = cross sectional area of roots (m²)
σ_a = root stress (kPa)

This linear relationship is validated by Waldron (1977) for roots of herbaceous plants and by Wu (1976) for woody plants.

The root cross-sectional area A_r occurring in a given soil cross-sectional area, A, can be derived: from the number of roots n_i in a diameter class and its average cross-sectional area, a_i:

$$A_r = \Sigma\, n_i a_i \qquad (4.2)$$

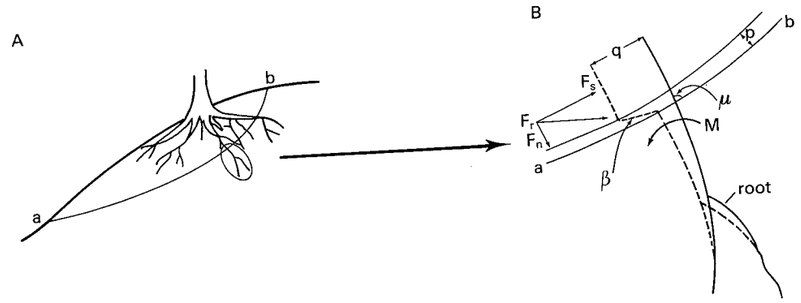

a-b	=	shear zone	
F_n	=	normal force	(N)
F_s	=	shear force	(N)
F_r	=	root force	(N)
β	=	angle between shear zone and root after displacement	(°)
μ	=	initial angle between shear zone and root	(°)
p	=	thickness of the shear zone	(m)
q	=	displacement of upper part	(m)
M	=	bending moment	(Nm)

Figure 4.1 Schematization of roots intersecting a shear zone (After Wu, 1984)

The root force, F_r, is resolved into a tangential component, F_s and in a normal component, F_n (figure 4.2). The tangential component produces an additional shearing resistance, while the normal component is added to the confining force on the shear zone intersecting a root zone.
The normal and tangential force components are:

$$F_s = F_r \cos\beta \text{ or } \tau_r = (A_r/A)\,\sigma_a \cos\beta \qquad (4.3a)$$
$$F_n = F_r \sin\beta \text{ or } \sigma_{nr} = (A_r/A)\,\sigma_a \sin\beta \qquad (4.3b)$$

A	=	cross-sectional area of shear zone	(m²)
A_r	=	cross-sectional area of roots	(m²)
σ_{nr}	=	normal stress on shear zone due to roots	(kPa)
τ_r	=	shear stress on shear zone due to roots	(kPa)

β	=	angle between shear zone and root after displacement	(°)
L	=	length of a root in the shear zone	(m)

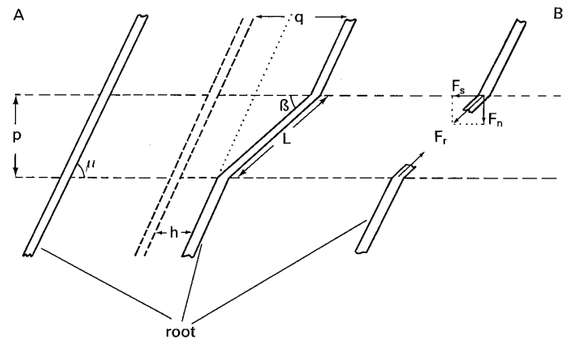

Figure 4.2 Forces acting on a root extending across a shear zone

Combination with the Coulomb Strength Law (equation 1.1) yields an expression for the shear strength of a root penetrated soil:

$$S_{rooted} = c + \tau_r + (\sigma_n + \sigma_{nr} - u) \tan \phi \qquad (4.4)$$

where:

σ_n	=	$\gamma.z$ = total normal stress	(kPa)
γ	=	unit weight	(kPa/m)
z	=	depth below the surface	(m)
S_{rooted}	=	shear strength root penetrated soil	(kPa)
c	=	cohesion	(kPa)
u	=	pore pressure	(kPa)
ϕ	=	angle of internal friction	(°)

The net effect of root reinforcement, S_r, is obtained by comparing the shear strength of a root penetrated soil with a root free soil:

$$S_r = S_{rooted} - S_{rootfree} = \tau_r + \sigma_{nr} \cdot \tan\phi = \sigma_a \cdot \left(\frac{Ar}{A}\right) \cdot (\sin\beta \cdot \tan\phi + \cos\beta) \qquad (4.5)$$

$$\beta = \tan^{-1} \frac{1}{\frac{(q-h)}{p} + \frac{1}{\tan\mu}} \qquad (4.6)$$

where:

S_r	=	root reinforcement	(kPa)
$S_{root\ free}$	=	shear strength of a root free soil	(kPa)
μ	=	initial angle between shear zone and root	(°)
p	=	thickness of the shear zone	(m)
(q-h)/p	=	shear strain	(-)
q	=	displacement of the upper soil mass	(m)
h	=	displacement of the root perpendicular to the root surface.	(m)

The influence on the root reinforcement of the initial angle of a root to the shear zone, S_r, is reflected in the factor ($\sin\beta \cdot \tan\phi + \cos\beta$) of equation 4.5. The factor depends on the shear strain, (q-h)/p, and the initial angle of the root to the shear zone, μ. Figure 4.3 shows this factor in relation to the shear strain (q-h)/p for different values of μ. The average of the factor ($\sin\beta \cdot \tan\phi + \cos\beta$) is calculated using 17 different values of initial angles, μ, with the shear zone. The initial angles ranging from 10° to 170° with the movement direction, at intervals of 10°. It is assumed that the average represents the situation of randomly oriented roots.
The factor ($\sin\beta \cdot \tan\phi + \cos\beta$) is sometimes simplified to 1.2 (Wu et al., 1979) or 1.15 (Greenway, 1987). As shown in figure 4.5, this factor depends strongly on the initial angle, μ, of the root to the shear zone. The assumption of Wu et al. (1974) and Greenway (1987) is an overestimation of this factor for small shear strains and may lead to erroneous estimations of the root reinforcement.
Figure 4.3 also shows that another simplification, β=0, i.e., the factor ($\sin\beta \cdot \tan\phi + \cos\beta$) equals 1 (Waldron and Dakessian, 1981), is valid at large shear strains. The contribution of roots to the root reinforcement, S_r, is in that case simply $\sigma_a \cdot (A_r/A)$ (see equation 4.5).

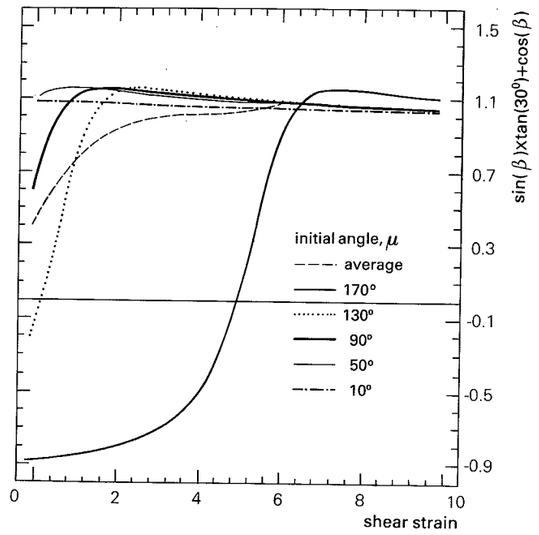

Figure 4.3 Plot of the factor ($\sin\beta \tan\phi + \cos\beta$) versus shear strain, (q-h)/p. $\phi = 30°$, β is given by equation 4.6.

A problematical parameter in equation 4.5 is the root stress, σ_a. What is its magnitude? What is the influence of the shear strain on the magnitude of the root stress? Is the root stress limited? Is a root capable to resist larger shear strains than a soil material before breaking? Most soils materials reach their peak strength at shear strains between 0.05 and 0.25 (Lee et al., 1983), while the ultimate strain before breaking of poplar and willow roots is about 0.16 (Hathaway and Penny, 1975). Two commonly used assumptions (Wu et al., 1979; Riestenberg and Sovonick-Dunford, 1983) are: (1) the root stress, σ_a, equals the rupture stress of the roots, and (2) the roots will break simultaneously.
These assumptions pay no attention to the influence of root elongation and soil deformation on the stresses in the shear zone, before the rupture stress of the roots is reached. This may lead to unrealistic situations as will be shown in the next paragraph, where a relation between root stress, friction between root and soil matrix and the elongation of a root due to displacements will be derived.

4.2.1 A relation between soil deformation and root stress

A root, which extends across a shear zone in a deforming soil, is elongated when a displacement takes place along this shear zone. This elongation, j, brings a root under stress. For simple uniaxial tension, the relationship between stress and elongation in the elastic range can be expressed as (Hook's law):

$$\sigma_a = E_r \frac{dj}{dx} \tag{4.7}$$

where:

σ_a	=	root stress	(kPa)
E_r	=	Young's modulus or elasticity modulus of a root	(kPa)
dj/dx	=	elongation of a root per length of a root	(-)

Assume a root as depicted in figure 4.2. The root extends across a shear zone of thickness p and is firmly anchored on both sides. If the upper mass of the soil is displaced over a distance, q, the elongation, j, of the root, with an initial angle of μ to the shear zone, will be:

$$j = L - \frac{p}{\sin\mu} = p\sqrt{\frac{2}{\tan\mu}\frac{q-h}{p} + \left(\frac{q-h}{p}\right)^2} \tag{4.8}$$

where:

$$j < 0 \quad if \quad \frac{2}{\tan\mu} + \frac{q-h}{p} < 0$$

$$j \geq 0 \quad if \quad \frac{2}{\tan\mu} + \frac{q-h}{p} \geq 0$$

where:

j	=	elongation of a root	(m)
L	=	length of a root in the shear zone	(m)
L^2	=	$(p/\tan\mu + q\text{-}h)^2 + p^2$	
μ	=	initial angle between shear zone and root	(°)
p	=	thickness of the shear zone	(m)
q	=	displacement of the upper soil mass	(m)
h	=	displacement of the root perpendicular to the root surface.	(m)

As shown in figure 4.4a and by equation 4.8, the elongation is negative, if $2/\tan\mu$ is smaller than the shear strain (q-h)/p. Therefore, roots with an initial orientation, μ, opposite to the direction of displacement, i.e $\mu > 90°$, will be in compression for small displacements. The average of the elongation was calculated using 17 different initial angles with the shear zone. The angle ranged from 10° to 170° with the movement direction and had an interval of 10°. As shown in figure 4.4b, an

enlargement of figure 4.4a, the average elongation is almost zero for shear strains less than 0.4. Because the elongation is almost equal to zero, the root stress is almost zero (equation 4.7), and therfore the root reinforcement will also be nearly zero (equation 4.6).
Figure 4.4 shows different elongations of roots, with a different initial angle, μ, to the shear zone, at the same displacement. The root stress is linearly related to the elongation of a root (equation 4.7). Therefore, the stresses in roots with different initial angles, μ, to the shear zone will not be the same at the same displacements. The roots will not reach simultaneously the rupture stress, as it is assumed by Wu et al. (1979) and Riestenberg and Sovonick-Dunford (1983).

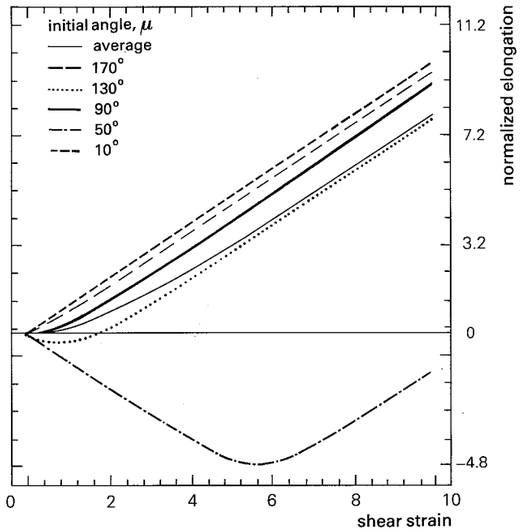

Figure 4.4a Simulations on basis of equation 4.8 of the dependence of normalized elongation on shear strain, (q-h)/p, as a function of different initial angles, μ, of the roots towards the shear zone. The normalized elongation is the ratio between the elongation of roots, j, and the thickness of the shear zone, p

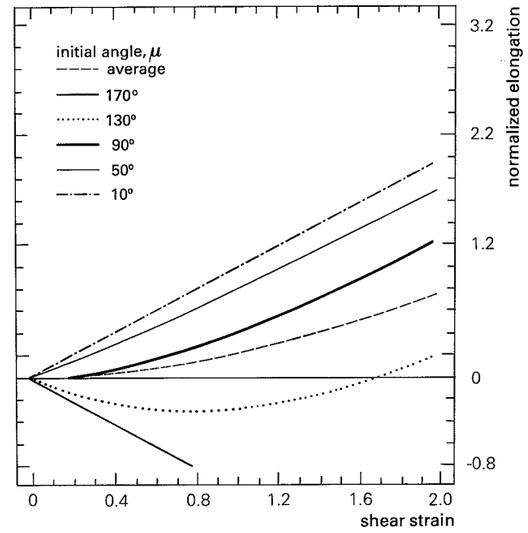

Figure 4.4b Enlargement of figure 4.4a

4.2.2 A relation between root-soil contact friction, root stress and root elongation

A root crossing a shear zone responses to a displacement along the shear zone either by elongation, breaking or slipping through a soil. The response of a root is determined by the anchorage of the root on both sides of the shear zone. The anchorage of a root in a soil is due to the friction that develops between a root and the soil material. This is the concept of reinforced earth as proposed by Vidal (1969). The friction stress is tangential to the root surface and develops as a reaction to the root elongation. Friction between root and the soil matrix can only develop when there is direct contact. Complete soil contact along the whole length of a root may be the exception rather than the rule (De Willigen and van Noordwijk, 1987). If a root has only over a fraction, CO, of his length a perfect contact, than the friction at the root-soil contact, B, has to be multiplied with CO to obtain the apparent friction, B', that is the friction stress measured in a pull-out experiment.
The following coordinate system is specified. An x-axis is defined with an origin at the shear zone. The x-axis is parallel to the principal length axis of the root. The values of x are increasing towards the end of the root. Under the assumption of equilibrium conditions for stresses in the x direction and a complete and perfect contact between root and soil, the following equation is obtained (Waldron, 1977; figure 4.6):

$$\pi r^2 \, d\sigma_a = 2\pi B r \, dx \quad \text{or} \quad r \, d\sigma_a = 2B \, dx \tag{4.9}$$

B = friction stress at the root-soil contact. (kPa)

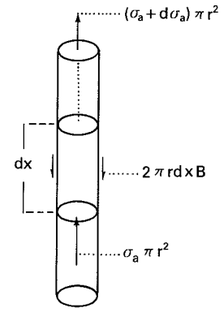

Figure 4.6 Cylindrical root section of radius, r, and length, dx, at equilibrium with root stress, σ_a, and tangential or friction stress, B. (after Waldron, 1977)

Under the assumption that B is independent of root stress and the place on a root, together with equation 4.9 yields (Waldron, 1977):

$$B = \frac{r}{2}\frac{d\sigma_a}{dx} = constant \tag{4.10}$$

Integration under the boundary conditions, x=0 and $\sigma_a=\sigma_0$, gives a relation between the root stress at x and root stress at the shear zone, σ_0:

$$\sigma_a(X) = 2B\frac{x}{r} + \sigma_0 \tag{4.11}$$

If the stress at the shear zone, σ_0, is known, than the distance along the root, x_0, before the root stress reaches zero, is given by:

$$x_0 = \frac{\sigma_0 r}{2B} \tag{4.12}$$

The elongation of a root gives rise to a stress with a maximum at the shear zone and decreasing to its end. The assumption (Waldron, 1977) of a symmetrical stress distribution around the shear zone implies a root length under stress, x_s, which is equally spread on both sides of the shear zone.

$$x_s = \frac{\sigma_0 r}{B} \tag{4.13}$$

x_s = length of root under stress (m)

In order to find an expression for the elongation of a root in relation to the friction stress at the root-soil contact and the elasticity modulus of a root, equation 4.11 and 4.7 can be combined to:

$$B = \frac{r}{2}\frac{d\sigma_a}{dx} = \frac{rE_r}{2}\frac{d^2j}{dx^2} \quad \vee \quad \frac{d^2j}{dx^2} = \frac{2B}{rE_r} \tag{4.14}$$

Integration under the conditions at x =0 of $\sigma_a=\sigma_0$ and at $x=x_0$ of $\sigma_a=0$, j =0, yields:

$$j(x) = \frac{B}{rE_r}x^2 + \frac{\sigma_0}{E_r}x + \frac{\sigma_0^2 r}{2BE_r} \tag{4.15}$$

j(x) = elongation of root at x (m)

The maximum stress of a root, σ_0, is found at the shear zone, x=0. A relation between the maximum stress in a root, σ_0 at x=0, with a radius of r, and the displacement, q, is obtained by combining equations 4.15 and 4.8:

$$\sigma_0^2 = \frac{2E_r Bj}{r} \tag{4.16}$$

$$j = p\sqrt{\frac{2}{\tan\mu}\frac{q-h}{p} + \left(\frac{q-h}{p}\right)^2}$$

$$\sigma_0 < 0 \text{ if } \frac{2}{\tan\mu} + \frac{q-h}{p} < 0$$

$$\sigma_0 \geq 0 \text{ if } \frac{2}{\tan\mu} + \frac{q-h}{p} \geq 0$$

4.2.3 Limitations to the root stress

The stresses inside a root are limited to a maximum by two factors: (1) the anchorage of a root in the soil is not sufficient, i.e. a root starts to slip through the soil, and (2) the root strength itself is limiting the stress that can be applied on a root, i.e. a root breaks.
When shearing of a soil causes roots to slip through the soil, they continue to contribute to the root reinforcement. The friction stress, B, on the roots is the resistance of a root against direct sliding. The tension in a root will be:

$$\sigma_0 = x_b \frac{B}{r} \tag{4.17}$$

x_b = length of root with a diameter of r slipping through the soil (m)

Roots do not contribute to the shear strength if they are broken at the shear zone. A root breaks when its stress due to the elongation is larger than its rupture stress, $\sigma_{r\,m}$. The magnitude of the rupture stress will be discussed in paragraph 4.3.5.
The length, x_f, required to mobilize the rupture stress, $\sigma_{r\,m}$, in a root of diameter r is obtained (equation 4.13):

$$\sigma_{rm} = x_f \frac{B}{r} \tag{4.18}$$

Let x be the actual root length. If $x > x_f$, the root can be broken.
Combining the effect of root stress, σ_a, on the shear strength of a soil (equation 4.5) and a relation between root stress, root diameter, r, and displacement (equation 4.16) yields a relation for the root reinforcement, S_r, omitting the index i for the different root diameter classes:

for stretching roots:

$$S_r = \sum \sqrt{\left|\frac{2E_r Bj}{r}\right|}\left(\frac{na}{A}\right)(\sin\beta\tan\phi+\cos\beta) \tag{4.19}$$

where :

$$j = p\sqrt{\frac{2}{\tan\mu}\frac{q-h}{p}+\left(\frac{q-h}{p}\right)^2}$$

$$\sqrt{\left|\frac{2E_r Bj}{r}\right|} < 0 \text{ if } \frac{2}{\tan\mu}+\frac{q-h}{p} < 0$$

$$\sqrt{\left|\frac{2E_r Bj}{r}\right|} \geq 0 \text{ if } \frac{2}{\tan\mu}+\frac{q-h}{p} \geq 0$$

$$\beta = \tan^{-1}\left(\frac{1}{\frac{q-h}{p}+\frac{1}{\tan\mu}}\right)$$

for slipping roots:

$$S_r = \sum \left(\frac{x_b na}{A_r}\right)(\sin\beta\tan\phi+\cos\beta) \tag{4.20}$$

after breaking of the roots:

$$S_r = 0 \tag{4.21}$$

where:

j	=	elongation of a root	(m)
μ	=	initial angle between shear zone and root	(°)
p	=	thickness of the shear zone	(m)
q	=	displacement of the upper soil mass	(m)
h	=	displacement of the root perpendicular to the root surface.	(m)
E_r	=	Young's modulus or elasticity modulus of a root	(kPa)
B	=	friction stress at the root-soil contact.	(kPa)
x_f	=	length of a root needed to break	(m)
x_s	=	length of the root under stress	(m)
x_b	=	length of root with a diameter of r slipping through the soil	(m)
x	=	actual length of root	(m)
σ_0	=	maximum stress in a root	(kPa)
$\sigma_{r\,m}$	=	rupture stress of a root	(kPa)
n	=	number of roots in different diameter classes	
A	=	cross sectional area of shear zone	(m^2)
A_r	=	cross sectional area of roots	(m^2)
a	=	average cross sectional of roots per diameter class	

The equations are essential the same as those of Waldron (1977). The major difference is the inclusion of the effect of the initial angle of a root towards the shear zone.
The calculation of the root reinforcement, S_r, is as follows:
For $\sigma_0 < \sigma_{rm}$ and $x_s < x$, equation 4.19 is used.
For $\sigma_0 >= \sigma_{rm}$, rupture will take place at the shear zone (place of maximum stress) and the root does not contribute anymore to the root reinforcement, $S_r=0$.
For $x < x_s < x_f$, a root start to slip and the root reinforcement is calculated using equation 4.20.
The model presented in the equations 4.19, 4.20 and 4.21 is validated using data presented in Waldron et al. (1983; see table 4.1). A plot of the measured values of the root reinforcement, S_r, and displacement shows a gradual increase (figure 4.6; line labelled 'experiment'). Waldron et al. (1983) claim that this curve can be produced using a model based on equations 4.19 to 4.21, in which it is assumed that the initial angle, μ, of all roots towards the movement direction is 90°. However, simulations with the same data set and putting μ=90° in the model reveal a different curve (line labeled 'Profile 1' in figure 4.6). The predicted root reinforcement rises to certain level and remains constant. Another simulation may be executed in which S_r is calculated for different angle of μ and the values of S_r are averaged (curve 'average' in figure 4.6). This simulation gives a continuing upward trend and follows the experiment curve more closely. Apparently an average of S_r, which is based on the S_r of roots with different initial angle, μ, to the shear zone, gives a good approximation of the observed root reinforcement with increasing displacement of randomly oriented roots.
The sensitivity of the model to parameters, fictions stress at the root-soil contact, B, the elastic modulus, E_r, and the rupture stress, will be considered in more detail in the next paragraphs.

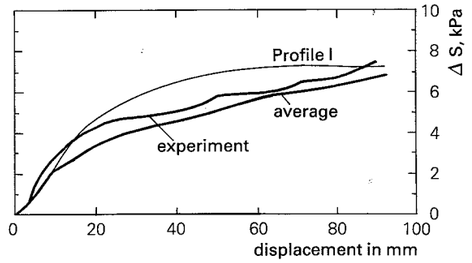

Figure 4.6 A plot of experimental measurement of the root strength increase, S_r, and prediction of the model presented in Waldron et al. (1983) and the model presented in this study.

Table 4.1 Soil and vegetation data of the shear displacement experiment by Waldron et al. (1983)

depth of shearing: 60 cm
angle of internal friction, ϕ: 38°
material: clay loam (11% sand, 41% silt, 48% clay)
bulk density : 1000 Kg/m^3
plants: *Pinus ponderosa*
elasticity modulus : $141 \cdot 10^5\ d^{-0.389}$ (kPa)
rupture stress : $8.820 \cdot 10^3\ d^{-0.116}$ (kPa)
d = diameter of the root (mm)
thickness shear zone : 2 cm

Pine root distribution at the shear plane.

root diameter, mm		number of roots
1		473
2		195
3		40
4		20
5		7
6		3
7		3
8		0
9		0
10		0
15		1
	total	742

$A_r/A = 2.06\ 10^3$

4.2.4 Limitations to the friction stress at a root-soil contact

The root stress is a basic parameter in explaining the higher values of the shear strength of a root penetrated soil compared to a root free soil. Root elongation causes the root stress. A root can only elongate, if it is firmly anchored in a soil. In the concept of Waldron and Dakessian (1981) and Wu (1984) stresses in the soil are transferred to the root by friction at the root-soil contact. They assume that the normal stress acting on the root-soil contact is due to overburden stress of the soil. A root will break if the friction between soil and root is large enough. The interaction mechanism between soil and root in sliding is shown in figure 4.7, under the assumption that a soil exerts a stress on a root.

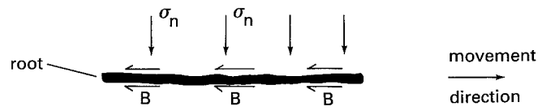

Figure 4.7 Interaction between a root and soil in direct sliding. Stresses in the soil are transfered by friction to a root.

The root-soil contact obeys the Coulomb friction-cohesion strength law (Milligan and Palmeira, 1987). The friction stress, B_f, increases linearly with the normal stress applied to the failure plane, which is parallel to the root surface. A variation to Coulomb's strength law for the friction at a root-soil contact is proposed by McKyes, 1985:

$$B_f = C_a + \sigma_n \cdot \tan\delta = C_a + \sigma_n \cdot R \cdot \tan\phi \qquad (4.22)$$

B_f	=	shear stress along the root-soil contact due to direct sliding	(kPa)
C_a	=	soil to root adhesion strength, independent of normal stress	(kPa)
σ_n	=	stress normal to shear zone	(kPa)
δ	=	root-soil contact friction angle	(°)
R	=	ratio of root-soil contact friction angle to soil friction angle	(-)
ϕ	=	angle of internal friction of the soil	(°)

The assumption of an equal shear strength of the root-soil contact and shear strength of the soil, means that R=1.
Assume a coefficient of friction of about 0.5 ($\phi \approx 30°$) and a overburden stress normal to the root surface. The use of equation 4.22 results in an estimation of the friction stress at the root-soil contact, B_f, of less than 4 kPa for a soil depth of less than 50 cm. This value may be compared with field data. Waldron (1977) estimated the friction of alfalfa roots in coarse gravel-sand mixture to be 40 kPa. Waldron and Dakessian (1981) gave a friction of about 2.5 kPa for barley and pine roots in a saturated clay loam. Stolzy and Barley (1968) measured the pull out resistance of single roots of field pea (*Pisum sativum*) that had penetrated a few millimeters into a compacted clay loam with a bulk density of 1.7 g/cm^3 at a matrix potential of -0.3 bar. They found values of about 10 kPa in absence of root hairs, and where root hairs extended into the dense unsaturated soil, the values ranged between 30-60 kPa.
So it appears that in field situations much higher values for the friction at the soil-root contact are found with a mean of 40 kPa. These values can hardly be explained with a friction generated by overburden stress alone (Waldron and Dakessian, 1981). The values of the friction calculated under the assumption of the soil exerting stresses on a

root (equation 4.22) seems especially low if one considers the fact that the calculation also assume a complete and perfect contact between the root and soil. If there is only a complete and perfect contact over a fraction of the root, CO, the calculated friction has to be multiplied with CO.
In the following paragraphs two mechanisms for higher friction stresses at the root-soil contact will be discussed. The difference with the concept of Waldron (1977) and Waldron and Dakessian (1981) is that in this case not the soil is exerting a stress on a root, but oppositely a root is exerting a stress on the soil. The stress in a root is transferred to the soil by friction. This friction stress on a soil may cause the soil to fail at a certain distance from the root. The first of the two mechanisms is considering a stress exerted by a root in a direction perpendicular to the root surface onto the soil. The second addresses to a stress applied by a root parallel to the root surface onto the soil.

4.2.4.1 Stresses exerted on the soil by a root perpendicular to its surface

If a root is firmly anchored in the soil, elongation of the root will make it to straighten. This straightening results in a root cutting through the soil. Assume the stress situation at the root-soil contact is analogous to a plough. McKyes (1985) proposed a model, which describes the movement of a soil and the stresses involved, when a plough cuts through a soil. The mechanisms taken into consideration are derived from the mechanics of deep foundation failure and are depicted in figure 4.8. Mckyes (1985) postulates that a vertical soil wedge is developed in front of the root, perpendicular to the direction of movement (figure 4.8b). The soil wedge has an included angle of $\phi=45°+\phi/2$. The soil fails to the sides of the root along planes in the form of logarithmic spirals with a limiting angle of α (figure 4.8b). The value of α differs for various practical applications. Several values of α mentioned in literature are: $\alpha = \phi$ (McKyes, 1985; agricultural equipment), $\alpha = 0$ (Craig, 1987; bearing capacity), α varies between 0 and $-\pi/4 + \phi/2$ (Milligan and Palmeira, 1987; stabilization of a slope by geotextile).
Outside the log spiral wedge acts the earth stress at rest, $P_0 = \gamma z(1-\sin\phi)$ (Craig, 1987). According to McKyes (1985) the stress, P_r, acting on the root face can be calculated with:

$$P_r = c\frac{(N_q - 1)}{\tan\phi} + P_o N_q \qquad (4.23)$$

where:

$$N_q = \tan^2\left(\frac{\phi}{2} + \frac{\pi}{4}\right) e^{(\pi + 2\alpha)\tan\phi}$$

c	=	cohesion	(kPa)
ϕ	=	angle of internal friction	(°)
α	=	limiting angle of the logarithmic spiral planes	(°)

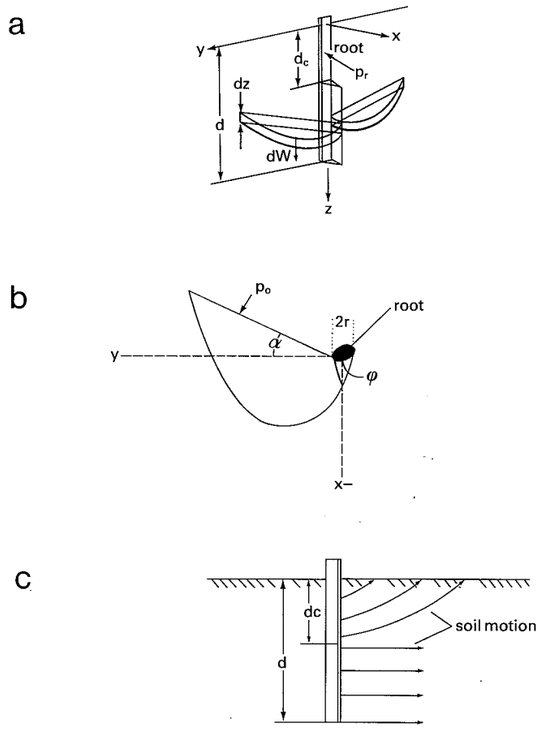

Figure 4.8 A mechanism for soil failure on a horizontal plane around a root below the critical depth due to a movement perpendicular to the root surface (adapted from McKyes, 1985)

If a root makes an angle ϵ with the horizontal, a correction has to be made. P_r is multiplied by sin ϵ, to correct for the angle, ϵ. Because P_r is due to movement perpendicular to the root surface, it is the normal stress to the root surface. Therefore the Coulomb friction law is rewritten to give a friction stress, B_b, at the root-soil contact due to perpendicular movement:

$$B_b = c+P_r \cdot R \cdot \tan\phi \cdot \sin\epsilon \quad \text{or} \quad B_b = c+N_q \cdot (c+P_o \cdot R \cdot \tan\phi) \cdot \sin\epsilon \qquad (4.24)$$

The model of Mckyes is only valid if the soil moves in a horizontal plane around the root. Above a certain critical depth, d_c, the soil is lifted upwards to the soil surface (Figure 4.8 a, c). Below this critical depth it requires less energy to compress the soil

and to move it horizontally around the root, than to slide the soil towards the surface. Experimental evidence of the critical depth phenomenon indicates that the ratio of critical depth to tool width (critical depth ratio) varies over a wide range and depends upon the consistency of the soil (Mckyes, 1985). For most soils the critical depth ratio seems to be less than 20 (McKyes, 1985). If the findings of Mckyes are applied to our problem, it appears that most roots grow below the critical depth. The assumption of a soil being compressed and moving around a root and not moving upwards seems reasonable.

4.2.4.2 Stresses exerted on the soil by a root,parallel to its surface

Let us assume: a friction stress, B_p, is generated at the root-soil contact by an elongation of a root along its longest axis.The root exerts a stress on the soil and there is perfect contact between the root and soil along the total root length. Under these assumptions, it is possible to establish a relation between the principal stresses and the direction of displacement.
If a root is exerting stress on a soil, than the major principal stress, σ_1, is parallel to the root surface. Because of the assumed stress equilibrium it is equal but opposite of sign to the friction stress. The angle between root and the horizontal, ϵ, is also the angle between the major principal stress and the horizontal.

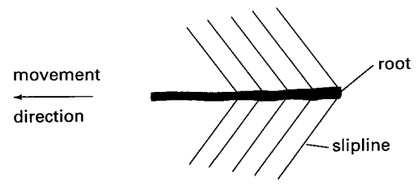

Figure 4.9 Slip lines due to a movement along the longest axis of the root (after Jones, 1985)

The assumption of a major principal stress parallel to the root surface implies, that if failure occurs, the failure plane makes an angle, δ_f, to the surface of a root. The angle of the failure plane relative to the major principal stress, σ_1, plane can be calculated with (McKyes, 1985):

$$\delta_f = 45° + \phi/2 \qquad (4.25)$$

The proposed stress situation results in a slip line patron as depicted in figure 4.9. Similar slip lines have been found in experiments where a fibre is pulled out of a glass plate (Jones, 1985).
The Mohr circle of stresses together with Coulomb strength law and equation 4.25, makes it possible to give a relation between the major, σ_1, and the minor, σ_3, principal stress (Craig, 1987).

$$\sigma_1 = \sigma_3.K_a^2 - 2.c.K_a \qquad (4.26)$$

K_a = $\tan(45° - \phi/2)$
c = cohesion (kPa)

If the angle ϵ between the major principal stress and the horizontal plane is known, together with σ_1 and σ_3, the following relation with the overburden stress, σ_z, is obtained (Scott, 1963):

$$\sigma_z = \sigma_1.\sin^2\epsilon + \sigma_3.\cos^2\epsilon \qquad (4.27)$$

From equation 4.26 and 4.27 it follows that the friction stress, B_p, at the root-soil contact is given by:

$$-B_p = \sigma_1 = \frac{\sigma_z + 2cK_a\cos^2\epsilon}{\sin^2\epsilon + K_a^2\cos^2\epsilon} \qquad (4.28)$$

4.2.4.3 Results of simulations of friction stresses at the root-soil contact

Table 4.2 presents different friction stresses: B_f, B_b and B_p, where B_f is based on the assumption of a soil exerting stress on a root (equation 4.22), B_b is based on the assumption of a stress exerted by a root perpendicular to its surface (equation 4.24) and B_p is based on a stress exerted by a root parallel to its surface (equation 4.28). The listed values of the friction stress are maximum estimates, due to the assumptions of a complete and perfect root-soil contact, CO=1, and of the same strength characteristics for soil and root-soil contact, R=1. According to De Willigen and Van Noordwijk (1987) a complete contact between soil and root is rather an exception than a rule. McKyes (1985) has estimated that the ratio between the friction angle of the soil plough contact and the soil friction angle to range from 0.4 to 1.

Table 4.2 Calculated values for friction stress (kPa)

depth=40 cm
cohesion = 10 kPa

ϵ	B_f	B_p	B_b
0°	13.66	50.73	92.28
10°	13.97	47.68	91.03
20°	14.16	40.18	87.32
30°	14.23	31.39	81.25
40°	14.16	23.53	73.03
50°	13.97	17.38	62.89
60°	13.66	12.96	51.14
70°	13.24	10.04	38.14
80°	12.72	8.38	24.29
90°	12.11	7.85	10.00

depth=40 cm
Cohesion = 0 kPa

ϵ	B_f	B_p	B_b
0°	3.66	19.34	14.35
10°	3.97	18.52	14.13
20°	4.16	16.51	13.49
30°	4.23	14.16	12.43
40°	4.16	12.05	10.99
50°	3.97	10.40	9.23
60°	3.66	9.22	7.18
70°	3.24	8.43	4.91
80°	2.72	7.99	2.49
90°	2.11	7.85	0.00

ϵ = 40°
cohesion = 10 kPa

depth (cm)	B_f	B_p	B_b
10	11.04	14.49	64.78
20	12.08	17.50	67.53
30	13.12	20.52	70.28
40	14.16	23.53	73.03
50	15.20	26.54	75.78
60	16.24	29.55	78.53
70	17.28	32.56	81.27
80	18.32	35.58	84.02
90	19.36	38.59	86.77

ϵ = 40°
cohesion = 0 kPa

depth (cm)	B_f	B_p	B_b
10	1.04	3.01	2.75
20	2.08	6.02	5.50
30	3.12	9.04	8.25
40	4.16	12.05	10.99
50	5.20	15.06	13.74
60	6.24	18.07	16.49
70	7.28	21.09	19.24
80	8.32	24.10	21.99
90	9.36	27.11	24.74

Assumptions:
complete contact between root and soil, CO=1.
the root-soil interface has the same strength characteristics as the soil, R=1.

with :
ϕ = 25°, angle of internal friction
α = 0°, limiting angle of the logarithmic spiral planes
γ = 18.2 kPa/m, unit weight
ϵ = angle of root to the plane parallel to the soil surface (°)
B_f = friction stress due to overburden pressure (kPa)
B_p = friction stress due to parallel movement (kPa)
B_b = friction stress due to perpendicular movement (kPa)

Table 4.2 reveals that the friction stress is strongly influenced by the cohesion of the root-soil contact. Only the mechanisms, where a root exerts stress on the soil, gave friction stresses, B_p and/or B_b, high enough to explain values of 40 kPa as found in field situations.
A realistic estimation of the friction stress between root and soil is still not feasible. The parameters, like R, CO, P_o and α, describing the stresses and the strength characteristics at the root-soil contact are difficult to quantify. But the mechanisms based on the assumption of a root exerting stress on a soil are explaining the high values of the friction stress mentioned in the literature.
The influence of the friction stress, B, on the root reinforcement, S_r, is shown in figure 4.10. The experimental results of Waldron et al. (1983) are also plotted in this figure. The simulations were done using equation 4.19, 4.20, 4.21 for different initial angles to the shear zone and the data presented in table 4.1. The results of the different angles were averaged. A friction stress of 6.4 kPa gave a good approximation of the line. The value of 6.4 kPa was obtained by trial and error.With increasing displacements all roots within the successive diameter classes break, causing an irregular rise of the curve.

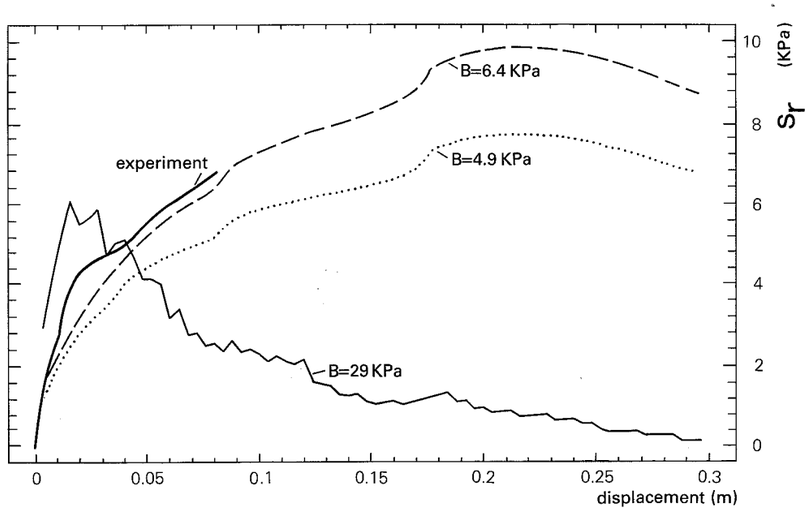

Figure 4.10 Simulations on basis of the equations 4.19, 4.20 and 4.21 of the dependence of the average root reinforcement, S_r, on the displacements as function of the friction stress, B (kPa)

Roots will break under high values of friction stress, B. At smaller displacements and with higher values of B, the increase in root reinforcement, S_r, is larger, but the overall maximum S_r is less compared to soils with only slipping roots (low values of B). The friction stress dictates at what displacements the maximum S_r is reached.

In the figures 4.8 and 4.9 the results of simulations of the root reinforcement, S_r, are shown in relation to the initial angle of the root to the shear zone, μ, while the friction stress is kept constant.
Figure 4.11 depicts the results of simulations using the data presented in table 4.1 and under the assumption of a friction stress at the root-soil contact of 6.4 kPa. Figure 4.11 is an example of root reinforcement due to slipping and stretching of roots. As long as the roots are mostly slipping, i.e. at small friction stresses, the simulated average increase in Sr is: (1) a little smaller than the root reinforcement due to roots at an angle of 90° to movement direction and (2) identical to results obtained using the average root reinforcement due to roots with different initial angles at the shear zone (figure 4.11).
These results are in agreement with the tests of Gray and Ohashi (1983) and Freitag (1986), showing that roots/fibers perpendicular to the shear zone provide a reinforcement, comparable to randomly oriented roots. This indicates that in their tests they may have had slipping roots/fibers.

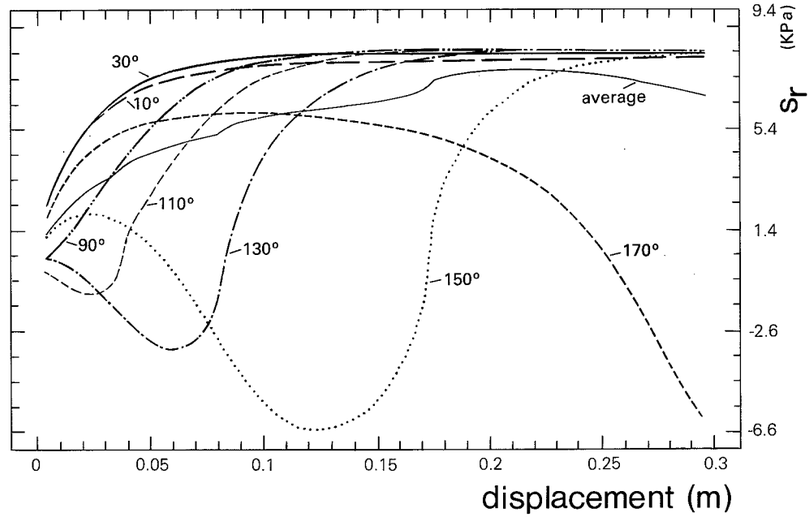

Figure 4.11 Simulations, based on the equations 4.19, 4.20 and 4.21, of the dependence of the root reinforcement, S_r, on the displacement as a function of μ, the initial angle of the root to the shear zone. The friction stress, B, is assumed to be 6.4 kPa.

Figure 4.12 depicts the results of simulations using the data presented in table 4.1 and under the assumption of a friction stress at the root-soil contact of 29.0 kPa. Figure 4.12 is an example of breaking and stretching roots. When roots are breaking, the simulated increase of S_r with increasing displacements is much higher for roots at an angle of 90° to movement direction than the average increase in S_r (figure 4.12).

Some of the simulations show a decrease in root reinforcement, S_r, in abrupt steps as roots in the successive root diameter classes were ruptured.
A distinct feature of figure 4.11 and 4.12 is a negative S_r for roots with an initial angle, μ, larger than 90° to the displacement direction, during one stage of the displacement. These roots are decreasing the strength of the soil. It should be noted that an initial angle, μ, larger than 90° to the displacement direction is not identical to a negative S_r. For a certain displacement both the root stress as the factor ($\sin\beta \tan\phi + \cos\beta$) are negative and therefore the resulting S_r is positive, see for example the curve of a root with an initial angle of 170° towards the shear zone in figure 4.11. Furthermore, it shows the influence of the initial angle of a root to the shear zone on the resulting root reinforcement. The peak strength for each initial angle of a root to movement direction is at another displacement. It will be clear that the inclusion of the initial angle of the root to the movement direction is essential when modelling the root reinforcement.
One of the parameters that might influence the friction stress, B, and therefore the root reinforcement, S_r, is the contact area between root and soil. CO is defined as the ratio between the total root surface and the root surface where the root makes contact with the soil. A CO value of 1 indicates complete and perfect contact. Figure 4.13 shows the influence this ratio CO. CO influences the magnitude of S_r, but not at what displacement /shear strains it is reached.

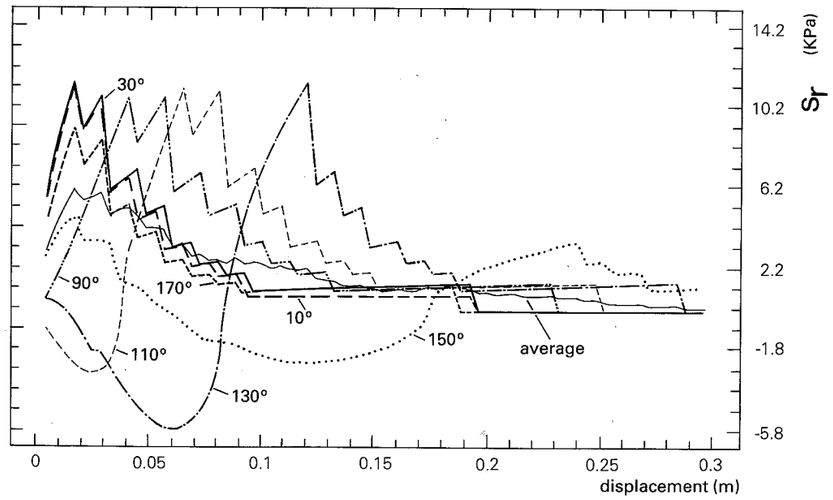

Figure 4.12 Simulations on basis of the equations 4.19, 4.20 and 4.21 of the dependence of the root reinforcement, S_r, on the displacement as a function of μ, the initial angle of the root to the shear zone. The friction stress, B, is assumed to be 29.0 kPa.

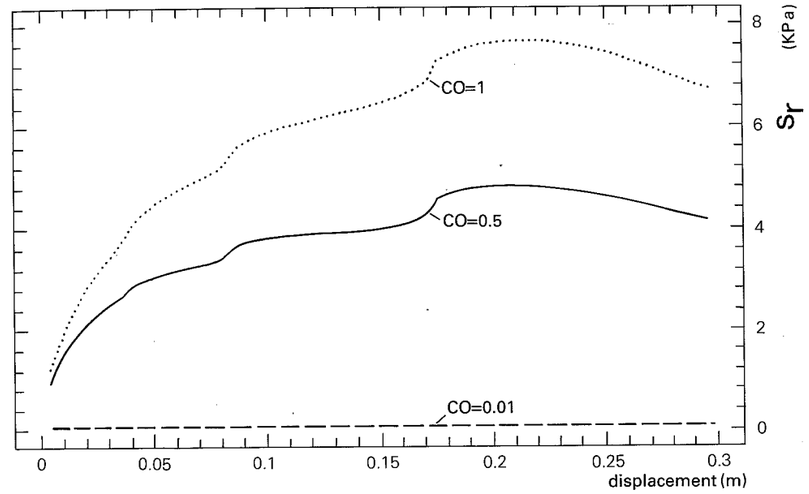

Figure 4.13 Simulations on basis of the equations 4.19, 4.20 and 4.21 of the dependence of the average root reinforcement, S_r, on the displacements as function of the contact area root-soil, CO.(B = 4.9 kPa)

4.2.5 Rupture of roots

In paragraph 4.2.4 the different concepts of friction stresses at the root-soil contacts and the effect on the reinforcement of the roots, S_r, in relation to deformation, were investigated. A second important parameter in the root reinforcement model is the rupture stress, $\sigma_{r\,m}$, of the roots. The rupture stress of a root has great influence on the root reinforcement, because it determines whether a root breaks or slips through the soil.
Imagine a shear zone, which intersects a root zone (figure 4.1a). As reaction to a displacement along a-b, the roots crossing the shear zone, start to stretch. The elongation of the roots continues until the root stress exceeds the rupture stress, or until the frictional force on the root-soil contact is less than the force applied on the root. A root is either in tension or compression when the applied force acts in the principal length direction of the root.
The variation in rupture stress of roots is considerable, both between and within species. In absolute values, the rupture stress of roots, $\sigma_{r\,m}$, appears to range from 6 to 100 MPa (Lee, 1985).
The rupture stress of a root, $\sigma_{r\,m}$, seems to depend on the structural and chemical characteristics of roots, governed by environmental factors (Hathaway and Penny,

1975; Greenway, 1987). Schiechtl (1980, 1973) demonstrated that roots, extending uphill, were stronger than those extending downhill. Burroughs and Thomas (1977) found that Douglas Fir roots in the Coastal Range (USA) are 4 times stronger than those from the Rocky Mountains (USA). Hathaway and Penny (1975) reported a seasonal fluctuation in rupture stress within poplar and willow roots, due to variations in specific gravity and lignin/cellulose ratio.

Estimation of the rupture stress

The rupture stress of *Pinus sylvestris* roots, gathered at plot 1, have been determined by using an unconfined uniaxial extension test, with an apparatus as depicted in figure 4.14. The roots are on both ends embedded in gypsum. Prior to the testing the gypsum is hardened, approximately 12 hours. The hardening is executed under water to prevent desiccation of the root. After the hardening the root is placed between the weigh-beam and cog-wheel. Stress is applied to the root by slowly turning the cog-wheel.
The method has some drawbacks. Some of the roots were broken because the gypsum was cutting the root, or the root was pulled out of its bark without breaking. Furthermore, it was impossible to measure the strength of small roots.They were already broken, due to the weight of the gypsum.
The results of 11 tests are shown in figure 4.15. The data indicate a rupture stress of 6.91 MPa.
Several papers suggest a decrease in rupture stress of the roots with increasing root diameter (Greenway, 1987; Turmanina, 1965; Burroughs and Thomas, 1977; Waldron and Dakessian, 1981; Tsukamoto and Minematsu, 1987). However, figure 4.15 does not show such a relationship. Hathaway and Penny (1975) and Ziemer and Swanston (1977) also found a rupture stress, independent of the root diameter.

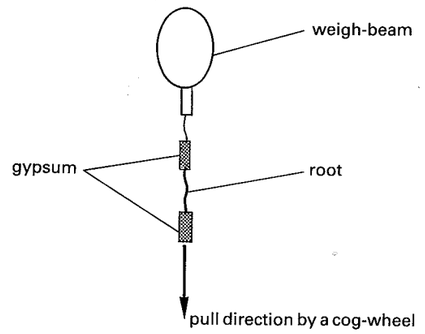

Figure 4.14 Tester for rupture stress of roots

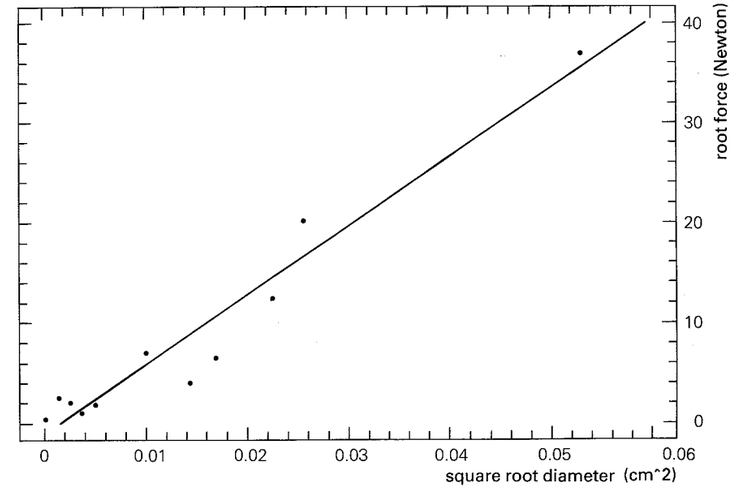

Figure 4.15 Relationship between force (N), needed to break the root and its squared root diameter (cm²)

Equation 4.8 (paragraph 4.3.3), which gives a relation between rupture stress, σ_{rm}, friction stress, B, and the minimum length of root, x_f, with a certain radius, r, needed to break the root, is used to answer the question: will a root break or slip though the soil. The equation is based on a stress equilibrium and given by:

$$\sigma_{rm} = B\frac{x_f}{r} \qquad (4.18)$$

A minimum value for the rupture stress of roots seems to be about 6 MPa (Lee, 1985). Assume furthermore that friction stress at the root-soil contact, B, is about 40 kPa (par. 4.3.4). This would result in a x_f/r of about 150. The ratio between x_f and r is about 2-5 for small roots (Lyford, 1975). It is expected that the smaller roots **never break** and only slip. This is in line with the conclusions of Waldron and Dakessian (1981), who found that root slippage, rather than breakage, may be the prevailing process, limiting root reinforcement of saturated, fine textured, soils.

4.2.6 Elastic modulus of a root

A third important parameter in the root reinforcement model is the elastic modulus, E_r. The elastic modulus determines the root stress at a certain elongation of a root (equation 4.6) and therefore the root reinforcement, S_r.
The elastic modulus, E_r, shows a wide variation between and within plant species (Whiteley and Dexter, 1981; Hathaway and Penny, 1975; Waldron and Dakessian 1981). Environmental factors, such as water potential and plant nutrition seem to have a significant influence on the elastic behavior of roots. Whiteley and Dexter (1981), in a study with 16 field crops, investigated the effects of nitrate concentration and water potential on the magnitude and linearity of the elastic moduli. They found, that differences in mechanical properties of roots were in general greater than the differences, observed between different plant species. However, no simple relation was found between the magnitude of either of these factors and the resultant modulus. Furthermore, the elastic modulus depends on chemical (cellulose and lignin content) and structural differences of the root tissue (Hathaway and Penny, 1975; Whiteley and Dexter, 1981). In absolute values E_r seems to range from 1 to 130 MPa (see table 4.3).
As shown in figure 4.16 variation in the elastic modulus of the roots influences the magnitude of the root reinforcement.

Table 4.3 Elastic modulus, E_r (MPa), for several plants

plant	E_r	reference
Poplar	8.7 - 16.4	Hathaway and Penny (1975)
Willow	10.8 - 15.8	Hathaway and Penny (1975)
Pinus ponderosa	141 - 100	Waldron et al. (1983)
Barley	24	Dexter and Hewitt (1978)
Lucerne	22	Dexter and Hewitt (1978)
Barrel	36	Dexter and Hewitt (1978)
Oats	97	Dexter and Hewitt (1978)
Pea	21	Dexter and Hewitt (1978)
Rye	17	Dexter and Hewitt (1978)
Soy Bean	57	Dexter and Hewitt (1978)
Triticale	61	Dexter and Hewitt (1978)
Wheat	45	Dexter and Hewitt (1978)

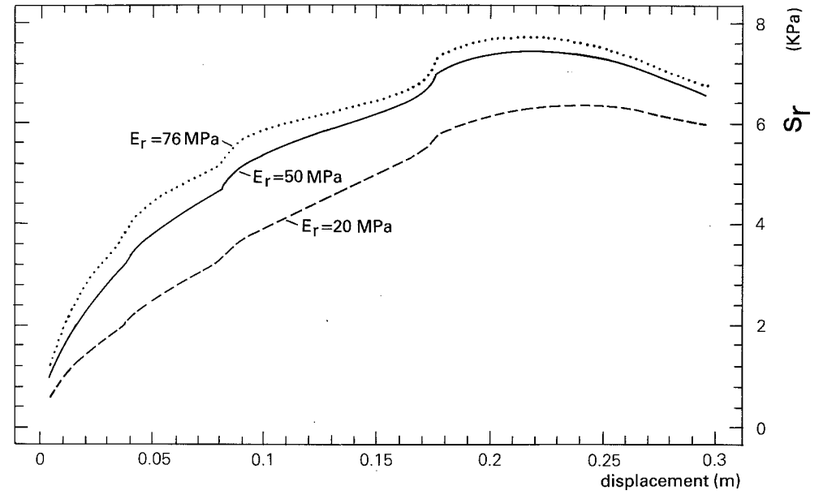

Figure 4.16 Simulations on basis of the equations 4.19, 4.20 and 4.21 of the dependence of the root reinforcement, S_r, on the displacement as a function of the elastic modulus, E_r. The friction stress, B, is assumed to be 4.9 kPa.

4.3 Conclusions and summary

The processes causing the reinforcement of the soil by roots are not well understood. Experimental data are scarce, sometimes conflicting and not always conclusive. To assess the mechanical effect of roots on the strength characteristics in a limit equilibrium analysis, is the purpose of this chapter. This led to the development of a model.
The model is based on the following concept of the processes involved. Due to a displacement along a shear zone, a root, which crosses the shear zone, will elongate. This elongation generates a stress inside the root. This root stress gives rise to additional stresses in the shear zone. The root stress is transferred to the soil by a friction stress at the root-soil contact. The friction stress at the root-soil contact causes the anchorage of a root in the soil. The total force, that can be applied to a root is limited either by breaking of the root, or slipping of the root through the soil.
The model is formulated by equation 4.19, 4.20 and 4.21 and needs as input variables: initial angle between the root and the shear zone, μ, the displacement along the shear zone, q, the elastic modulus of roots, E_r, the rupture stress of root, $\sigma_{r\,m}$, a friction stress, B, at the root-soil contact, and the cross sectional area of roots per cross sectional area soil.
A basic assumption of this model is, that the friction is independent of the root stress and the place on the root.

The model was validated against the well documented experiments of Waldron et al. (1983). It appeared, that averaged root reinforcement of the soil due to roots with different initial angles to the shear zone is in good agreement with the data of Waldron et al. (1983; see figure 4.6)
The following tentative conclusions and remarks result form the analyses:
- The average elongation of randomly oriented roots crossing a shear zone remains aproximately zero, upto a shear strain of 0.4. This shows that roots are contributing to the shear strength of a soil only at shear strains larger than 0.4. At these shear strains, most soils are already at their residual strength (Lee et al., 1983). Therefore, the mechanical effects of roots increase the residual strength of a soil, i.e. roots make a soil less brittle. This also explains why no relationship was found between root content and the strength characteristics of a soil (paragraph 3.3.3). Shear strains beyond 0.4 are hardly reached on small samples, i.e. conventional direct shearing and unconfined compression shear tests are unsuitable in estimating the effects of roots on the peak strength.
- A limit equilibrium analysis is based on the assumption of static equilibrium, i.e. no movement takes place. Root reinforement of a soil only starts after displacements have taken place. Thus root reinforcement needs no consideration in a limit equilibrium analysis.
- The elongations of roots, with different initial angles, μ, to the shear zone, vary for a given displacement (figure 4.4). The root stress is linearly related to the elongation of a root (equation 4.6). Therefore, the stresses inside roots with different initial angles, μ, to the shear zone will vary at any displacement. The roots will not simultaneously reach the rupture stress, as is assumed by Wu et al. (1979) and Riestenberg and Sovonick-Dunford (1983).
- A realistic estimation of the friction stress between root and soil is still not feasible. The parameters, like R, CO, P_o and α, describing stresses at and strength characteristics of the root-soil contact, are difficult to quantify. Two proposed mechanisms, however, related to roots exerting stress on a soil, explain the high values of the friction stress, as mentioned in literature.
- Roots will break under higher values of friction stress, B at the root-soil contact. At smaller displacements and with higher values of B, the increase in root reinforcement, S_r, is larger, but overall maximum S_r is less, compared to soils with only slipping roots (low values of B). The friction stress dictates which displacements the maximum S_r have reached (figures 4.8 and 4.9).
- Root slippage rather than breakage of roots may be the prevailing process, limiting root reinforcement.
- The following concept of the development of a landslide and the influence of the roots on the strength of the soil may be outlined: at maximum groundwater levels, in early spring, a slope may fail for the first time. This initial failure of a slope happens as the soil is at peak strength. After failure and sufficient displacement have taken place (shear strains > 0.4), the soil is at its residual strength and the root reinforcement of a soil increases. This may enlarge the total shear strength (root reinforcement, plus the residual strength of the soil) and may cause the landslide to stop sliding. It may even be possible, that the total strength rises to a level above the peak strength of the soil material alone. The influence of the root reinforcement on

the total strength of the soil will be most obvious in soil materials, which do not exhibit a clear difference between peak and residual strength like, for example, sandy soils. After the landslide stops, the root stress and therefore the root reinforcement may decrease, due to processes like root growth or creep at the root-soil contact.

5 EXAMPLES OF LANDSLIDE HAZARD ANALYSIS ON A LOCAL SCALE

5.1 Introduction

The presence of morainic material on top of impervious marl (terres noires) in combination with relief - and hydrological factors induce a large number of mass movements in the study area of the Barcelonnette basin (see par. 1.4). Many of these mass movements have been (re-)activated during the 18th and 19th century, due to abandoning of agricultural land and the logging of large areas.
Three slope profiles typical for situations in the study area, have been used to exemplify the application of a probabilistic limit equilibrium analysis to assess the landslide hazard on a local scale. Two profiles are located at plot 1, Riou Bourdou: one representing the stable locations, the other illustrating a landslide typically for colluvium. The third profile is located at plot 2, the landslide next to "la maison forestiere Le Treou"; this landslide is one of the few that partly have developed in coarse morainic material. Both plots are described in paragraph 1.4.
Because no movement has taken place on the monitored landslides from november 1984 till may 1988, an estimation of the location and shape of the failure surface had to be made, before a stability analysis could be performed. Methods that can assist in the estimation of the shape and the location of the failure surface will be considered in the next paragraph.

5.2 Estimating the location of the failure surface

There are several considerations that can assist the estimation of the location and the shape of a failure surface.
- The terrain itself may provide clues like location of the scarp and toe of a landslide, or material characteristics may dictate the location.
- Assumptions about the shape. It is often noted (Narayan et al, 1982) that the critical failure surface deviates from the circle. The actual failure surface resembles a logarithmic spiral (Peck and Terzaghi, 1968), that is the curvature has its apex towards the lower boundary (toe) and the upper portion has a flat curvature. The static moment of this type of curves is independent of the normal stress distribution (De Josselin de Jong, 1981).
- Statistical reasoning. Read and Harr (1988) assume on the basis of the maximum entropy principle that the most critical failure surface will have the highest entropy and highest probability of failure.
- Mathematical reasoning. The calculus of variations provides mathematical procedures to minimize a functional F[y(x)], where y(x) is a mathematical function, describing the slip surface and the functional itself is describing the stability or safety factor of a slope. In literature several examples of this approach can be found (Greco and Gulla, 1988; Oboni and Bourdeau, 1983; Narayan et al, 1982). The mathematical approach is not always feasible, because the functional not always satisfies the

Legendre, Weierstrass and Jacobi conditions of positive definiteness and global extreme (Narayan et al, 1982; De Josselin de Jong, 1980, 1981). A functional, which is discontinuous or contains a cusp, is most susceptible not to satisfy the conditions.
A computer program was used to estimate the failure surface with the smallest safety factor based on the DLEA method (paragraph 2.21). Two possible shapes of the failure surface will be considered: (1) a circular, this type of failure surface can be described by the coordinates of its center and the radius of the circle and (2) a parabolic, this type of failure surface can be described by function in the form of ax^2+bx+c, where x is the x-coordinate of the profile and a, b, and c are constants.
The programmed minimizing algorithm is given in Press et al (1986). It is a so-called conjugate direction set method first described by Powell (Press et al, 1986). The Powell procedure is as follows: starting from a circular or parabolic surface defined by the user, the program derives the 3 parameters describing the surface. During the iteration two of the parameters are held constant, while the third is shifted until a local minimum of the safety factor is located. The optimum position, corresponding to a minimum safety factor, is obtained if the change of the parameters is below a certain tolerance, given by the user. The Powell procedure was chosen because it doesn't need partial derivatives with respect to the parameters used.
Although the algorithm appears to be very efficient, it should be noted that the minimum safety factor found is quite often an approximation of a local minimum (Press et al, 1986; Greco and Gulla, 1988). There is no guarantee that it represents the global minimum of the safety factor (if one is present). This limitation is partly overcome by starting the procedure over again only from another starting point. If the various critical failure surfaces are sufficiently close, it is assumed to be the global minimum of the safety factor. If the various failure surfaces are still scattered, the one with the highest overall probability of failure is assumed to be the global minimum.
Experience with the program showed that it is difficult to find the global minimum of the safety factor and its corresponding failure surface of a natural slope, because:
- more often there are several local minima in the safety factor which hardly differ from each other, but each with a complete different failure surface.
- due to the irregular topographic surfaces and/or a stratification having different geotechnical characteristics, the functional is all but, smoothly declining to its global minimum of the safety factor.
Thus the estimate of the failure surface may not be the real failure surface, but the estimated safety factor and its corresponding probability of failure is often several magnitudes smaller as one obtained after a visual estimation of the failure surface.

5.3 Examples of landslide hazard analysis for the study area

The landslide hazard analysis has been based on the VARCON method (see par. 2.2.2.4); the method, most appropriate to be applied to slopes with heterogenous material (see 2.5).

5.3.1 Landslide in colluvium (Profile *Caris*)

Profile *Caris* is situated at plot 1, Riou Bourdou (paragraph 1.4) and runs from the road to the scarp (figure 5.1). It is an example of the many landslides, developed in the colluvium.
The data of this profile are kindly provided by J. Caris. It is the only profile where both the surface and the location of the boundary, between the colluvium and the solid terres noires, was measured by electro-resistivity methods.
Five different conditions of the profile are compared, to reveal the landslide hazard of the slope and the influence of vegetation, pore water pressure and strength parameters on it. The following cases will be discussed:

Case 1 The profile is outlined in figure 5.1. The groundwater level is at 0.3 m below surface. The profile embodies three layers. The root zone (labelled 1) is 1 m thick. It has the same strength parameters as the sub soil (layer 2), consisting of colluvium. The layer, labelled 3, consists of solid terres noires. Strength parameters are listed in table 5.1.

Case 2 Same as case 1, except with groundwater level at 3 m below surface.

Case 3 Same as case 1, except with trees covering the landslide The influence of the vegetation is assessed, by adding 5 kPa to the stress, acting in the vertical direction. Gray and Megahan (1981) give a range from 0 to 10 kPa for the extra vertical stress due to the vegetation. An extra stress of 5 kPa is comparable to a soil layer of 25 cm with a bulk density of 2 g/cm^3.

Case 4 Same as case 1 except with layer 2 at residual strength.

Case 5 Same as case 2 except with layer 2 at residual strength.

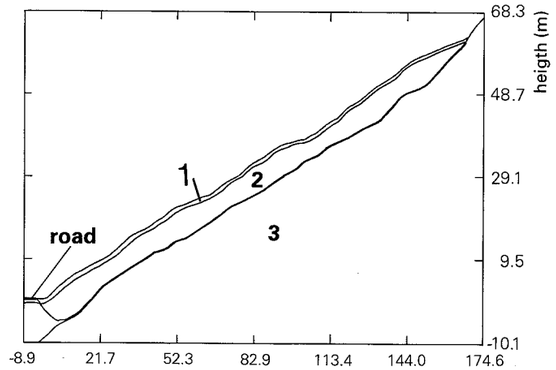

Figure 5.1 Morphometry of the *Caris* profile for *case 1*
The scarp at 169.57 m and the toe at -3.86 m

Table 5.1 Material descriptions

peak strength parameters

mean values		layer 1	2	3
bulk density	(g/cm³)	2.02	2.02	2.30
cohesion	(kPa)	16.55	16.55	72.0[ss]
phi	(°)	27.8[s]	27.8[s]	28.7[ss]

variance	layer 1	2	3
cohesion	53.71	53.71	13.00[ss]
phi	3.83[s]	3.83[s]	1.70[ss]

Residual strength parameters (Van Asch et al, 1989)

mean values		layer 1	2	3
cohesion	(kPa)	0.6	0.6	--
phi	(°)	25.6	25.6	--

[s] = estimated using the straight line approximation to the failure envelope at normal stress between 30 and 55 kPa. The failure envelope was estimated with the direct shear tests.
[ss] from Antoine et al, 1988

The strength parameters were obtained from literature and measurements. Literature provided estimations of the residual strength of colluvium (van Asch et al., 1989) and of the peak strength of solid terres noires (Antoine et al., 1988). The results of direct shear tests were used to estimate the peak strength of the colluvial material. The tests are discussed in chapter 3. It is found that the failure envelope was curved in the lower normal stress ranges. The failure envelope is the line connecting the different combinations of the shear stress and the normal stress where failure occurs. For calculation purpose the curved failure envelope is replaced with a straight line. This is done by providing a best fit over the stress range 30-55 kPa, coincides with a normal stress due to a soil layer of 1.5-3.0 metres. The fitting results in the following mean values; 16.55 kPa for cohesion and 27.8° for the angle of internal friction and a variance of 53.71 for the cohesion and 3.83 for $\tan\phi$.
The positions of the scarp and toe of the landslide are estimated by using the search program for the smallest safety factor, based on DLEA (see explanation of the search program paragraph 5.2). The estimated scarp coincides with the actual scarp, while the estimated toe is 2 m below the (actual?) toe near the road.
It is assumed that the coefficient of variation of the water pressure and variables b_1 and b_2 in the safety factor variance equations (2.11 and 2.14) are constant and equal to 0.1.

Table 5.2 Comparison of the overall values of the safety factor, variance of the safety factor and probability of failure of profile *Caris* under different conditions along the failure surface

	safety factor	variance of the safety factor	probability of failure	ratio λ
case 1	1.156	0.333	0.538	0.293
case 2	1.415	0.147	0.332	0.297
case 3	1.164	0.321	0.513	0.296
case 4	0.705	0.331	0.823	0.823
case 5	0.932	0.269	0.690	0.823

Description failure surface:
Failure surface follows boundary layer 2-3, i.e. boundary colluvium - solid terres noires.
Toe at -3.86 m : scarp 169.57 m

Figure 5.2 shows the plots of the distribution of the vertical shear forces for case 2 (peak strength, groundwater at 3 m below the surface). The plot of the vertical interslice forces, T, shows after a sharp rise near the toe, a line, which fluctuates around a constant value, (figure 5.2). Only at the toe the shear stress, T_{stress}, along the sides of the slices exceeds the shear strength of the soil. This indicates that the assumptions of the VARCON method results in physically realistic stress situations, with a possible exception of the area near the toe. Similar plots and conclusions were derived for the other cases.
The VARCON method indicates a landslide with a probability of failure of 53% in early spring, when groundwater levels reach to 0.3 metre below the surface (case 1 table 5.2). The landslide still has a probability to fail of 30 %, when groundwater levels drop below the 3 metres below the surface (case 2 table 5.2).
The landslide under field conditions of peak strengths and groundwater at 0.3 below the surface, consists of five blocks with almost equal probability of failure (figure 5.3). The probability of failure does not changes much along the failure surface, if the profile is considered to be under residual strength conditions, i.e. the slide may reacts as one block (figure 5.4).
The extra normal stress due to the vegetation biomass hardly effects the safety factor and the probability of failure (compare case 1 and 3 in table 5.2).
The influence of the pore water pressure at the failure surface on the probability of failure is higher under peak strength conditions, than under residual conditions. This indicates that changes in the hydrology of a slope have a larger influence on initial failure, than on the continuation of movement of an already failed soil mass, at residual strength (compare case 1, 2, 4, 5 in table 5.2).
The overall value of variance of the safety factors along the failure surface changes a little between the different cases. Higher variances are associated with higher pore pressures at the failure surface and with residual strengths.

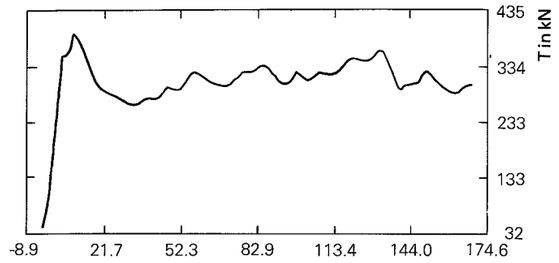

Figure 5.2 The distribution of vertical interslice forces along the failure surface of profile *Caris* for *case 2*
The scarp at 169.57 m and the toe at -3.86 m

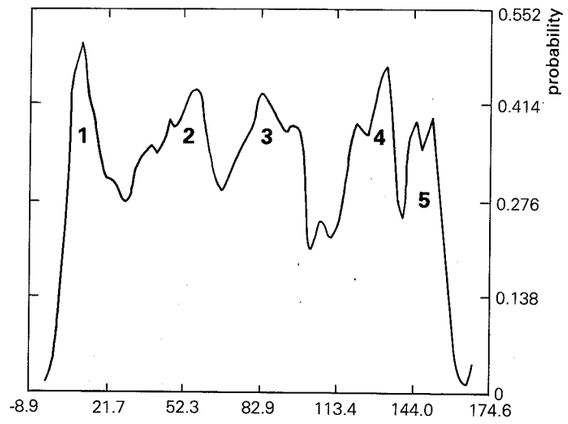

Figure 5.3 The probability of failure along the failure surface of profile *Caris* for *case 1*
The scarp at 169.57 m and the toe at -3.86 m

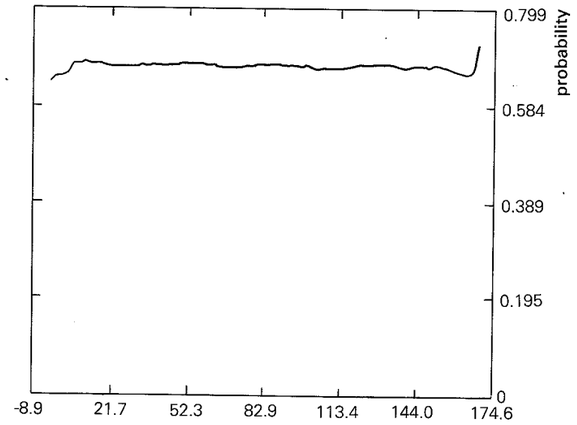

Figure 5.4 The probability of failure along the failure surface of profile *Caris* for *case 5*
The scarp at 169.57 m and the toe at -3.86 m

5.3.2 A stable slope (profile *Rbprof3*)

Profile *Rbprof3* is situated at plot 1, Riou Bourdou (paragraph 1.4). It is an example of a stable slope in the study area. The depth of the boundary between colluvium and the solid terres noires was not measured systematically. Some indications were obtained from hand auger data. The maximum depth reached with the auger, was about 4 meters. At this depth weathered terres noires were found.
The profile is depicted in figure 5.5. The groundwater levels,observed in the field, never came within 3 meters of the surface. It is assumed that both groundwater level and the boundary between the solid terres noires and the colluvium parallels the surface. Another assumption is that the position of the failure surface lies at the boundary between layer 2 (colluvium) and layer 3 (solid terres noires). Layer 1 is a root zone of 1 meter developed in colluvium.
Four different conditions of the profile are compared to reveal the landslide hazard of the slope and the influence of vegetation, pore water pressure, strength parameters and the assumption of sliding depth on it. The following cases will be discussed:

Case 1 Groundwater level at 3 m below the surface. The strength parameters are listed in table 5.1. layer 1 and layer 2 consists of colluvium, while layer 3 contains solid terres noires. The boundary between layer 2 and 3 is at 4 meter below the surface. The failure surface lies at the boundary of layer 2 and 3.

Case 2 Same as case 1 except with groundwater level at 0.3 m below surface.

Case 3 Same as case 1 except with trees covering the landslide and adding 5 kPa to the normal stress.

Case 4 Same as case 1 except with failure depth at 2.5 meters below the surface.

Table 5.3 Comparison of the overall values of the safety factor, variance of the safety factor and probability of failure of profile *Profrb3* under different conditions along the failure surface

	safety factor	variance of the safety factor	probability of failure	ratio λ
case 1	1.077	0.031	0.475	0.641
case 2	0.846	0.038	0.767	0.636
case 3	1.057	0.029	0.497	0.643
case 4	1.493	0.068	0.128	0.717

Description failure surface:
Failure surface follows boundary layer 2-3, i.e. boundary colluvium - solid terres noires.
Toe at 5.93 m : scarp 85.08 m

Material description and calculation parameters for *Profrb3* profile are identical to the *Caris* profile and given in table 5.1.
The positions of the scarp and toe of the landslide are estimated using the search program for the smallest safety factor based on DLEA (see explanation of the search program paragraph 5.2).
The stability of profile *Rbprof3* is strongly influenced by changes in groundwater levels and the assumption of the failure depth.
The VARCON method indicates, that this profile has, under field situations (case 1 and 3), an overall probability of failure of about 48%, which is comparable with the 53 %, obtained for profile *Caris*. Although there is a considerable difference in geometry of both profiles, there is not much difference in the probability of an initial failure under the field conditions. Apparently the landslide area and the stable area have under the conditions of peak strength and their shallowest groundwater levels of 0.3m below the surface for the landslide and 3.0 metres for the stable area, an almost equal probability of failure.
The distribution of probability of failure along the failure surface is only slightly fluctuating, as shown in figure 5.6 for case 1 and case 2. It seems that if an initial failure occurs, the landslide will move as one block: because there are hardly any changes in the probability of failure along the potential failure surface.
Alterations in the groundwater level change the probability with 27 %. Under normal field conditions (case 1; groundwater levels below the 3 metres beneath the surface) the failure probability is 48%, while extreme groundwater levels of 0.3 metres below the surface give a probability of 76 % .
A decrease from 4 to 2.5 metres below the surface, in the assumed depth of sliding, reduces the probability of failure to 12.8 %.

The overburden of vegetation hardly affects the stability of this slope (compare case 1 and 3, table 5.3).

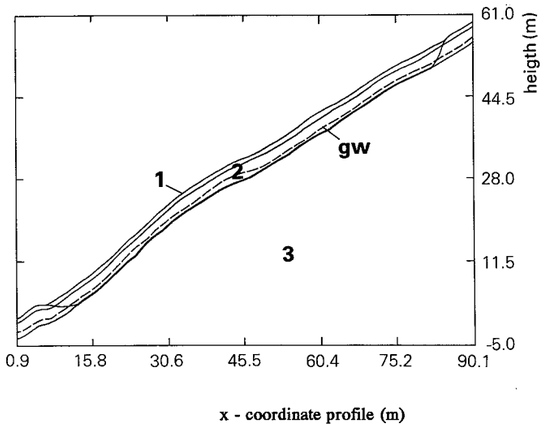

Figure 5.5 Morphometry of the *Profrb3* profile for *case 1*
The scarp is at 85.08 m and the toe at 5.93 m

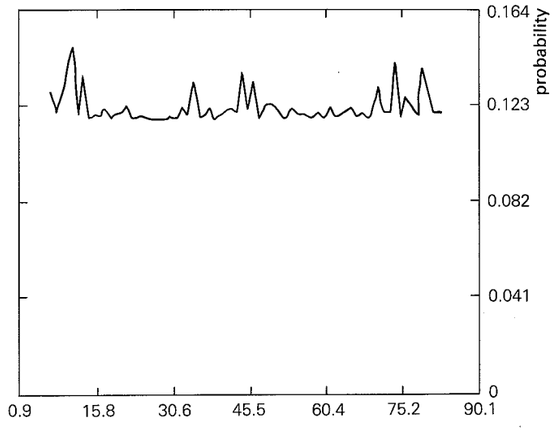

Figure 5.6a The probability of failure along the failure surface of the *Profrb3* profile for *case 1*
The scarp is at 85.08 m and the toe at 5.93 m

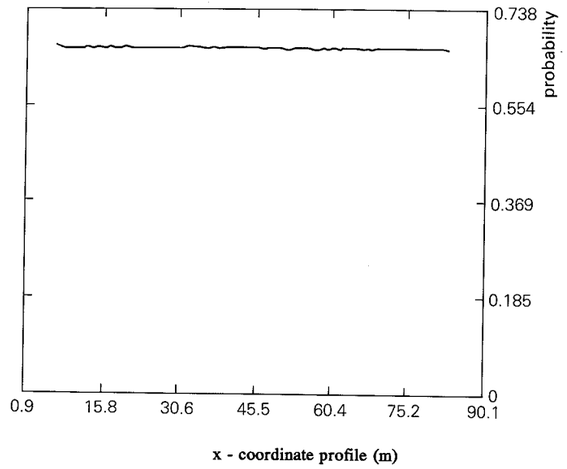

Figure 5.6b The probability of failure along the failure surface of the *Profrb3* profile for *case 2*
The scarp is at 85.08 m and the toe at 5.93 m

5.3.3 A landslide in coarse morainic material (profile *FT1*)

Profile *FT1* is situated 20 meters west of 'La Maison Forestiere Le Treou' at an elevation of 1450 m (paragraph 1.4) and is an example of a landslide that partly developed in coarse morainic material. The boundary of the solid terres noires is assumed to be at 5.5 meters below the surface. This is based on information obtained during the drilling of holes for positioning open stand pipes. It is further assumed that the failure surface lies at the boundary between layer 2 (morainic material) and layer 3 (solid terres noires).In the surface layers the material of this landslide consists of a mixture of fine to very coarse morainic material (stones up to 2 meter diameter). Nevertheless the strength characteristics of the colluvium, estimated at plot 1, have been applied in the calculations. This seems to be justified, because the coarse material does not reach up to the boundary of the terres noires. The interface between layer 2 and 3 (see figure 5.7), shows material with a comparable nature to that at plot 1. The main differences between this profile and profile *Caris* are its hydrology and geometry. For profile *FT1* the maximum groundwater level is at 0.5 meter below the surface. The root zone (layer 1) is estimated to be 1 m. The location of scarp and toe were estimated using the search program for the smallest safety factor based on DLEA (see paragraph 5.2). The estimations of the toe and scarp appeared to coincide with the actual ones.
Four different conditions of the profile are compared to reveal the landslide hazard of the slope and the influence of vegetation, pore water pressure and strength parameters on it. The following cases will be considered:

Case 1 Groundwater level at 0.5 m below the surface. For layer 1 and 2 the strength parameters of the colluvium are used, and for layer 3 those of the solid terres noires (table 5.1).
Case 2 Same as case 1 except with groundwater level 3 m below surface.
Case 3 Same as case 1 except with trees covering the landslide and adding 5 kPa to the normal stress.
Case 4 Same as case 1 except with layer 2 at residual strength.

An alteration in the groundwater level changes the probability of failure by 25 %. Under springtime conditions, characterized by groundwater levels at 0.5 metres below the surface (case 1), the probability is 50 %. Under autumn conditions, characterized by groundwater levels below 3 metres beneath the surface, the probability of failure is 25 % (table 5.4).
The assumption of the residual strength results in an increase of the probability of failure of 30 % compared with peak strength conditions (table 5.4; case 1 and 4).
The distribution of the probability of failure along the failure surface, as shown in figure 5.8, suggests at least three blocks with equal probability of failure. Block 1, actually has moved after some excavation took place at the toe, for an enlargement of the road. The sharp dip in probability of failure between block 1 and 2 is the basis for hypothesis, that failure of block 1 is not affecting the probability of failure of the other blocks.
The extra normal stress, applied by trees, hardly results in any change of the probability of failure (compare case 1 and 3, table 5.4).

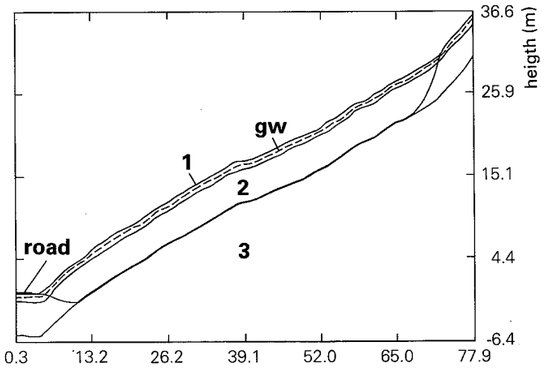

Figure 5.7 Morphometry of the *FT1* profile for *case 1*
The scarp is at 72.88 m and the toe at 5.81 m

Table 5.4 Comparison of the overall values of the safety factor, variance of the safety factor and probability of failure of profile *FT1* under different conditions along the failure surface

	safety factor	variance of the safety factor	probability of failure	ratio λ
case 1	1.171	0.203	0.503	0.400
case 2	1.450	0.187	0.250	0.402
case 3	1.161	0.234	0.487	0.409
case 4	0.682	0.228	0.819	0.404

Description failure surface:
Failure surface follows boundary layer 2-3, i.e. boundary colluvium - solid terres noires.
Toe at 5.81 m : scarp 72.88 m

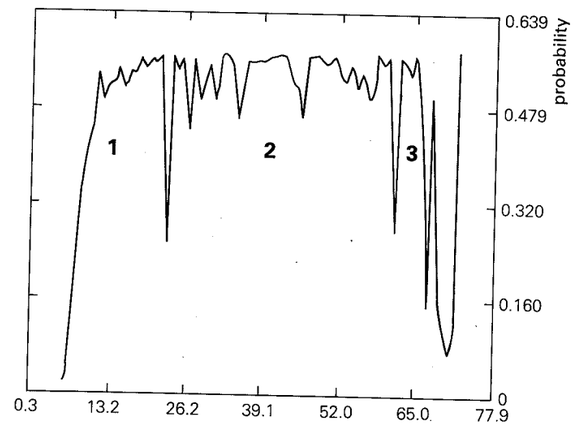

Figure 5.8 The probability of failure along the failure surface of the *FT1* profile for *case 1* The scarp is at 72.88 m and the toe at 5.81 m

5.4 Conclusions

Some tentative conclusions for the landslide hazard in the study area may be drawn from the analyses of the three slope profiles.
- The landslides have a failure probability of 50% in early spring, when groundwater levels are close (0.2-0.5 m) to the ground surface. The failure probability decreases to 30 %, when the groundwater levels drop to more than 3 metres below the surface (autumn condition).
- The stable areas have under field conditions of peak strength and a groundwater level of 3 metres below the surface, a landslide hazard, that is slightly lower than that of a landslide, with a groundwater level at 0.3 metres below the surface and peak strength.
- The distribution of the probability of failure along the failure surface indicates landslides, consisting of several 'blocks' of material with a comparable probability, separated by stretches of lower probability of failure.
- The influence of water pressure at the failure surface on the probability of failure is higher under peak strength conditions than under residual conditions. This shows, that changes in the hydrology of a slope have larger influence on initial failure, than on the continuation of movement of an already failed soil mass.
- The overburden of vegetation hardly affects the mean and the variance of the safety factor of a slope. Removal of the vegetation may increase the landslide hazard, due to their effect on the hydrology of the slope: the removal reduces water losses through interception and evaporation, thus increasing the amount of infiltrating water. This may result in groundwater levels closer to the surface. This condition increases the landslide hazard.

6 ASSESSMENT OF LANDSLIDE HAZARD ON A REGIONAL SCALE

6.1 Introduction

The estimation of landslide hazard on a local scale is based on a soil mechanical approach (chapter 2, 3, 4, 5). On a regional scale, usually statistical methods are used. In this chapter a soil mechanical approach is proposed to assess the landslide hazard on a regional scale. Both a statistical and soil mechanical approach are applied to the study area (see par. 1.4).
A general procedure for preparing landslide hazard zonation maps of a region usually involves four steps (Carrara, 1983; Aniya, 1985): (1) selection of critical terrain factors; (2) assessment of the relative contribution of the critical terrain factors in generating mass movements; (3) mapping of the different critical terrain factors; and (4) production of a landslide hazard zonation map by superimposing these terrain factor maps according to an appointed weight.
This chapter focusses on the abilities of the statistical and the soil mechanical approaches to select the critical terrain factors, assess their relative contribution to the landslide hazard and the assessment of the landslide hazard itself.

6.2 A statistical approach to the assessment of landslide hazard on regional scale: an example of the use of a discriminant analysis

In a statistical approach, the degree of landslide hazard may be assessed by a statistical (multivariate) analysis (Reger, 1979; Carrara, 1983). The most significant factors, contributing to the instability, are weighted quantitatively, according to their statistical significance.
A standard technique is the discriminant analysis (see for example Carrara et al., 1977; Neuland, 1976; Aniya, 1985; Haigh et al., 1988). The analysis can be used to select the critical terrain parameters and to give an assessment of their relative contribution to the landslide hazard. In the following paragraph the use of a discriminant analysis for the assessment of the landslide hazard in the Ubaye River Valley, will be tested.

6.2.1 Methods of data collection and -analysis

Data collection

The collection of quantitative and objective information on a large number of terrain parameters, related to slope instability phenomena, is simplified by the use of a standardized form (Carrara and Merenda, 1976).
Collecting the data, the study area has been divided into squares of 500 by 500 m. In each square one standardized form was compiled on (1) the land unit with the greatest

vegetation coverage and on (2) each landslide, encountered in a field reconnaissance of the entire square. The form used to gather the data is shown in table 6.1. It covers aspects of geomorphology, geology, hydrology, vegetation and morphometry of the mass movements of an area. Geological factors, determining the susceptibility of slopes to mass movements, are related to cohesion and angle of internal friction and include rock composition, structure and bedding sequence. Actual or potential failure planes may form, when downslope dipping planes separate rocks of different competence. Other geological situations, favorable to mass movements are: a soil poorly attached to the underlying bedrock, or an impermeable bedrock.
Soil factors, related to slope stability, are cohesion, angle of internal friction and water retention and transmissibility.
Hydrological processes determine the pore water pressure in the potential slip plane. Infiltrating water can decrease the stability of a slope by increasing the weight of the soil and by eventually creating positive pore water pressures. A perched groundwater table, creating positive pore pressures, will form within the soil mantle, if the subsurface flow is lower than the infiltration rate, for an extended period of time. The height and the persistence of a groundwater table depends furthermore on rainfall or snow melt intensity and duration, type of vegetative cover, agricultural practice, morphology and soil physical properties, like hydraulic conductivity and void ratio. The large interconnected soil pores, like soil pipes and cracks, are important passageways for the transport of water on a slope. Although piping networks are interconnected over large areas, small breaks in this network create sites of extensive pore water pressures (Sidle et al., 1985).
Vegetation influences the hydrology and the normal stress on the failure surface.
Slope gradient is the most prominent geomorphological factor. It governs directly the normal and shear stress. Slope shape and gradient influence the water distribution in and on the slope. Convex slopes disperse subsurface water and therefore tend to be more stable than concave slopes, which concentrate subsurface water into small areas. The frequent association of shallow mass movements and slope depressions is not surprising.
The geotechnical information gathered, was limited.
Micro-relief is defined as smaller relief elements of a hillslope within an area, not more than 100 m². Meso-relief is composed of larger relief elements of a hillslope in an area, more than 100 m². Slope length is the distance of a sampling point to the main water divide. Slope length has been estimated by using a topographic map, scale 1:25.000. Distance to the water divide, is the distance of the sampling point to the nearest water divide.
In total 392 forms have been processed. 211 sites have been classified in the field as a stable site, 155 as a landslide and 26 as unknown.

Discriminant analysis

In a two-group discriminant analysis,discriminating between stable sites and landslides, a linear discriminant function is given by (Norusis, 1985) :

$$DS = B_0+B_1X_1+B_2X_2+.....+B_nX_n \qquad (6.1)$$

The discriminant function is similar to the multiple linear regression equation. The X's are the values of the variables and the B's are the coefficients estimated from the data. If a linear discriminant function is used to differentiate between stable sites and landslide sites, the two groups must differ in their discriminant score (DS). The estimation of the coefficients of the B is such, that the discriminant scores differ as much as possible between the groups, i.e the own value or the ratio of the variability between the groups and the variability within the groups, is at a maximum. The variables, used in the discriminant function may be considered as the critical terrain parameters and the standardized constants B are often seen as their relative contributions to the landslide hazard (Carrara et al., 1977)
The discriminant score can be used, to obtain a rule for classifying sites into one of the two groups. The classification technique, used in SPSS-x version 2.0 is based on Bayes' rule. The probability, that a site with a discriminant score of DS belongs to group i, represented by $P(G_i \mid D)$, is estimated with (Norusis, 1985):

$$P(G_i|D) = \frac{P(D|G_i)P(G_i)}{\sum_{i=1}^{g} P(D|G_i)P(G_i)} \qquad (6.2)$$

Where $(P(D \mid G_i))$ is a conditional probability. The prior probability, $P(G_i)$, is an estimate of the likelihood of a site to belong to a specific group, when no information about the site is available. For example, if 40 % of the sites is a landslide, the prior probability that a site is a landslide is 0.4.
The conditional probability $(P(D \mid G_i))$, for obtaining a particular discriminant score (DS), given the group membership of the site, can be estimated, when the discriminant scores are normally distributed for each of the two groups and the main and variance of each group can be estimated. A site is classified, based on its discriminant score DS, in the group for which $P(G_i \mid D)$ is the largest. The discriminant score has been related by Carrara (1983) and Neuland (1976) to the degree of stability.
The percentage of sites classified correctly is often taken as an index of the effectiveness of the discriminant function. During an evaluation of this index, it is important to compare the observed misclassification rate to the rate expected by chance alone. Two groups with equal prior probabilities result in an expected misclassification rate of 50 %. A discriminant function with an observed misclassification of 50 % is not performing better than chance.
In this study two assumptions about the prior probability have been tested separately:

Table 6.1a Form for landslide inventory of the Barcelonnette basin

GENERAL INFORMATION

1. Surveyor .....
2. map coordinates x ..... y ..... z ..... m
3. Date / / 86
4. Weather .....

MICRO RELIEF

1. steps/ terracettes ☐ mean height ..... cm
   depressions ☐
   undercutting by human ☐
   nature ☐

2. slope morphology micro relief

	down slope	parallel
straight	☐	☐
concave	☐	☐
convex	☐	☐

MESO RELIEF

1. slope morphology

	down slope	parallel
straight	☐	☐
concave	☐	☐
convex	☐	☐

2. ground area (m²)

< 100	☐
100- 200	☐
200- 500	☐
500- 1000	☐
1000- 2000	☐
2000- 5000	☐
5000-10000	☐
>10000	☐

3. length slope (m)

< 20	☐
10- 20	☐
20- 50	☐
50-100	☐
100-200	☐
200-500	☐
>500	☐

4. max. slope angle ..... %
   min. slope angle ..... %

REGOLITH

1. material type
   morainic ☐
   weathered 'terres noires' ☐
   other ☐

2. texture
   clayey ☐
   sandy ☐
   loamy ☐

3. depth to solid rock (cm)

< 5	☐
5- 10	☐
10- 20	☐
20- 50	☐
50-100	☐
100-200	☐
200-500	☐
>500	☐

4. bare ground (%)

< 5	☐
5-10	☐
10-25	☐
25-50	☐
50-75	☐
75-90	☐
90-95	☐
>95	☐

5. stoniness (%)

<10	☐
10-50	☐
>50	☐

SOLID ROCK

1. Discontinuity surfaces:

Steep dips of the joints into topographic slope ☐
Moderate slopes of the joints opposite to topographic slope ☐
Horizontal or nearly vertical joints ☐
Moderate dip of the joints in direction of topographic slope ☐
Steep dip of joints out of the topographic slope ☐

2. strength

very soft=1 / soft=2 / moderate strong=3 / strong=4 / very strong=5

limestone ☐
dolomite ☐
sandstone ☐
breccia ☐
conglomerate ☐

shale ☐
loamy-limestone ☐
marl ☐
gypsum ☐

HYDROGRAPHY

1. spring ☐
   stagnating water ☐
   streaming water ☐
   disturbed water pattern ☐

Table 6.1b Form for landslide inventory of the Barcelonnette basin

2. distance to gully downhill (m)

< 10	☐
10- 20	☐
20- 50	☐
50-100	☐
100-200	☐
200-500	☐
>500	☐

3. distance to watershed (m)

< 10	☐
10- 20	☐
20- 50	☐
50-100	☐
100-200	☐
200-500	☐
>500	☐

4. catchment area (m²)

< 100	☐
100- 200	☐
200- 500	☐
500- 1000	☐
1000- 2000	☐
2000- 5000	☐
5000-10000	☐
>10000	☐

MASS MOVEMENTS

1. The mass movement was:
   sheet ☐
   rotational ☐
   unknown ☐

2. Morphometry of the movement:
   length ..... m slope scarp .... %
   width ..... m height scarp .... m
   depth ..... m

VEGETATION

1. the following vegetation layers were found:
   trees ☐ herbs ☐
   shrubs ☐ moss ☐

2. tree coverage (%)

>75	☐
25-75	☐
10-25	☐
<10	☐

homogeneous ☐
cluster ☐
solitaire ☐

3. type of forest (% pine)

>75	☐
25-75	☐
10-25	☐
<10	☐

4. dominant tree species and genera

Pinus cembra ☐ *Larix decidua* ☐ *Populus* ☐
Pinus sylvestris ☐ *Abies alba* ☐ *Fraxinus excelsior* ☐
Pinus uncinata ☐ *Picea abies* ☐ *Salix* ☐

5. basal area ..... m²/m² 6. number of trees per 100 m² .....

7. number of trees with:
   straight trunk ☐ leaning trunk ☐
   curved trunk ☐ curved lower part ☐
   "swan" trunk ☐ death ☐

8. number of trees with a length of:

5 m	9 m	13 m	17 m	21 m .....
6 m	10 m	14 m	18 m	>21 m .....
7 m	11 m	15 m	19 m	
8 m	12 m	16 m	20 m	

9. max. rooting depth ..... cm.
   mean rooting depth ..... cm.

10. vitality forest
    scanty ☐
    normal ☐
    abundant ☐

11. shrubs

coverage (%)

>75	☐
25-75	☐
<25	☐

homogeneous cluster ☐

height (cm)

< 50	☐
50-100	☐
100-200	☐
200-500	☐

12. herbs

coverage (%)

>50	☐
10-50	☐
<10	☐

homogeneous cluster ☐

13. depth litter layer (cm)

<1	☐
1-3	☐
>3	☐

HUMAN ACTIVITY

arable land ☐ supporting wall ☐
building area ☐ ski run ☐
talus ☐

STABILITY OF THE AREA

1. the area was:
   stable ☐
   movement ☐
   complex of movements ☐

2. the movement was:
   old ☐
   not recent ☐
   recent ☐
   unknown ☐

- the probability for a certain group member is proportional to the number of sites in each group, i.e. sites will more likely be assigned to the greater group of stable sites.
- the probability of group membership is equal, i.e. there is no difference in the probability of assignment between the groups, stable or landslide sites.

A discriminant analysis assumes that the classification variables are from a multivariate normal distribution and the covariance matrices of all groups are equal. If these assumptions are violated, the linear discriminant analysis is less optimal (Norusis, 1985).
The Box's M test tests the equality of the group covariance matrices (Norusis, 1985). For the data used,the test gave a significance of 0.43, indicating two matrices, which are not too dissimilar.
There is reason to suspect that the multivariate normality assumption is violated, because some of the variables have markedly non-normal distribution. But Norusis (1985) states that the linear discriminant function performs quite well if the covariance matrices are not too dissimilar and in case of dichotomous classification variables, especially when the data sets are small.

6.2.2 Results of discriminant analysis

Before any further analysis is performed, it is tested how successful the obtained discriminant function is in differentiating stable sites from landslide sites.For this purpose the variability between the groups, within the groups and the total variability of the data were estimated.
The ratio of the variability between the groups and the variability within the groups or eigenvalue of the discriminant function is maximized in a discriminant analysis. Large eigenvalues are associated with a good discrimination (Norusis, 1985). The data had a eigenvalue of 1.3423, which indicates a rather good discrimination (Norusis, 1985).
Another measure of the success of discrimination is the Wilks' λ. This is the ratio between the variability between the groups with the total variability. Small values are associated with analyses with much variation between the groups and less within the groups. A Wilks' λ of 1 indicates that all group means are equal to each other. The gathered data had a Wilks' λ of 0.4269, which indicates a reasonable discrimination. This was confirmed by a Chi-square test. The Chi-square test indicates that the groups of stable and landslide sites are significantly different at the 0.00005 level.
For each site a discriminant score or group membership was calculated using the discriminant function. By comparing the predicted group membership with the actual group membership, one can empirically measure the success of the discrimination. Table 6.2 shows that 87.7 % of the sites were correctly classified.
The percentage of correctly classified sites will always be too optimistic, when the same sites are used, both to compute the discriminant function and to classify (Nie et al., 1981). To get an unbiased estimate of percentage of correctly classified sites, the sample has to be split randomly into two parts: one for computing the discriminant function and one for estimating the percentage of correctly classified sites. This way of testing gives a good indication of the reliability of the predictive power of the discriminant function (Nie et al., 1981).

Table 6.2 Percentage of incorrectly and correctly classified sites due to two different assumptions about the prior probability

	Prior probability	
	equal	group size
total correctly classified	87.7	87.7
incorrectly classified as stable	10.2	15.7
correctly classified as stable	86.3	90.0
incorrectly classified as landslide	13.3	10.0
correctly classified as landslide	89.8	84.3

Table 6.3 Percentage of correctly classified sites as function of the percentage of the total number of sites used to compute the discriminant function

% of forms used to compute discriminant function	biased	unbiased
100	87.7	--
80	86.8	78.2
60	92.7	68.3
40	94.3	71.6

Table 6.3 gives the percentage correctly classified sites; 'biased' stands for the percentage of correctly classified sites in the sample population, used to determine the discriminant function; 'unbiased' stands for the percentage of correctly classified sites, not used in the determination of the discriminant function.
Table 6.3 demonstrates that the unbiased percentage of correctly classified sites is always less than the biased percentage, indicating a moderate reliability of the discriminant function for classification.
Although the biased percentage of correctly classified sites is about 90%, the discrimination between stable and landslide sites is not optimal. Figure 6.1 depicts a plot of the cumulative frequencies of the discriminant scores, of landslide and stable sites groups. There is a transition zone between both groups and just this transition zone is interesting for landslide hazard mapping.
Interesting in aspect to landslide hazard mapping, are those sites, classified as a landslide by the discriminant function, but which are found to be a stable site in the field. Carrara (1983) and Neuland (1976) consider these "incorrectly classified" areas as a potential landslide and hence very dangerous. This interpretation is based on the assumption that slope failure, in the future, will be more likely to occur under circumstances, which both in the past and recently, have led to slope failure.
The group of incorrectly classified sites should be interpreted with some care: one might neglect the fact, that the classification can be incorrect, because of methodological errors. The methodological errors are related to sampling or data processing or to using the incorrect discriminating factors.

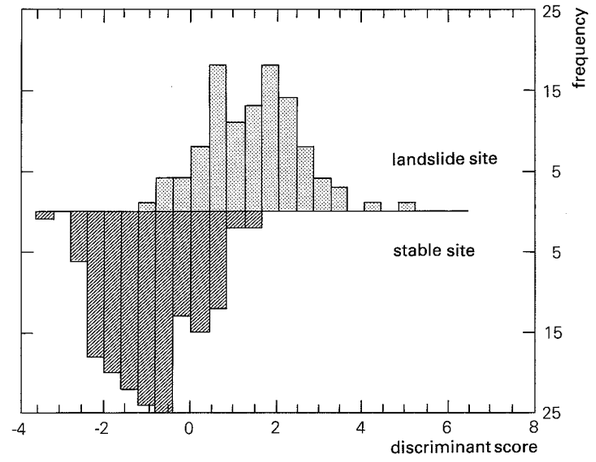

Figure 6.1 Frequency plot of the discriminant score for stable and landslide sites.

There also is a group of sites, which are classified as stable, but have proved to be a landslide in the field (see table 6.2). For this group is no physical explanation and it can only be interpreted as a result of methodological errors. A significantly larger percentage of sites, incorrectly classified as landslides, than the percentage of sites, incorrectly classified as stable, indicates that some sites can be considered as a potential landslide and thus dangerous. In this way, discriminant analysis may detect potential landslides. However, table 6.2 shows that in the study area, there is not a larger percentage of sites, incorrectly classified as a landslide. This makes it doubtful, that these sites can be considered as potential landslides.
In the presented analysis, large discriminant scores are associated with landslides, while small discriminant scores are associated with stable sites. Larger values of variables, with a positive coefficient B of the discriminant function, contribute to an increase in the discriminant score and have a negative effect on the slope stability. Larger values of variables, with a negative sign, are associated with an increase in stability.

Table 6.4 The seven most important variables in the discriminant function, with their standardized coefficient

steps/terracettes	0.57
maximum rooting depth	0.21
ground area of meso relief	-0.29
material type	-0.45
maximum slope angle	0.28
thickness of litter layer	0.15
basal area of trees	0.13

Table 6.4 lists the 7 most important variables in the discriminant function, together with their standardized coefficients: the presence of steps/terracettes, maximum rooting depth, ground area of meso relief, material type, maximum slope angle, thickness of litter layer and basal area of trees.

Table 6.5 Correlations between variables used in discriminant function

	A	B	C	D	F	G
B	.2602	1.0000				
C	.0088	-.1375	1.0000			
D	-.0990	-.0620	-.0904	1.0000		
E	.0583	.0682	-.0391	.1747	1.0000	
F	.0792	.3612	-.2243	.0566	.0424	1.0000
G	-.2672	-.1062	-.1108	-.1184	-.0244	.1363

A = Steps / terraccettes
B = Maximum rooting depth
C = ground area of meso relief
D = material type
E = maximum slope angle
F = thickness of litter layer
G = basal area of trees

Since some of the variables are correlated (table 6.5), it is not possible to assess the importance of an individual variable by the magnitude of his standard coefficient. The coefficient for a particular variable depends on the other variables, included in the function (Norusis, 1985).
Despite this, a general trend for the study area can be deduced. Generally is observed that the discriminant score increases, with increasing values of the variables: maximum rooting depth, thickness of the litter layer and basal area of trees, points at a frequent association between landslide and forests. A possible explanation for the association between landslide and forest is the planting of trees at the turn of the century, on areas, that suffered most from erosion, including mass movements. Apparently these landslides are still active.

6.3 A soil mechanical approach to the assessment of landslide hazard on regional scale

The use of soil mechanical methods in the assessment of landslide hazard on regional scale may give more predictive answers on the effects of human activities than the statistical approach, because the soil mechanical methods are based on the laws of physic and causality. The factors, which have a strong influence on landslide hazard, may be deduced from a sensitivity analysis using limit equilibrium methods (paragraph 6.3.1). The landslide hazard will be assesses using Monte Carlo simulations (paragraph 6.3.2)

6.3.1 Landslide hazard modelling using limit equilibrium methods

To determine the landslide hazard of slopes,the infinite slope model was used. This model assumes the sliding of a slab of soil on a failure surface, which is parallel to the ground surface. The safety factor equations, resulting from a force equilibrium perpendicular, and parallel to the slope, are simple. Since the slope is infinite,the interslice forces can be neglected, i.e their line of action is parallel to the ground surface and they are of equal magnitude, but opposite of sign (Nash, 1987).
The resulting equation describing the safety factor can be written as (Gray and Megahan, 1981):

$$F = \frac{\frac{2c}{\gamma_w H \sin 2\beta} + [\frac{q_o}{\gamma_w H} + (\frac{\gamma_{sat}}{\gamma_w} - 1)M + \frac{\gamma}{\gamma_w}(1-M)]\frac{\tan\phi}{\tan\beta}}{\frac{q_o}{\gamma_w H} + \frac{\gamma_{sat}}{\gamma_w}M + \frac{\gamma}{\gamma_w}(1-M)} \qquad (6.3)$$

where:

F	=	safety factor	
M	=	relative height of piezometric surface = Hw/ H	(-)
Hw	=	height of piezometric surface above potential failure surface	(m)
H	=	thickness above potential failure surface	(m)
c	=	effective cohesion of the soil	(kPa)
γ	=	unit weight of moist soil above piezometric surface	(kPa/m)
γ_{sat}	=	saturated unit weight of the soil	(kPa/m)
γ_w	=	density of water	(kPa/m)
q_o	=	vertical surcharge due to the vegetation weight	(kPa/m)
β	=	slope angle	(°)
ϕ	=	angle of internal friction	(°)

6.3.2 Sensitivity analysis for the study area

In order to obtain an impression of the relative importance of different parameters, given their range found in the study area, a sensitivity analysis was carried out, using the infinite equilibrium model (equation 6.3). In the analysis only one parameter was changed, all other parameters were kept constant at their median value. The changed parameter was increased stepwise, from its minimum to its maximum value.
Figure 6.2 shows the results of sensitivity analyses carried out on the colluvium soils, found in the Barcelonnette Basin and done for two depths of slippage: 0.4 to 0.6 metres, the depth of the root zone, and 4 to 6 metres, the variation in the depth of the colluvium cover. The results in figure 6.2 indicate slope angle as a very sensitive parameter, while the strength parameters and the groundwater height only have a moderate influence on the safety factor. Remarkable is the fact that the depth of the colluvium, the surcharge of the vegetation and the bulk density parameters become relatively unimportant, if slippage occurs in deeper soil layers (figure 6.2b).

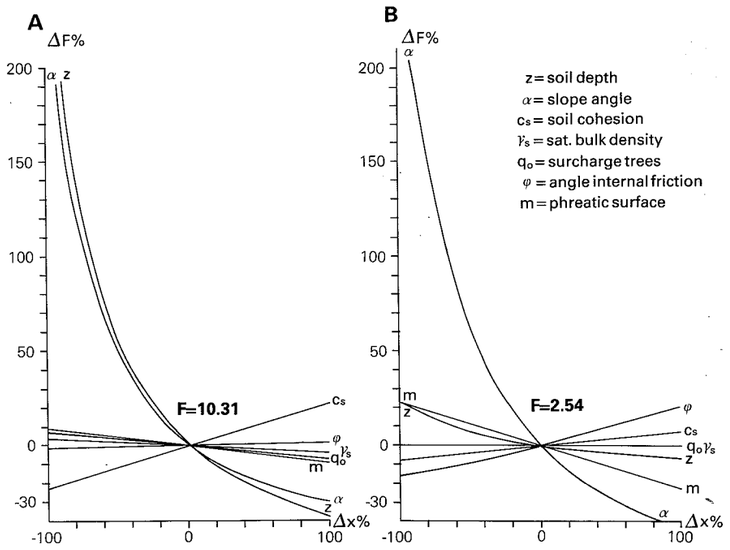

Figure 6.2 The sensitivity of the input parameters in the infinite slope model. Percentage change in safety factor (F), versus percentage change in the input variables (x).

6.3.3 Assessment of landslide hazard

The best way to construct hazard zones in a region is, to subdivide the landscape into land units, according to the most sensitive parameter. The sensitivity analysis indicated that the slope angle is under all circumstances a sensible parameter; fortunately this parameter is easy to map. Depth of slipping is especially important, if it occurs in the first 2 metres. The soil strength proved to be also an important parameter. However, it is not suitable for a further division of the landscape into units, because the values of this parameter vary considerable over short distances (see chapter 4). In the calculation of the hazard within each land unit, for the two soil depths, it is assumed, that the groundwater will rise once to the maximum level (M=1). This might give conservative estimates, especially for the upper (root-) zone. Five slope classes were chosen for subdivision of the landscape into land units. For the assessment of the hazard degree, the variability of the safety factor in each slope zone was calculated by means of the Monte Carlo method (Benjamin and Cornell, 1970). A Monte Carlo method consists of drawing a large, but finite number, of values from a probability distribution. In this case the probability distributions of parameters, used in the equilibrium model (equation 6.3). This equation 6.3 is used to calculated the safety factor.

Monte Carlo simulation within each land unit resulted in a distribution of the safety factor. The probability of sliding of a slab of soil is expressed as the percentage of the safety factors with a value below unity.

Many probability distributions have been proposed for the angle of internal friction and the cohesion. Lumb (1966) concluded that the cohesion and tan(ϕ) followed a normal distribution. The normal distribution provided a good fit at the central values, but it deviated significantly at the marginal values. The use of a normal distribution implies, that there is a small, but finite probability for a negative value. The use of normal probability for the shear strength would imply, that negative shear strength is possible, which is impossible in the commonly used models of soil strength parameters. Two alternative distributions were suggested: lognormal, a distribution in the range 0-∞ (Wu and Kraft, 1969), and a beta distribution, a distribution bounded on both extremities (Harrop-Williams, 1986; Oboni and Bourdeau, 1983; Lumb, 1970; Harr, 1977).

The histograms of the distributions of cohesion and tan(ϕ) estimated on the 131 sample cores taken at plot 1, Riou Bourdou, are given in figure 6.3. The Chi-square goodness of fit test was used to compare the experimental distributions of the cohesion and of tan(ϕ) with the normal, lognormal and beta distribution. The results are given in table 6.6.

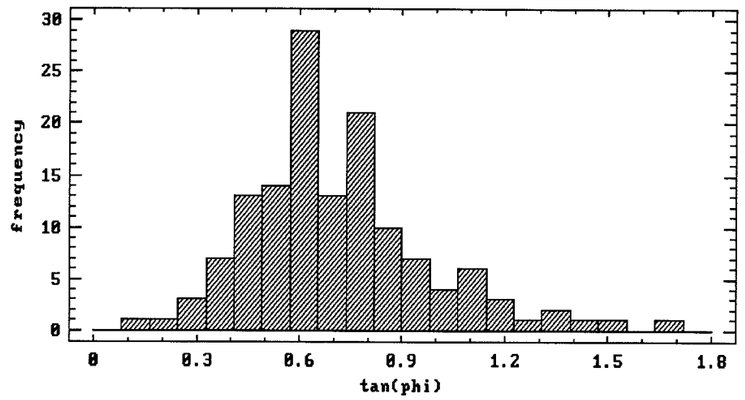

Figure 6.3a Frequency histogram of tan(ϕ) (°)

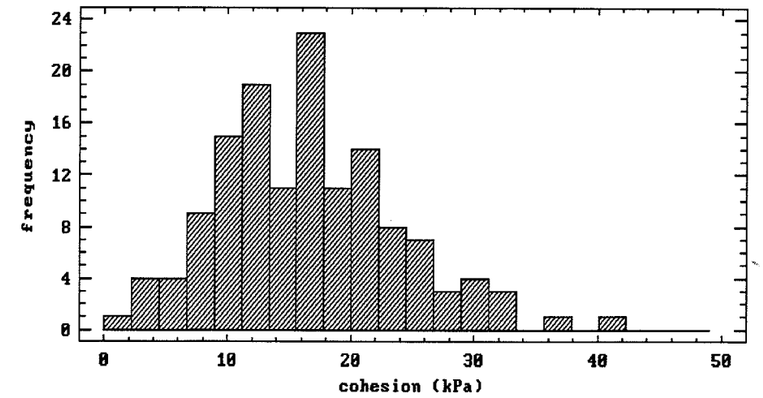

Figure 6.3b Frequency histogram of cohesion (kPa)

Table 6.6 reveals, that the experimental distribution of the cohesion can be approximated with a lognormal distribution, with a mean of 13.55 kPa and a variance of 49.17, while the distribution of tan(ϕ) best is approximated with a normal distribution, with a mean of 0.71 and a variance of 0.068.
The experimental distribution of dry bulk density is plotted in figure 6.4. Nielsen et al

Table 6.6 The results of a Chi-square test for fitting the experimental distribution of cohesion and tan(ϕ) on a lognormal, normal and beta distribution.

	normal	s	lognormal	s	Beta	s
cohesion (kPa)	12.20	0.708	24.36	0.006	11.30	0.255
tan(ϕ) (°)	23.19	0.994	16.91	0.050	14.45	0.008

s: significance level of equalling the proposed distribution.

(1973) and Russo and Bresler (1980) approximate the experimental distribution of the bulk density with a normal distribution. Both normal and lognormal distributions were used to fit the experimental distribution. The outcomes of the Chi-Square goodness of fit test appeared to be slightly higher for the lognormal distribution (normal Chi^2 = 25.86, lognormal Chi^2 = 26.78, both 12 degrees of freedom).
There are few estimates available about the depth of the colluvium. Augering on the plots and exposures in the 'terres noires' badlands revealed, that the colluvium cover has a minimum thickness of about 4 m. and a maximum of about 6 m. Therefore a uniform distribution is introduced in the Monte Carlo simulations for the colluvium depth of 4 to 6 metres.

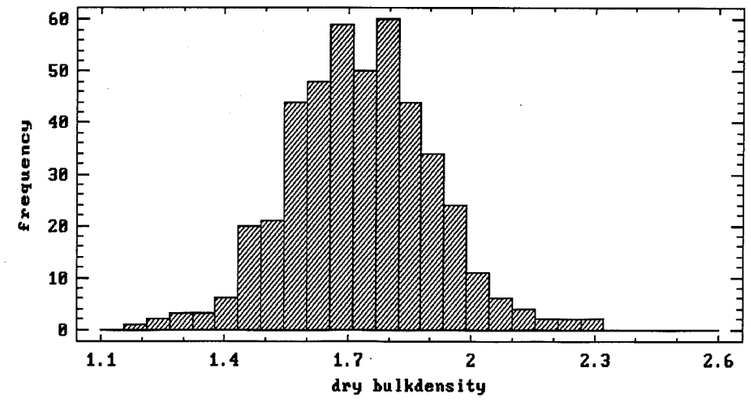

Figure 6.4 Frequency histogram of dry bulk density (g/cm³)

The variation of slope angle and the groundwater depth, within each class, were assumed to be uniform in the Monte Carlo simulations.
The distribution of vertical normal stress, due to vegetation, is assumed to be uniform and between 0-10 kPa. Gray and Megahan (1981) give a range of 0-10 kPa for the extra vertical stress, due to vegetation. An extra stress of 5 kPa is comparable to a soil layer of 25 cm, with a bulk density of 2 g/cm³.
The time component in the landslide hazard analysis may be neglected if the most dynamic variable, the groundwater level is assumed to be at its maximum. This is achieved by assuming, that groundwater reaches the surface everywhere at the same moment. It is interesting to compare such a conservative calculation with the landslide frequency, found in the field. Therefore, in figure 6.5 the normalized distributions over five slope classes of the cumulative probability of sliding (% F< 1), is compared with the normalized distribution of the number of landslides per unit area. The figure shows that the predicted relative chance is too low for the lower slope classes and too high for the higher slope classes.The conclusion is, that the distribution of the maximum groundwater levels cannot be considered independently from the slope angle. Obviously, lower slope angle classes give relatively higher maximum groundwater levels than the higher slope angle classes.

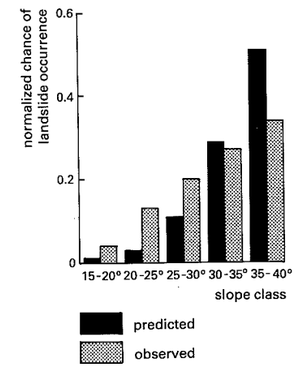

Figure 6.5 A comparison between the normalized distribution over five slope classes of the cumulative probability of sliding (% F < 1) and the normalized distribution of the number of landslides per unit area, as compiled in the study area.

Table 6.7 gives for five slope classes the mean and standard deviation of the F-values and the percentage probability, that the safety factor (F) has a value lower than one, indicating instability. The hazard analyses were carried out for three different depths of sliding: (1) 0.4-0.6 m (maximum density of the roots), (2) 1.8-2.0 m (maximum

Table 6.7 The probability of landslide occurrence (% F<1, column 3, 6, 9) for different slope classes in the basin of the Riou Bourdou (France)

slope class	depth of slip surface	max. GW level			max. GW level without trees			GW <3m		
		% F<1	mean	S.D.	% F<1	mean	S.D.	%F<1	mean	S.D.
40°-35°	O	0.0	10.6	4.9	0.0	5.6	2.4	0.0	11.1	5.0
	M	0.0	3.4	1.2	12.4	1.8	0.6	0.0	4.9	1.5
	D	51.8	1.1	0.4	50.8	1.0	0.4	16.6	1.7	0.6
35°-30°	O	0.0	10.9	5.3	0.0	6.5	2.9	0.0	12.9	5.1
	M	0.0	3.8	1.3	8.4	2.0	0.7	0.0	5.4	1.9
	D	36.1	1.2	0.4	35.6	1.2	0.4	7.4	2.0	0.8
30°-25°	O	0.0	12.2	5.0	0.0	6.9	2.0	0.0	12.5	5.6
	M	0.0	4.3	1.5	3.2	2.3	0.8	0.0	6.8	1.8
	D	23.2	1.5	0.6	23.9	1.5	0.5	1.6	2.1	0.8
25°-20°	O	0.0	13.3	6.6	0.0	7.1	3.0	0.0	15.5	7.1
	M	0.0	4.9	1.7	1.6	2.8	0.9	0.0	7.6	2.3
	D	10.2	1.8	0.6	11.0	1.8	0.6	0.0	2.9	1.0
20°-15°	O	0.0	17.7	8.6	0.0	10.2	4.3	0.0	20.5	8.3
	M	0.0	6.4	2.2	0.0	3.6	1.2	0.0	9.1	3.0
	D	1.4	2.1	0.8	1.4	2.3	0.8	0.0	3.9	1.3

Three situations are simulated: maximum groundwater level (column 3-5); maximum groundwater level without trees (column 6-8); groundwater 3 metres, below the surface with trees (column 9-11). Three depths of potential slip surface has been analyzed (column 2) : 0.4-0.6 (O); 1.8-2.0 metres (M); 4-6 metres (D). Mean = mean value of safety factor after 500 Monte Carlo simulations; S.D = standard deviation of the safety factor values.

possible depth of roots), and 4-6 m (expected thickness of colluvium material).
Table 6.7 shows there is a real danger for deeper landslides (4-6 m), if the groundwater level is at its maximum. Piezometric measurements on the plots revealed that in the landslides groundwater reaches to the topographical surface, while at the same time in the stable areas groundwater remains 2 to 3 metres below the surface. It indicates that in case of lower groundwater levels for all slope classes, the landslide hazard is very low. This again stresses the fact, that an estimation of maximum groundwater levels in the colluvium, within each land unit, is very important for the a more precise assessment of the landslide hazard. An indication of the maximum groundwater height within the slope class zones in the field gives more precise information about landslide hazard, than can be deduced from table 6.7. This can be done by introducing simple groundwater models, relating input of rain, slope angle and groundwater height.
Table 6.7 also shows the mechanical effect of the forest cover on the stability within the different land units. It appeared that after the removal of trees, there is a slight increase in hazard for mass movements with slippage at a depth of about 2 metres.

6.4 Conclusions

The use of discriminant analysis for landslide hazard zonation in the Ubaye river valley is questionable The reasons are:
- The high percentage of incorrect classified sites due to methodological errors. This large methodological error is caused by the uniformity in the study area of several of the terrain parameters.
- The low unbiased percentage of correctly classified sites. This indicates a low reliability of the predictive power of the discriminant function.

Some tentative conclusions may be drawn:
- The analysis gives no indication of the relative contribution of the various terrain parameters to the landslide hazard, because the parameters are correlated. The most important parameters of the discriminant function were: the presence of steps-/terracettes, maximum rooting depth, ground area of meso relief, type of material, maximum slope angle, thickness of litter layer, and basal area of trees.
- The analysis indicates a frequent association between forests and the landslides in the study area. This is probably due to the planting of trees at the turn of the century in areas, which suffered most from erosion, including mass movement. Apparently these mass movements are still active.

A more laborious way of quantitative hazard analysis is the use of soil mechanical models, in order to determine the probability of failure within a certain land unit. The case study here presented, used the infinite slope model. It shows that the use of sensitivity analysis enables the selection of the most important factors. A very sensitive factor proved to be the slope angle. Therefore, it was proposed to distinguish hazard zones, according to the slope angle. For all other parameters, a randomized value was introduced. It is assumed that this randomized value is drawn from a probability distribution, which is valid for the whole area under investigation. This probability distribution can be assessed with little effort.
Given the probability distributions of these parameters, the probability of a safety factor, less than one, can be calculated using Monte Carlo simulations. This probability is considered to be a measure for landslide hazard within a land unit.
The results show that a reliable estimate of maximum groundwater levels can lead to a more precise assessment of the landslide hazard. The soil mechanical approach also shows that different scenarios can be developed to study the effect of human activity on landslide hazard. In this case the effect of deforestation and changes in groundwater level on the landslide hazard was analyzed. It showed a relatively weak influence of the mechanical effect of a forest cover on the landslide hazard, while changes in the groundwater level did considerably change the landslide hazard. Groundwaterlevel close to the surface are assiociated with high probabilities of failure.
A combination of the qualitative and quantitative assessment of the landslide hazard, on basis of detailed geomorphological mapping and soil mechanical analyses may lead to a more valuable hazard assessment of landslides on regional scale.

SUMMARY AND GENERAL CONCLUSIONS

Mass movement is the major denudational process in steeply sloping terrain. Field observations indicate that human activity influences the initiation and frequency of mass movement. On the other hand mass movements also affect human activities. Therefore it is evident that, when human activities are planned, there is a need for methods to assess and evaluate the hazard of mass movement.
This study focuses on the assessment of the hazard on local and regional scale of a particular type of mass movement, the landslide. A landslide is a mass movement, in which movement occurs along a specific surface.
Landslide hazard is defined by Varnes (1984) as the probability of occurrence of landslides within a specific period of time (temporal hazard) and within a given area (spatial hazard).
The assessment of landslide hazard involves the use of analytical or numerical methods. Such methods are commonly based on the assumption of limit equilibrium. The limit equilibrium method postulates that a slope fails, if a rigid soil mass starts to slide over a failure surface. The assumption is, that the overall slope and each part of it are in static equilibrium at the moment of failure. Such a method explicitly takes into account the primary factors, unit weight, cohesion, angle of internal friction, slope angle and pore pressure, and is based on the safety factor (equation 1.1).
The deterministic safety factor concept is limited in its use for landslide hazard assessment. The limitations are due to following problems:
- the translation of a safety factor into a landslide hazard. This translation is not easy. In the deterministic safety factor concept the actual landslide hazard is assessed on the basis of past experiences. This translation can be criticized: the assessment of a landslide hazard depends on personal judgement and is therefore subjective and often arbitrary. Furthermore, the translated safety factor does not result in a linearly scaled landslide hazard in any of the limit equilibrium methods.
- the assumption of a constant safety factor for all individual slices of a slide is not valid. Numerous stress-deformation studies on the basis of finite element method have shown that the safety factor may be quite different (Chowdhury and A-Grivas, 1982).
- the inherent variability of vegetation, soil or rock properties is not accounted for in a deterministic safety factor concept.
An alternative to the deterministic safety factor concept is the probabilistic safety factor concept where the landslide hazard is expressed in terms of the probability of a safety factor less than unity. The probability of failure can be estimated when in addition to the safety factor, its variance is known. The mean and variance of the safety factor of each slice may be calculated on the basis of the mean and variances of the primary factors.
In the probabilistic safety factor concept, the translation of a safety factor into a landslide hazard is standardized. It is still a subjective method, because of the need to choose a probability function of the safety factor.

Soil mechanical methods to assess landslide hazard on a local scale (chapter 2)

In the conventional analysis a constant value of the safety factor is assumed for all individual slices along the failure surface. Two conventional analyses were extended with a variance equation, (1) GLEA, a method that satisfies all equilibrium conditions and is not redundant and (2) the Fellenius method.
The probabilistic safety factor concept provides alternatives to the assumption of a constant safety factor along the failure surface. Two alternative methods were formulated:
(1) a method based on the assumption of a constant probability of failure along the failure surface (PROBCON)
(2) a method based on the assumption of a constant variance of the safety factor along the failure surface (VARCON).
The methods based on the probabilistic safety factor concept may provide more details on the stress situation in a landslide. However, comparing the probabilistic methods it appears that there are considerable differences in the outcomes of the distribution of the safety factors, variance and the ratio λ of the vertical and horizontal interslice forces. This indicates that the four methods incorporate different stress distributions along the failure surface. This implies that probably neither one of the methods describes the actual stress situation and that the results should be interpreted with some caution.
The variance of the safety factor seems to be influenced primarily by the normal stress at the failure surface. The normal stress is a function of location of the failure surface, the internal forces and bulk density. Furthermore, the variances of the safety factors estimated by the VARCON method are nearly independent of the conditions in shear strength or hydrology of the slope.
The results of the probabilistic Fellenius method are quite different from the other probabilistic methods. This indicates that the way the interslice forces are incorporated in the method influences the results considerably.
The assumption of a constant probability of failure along the failure surface or a constant safety factor along the failure surface is questionable in case of heterogeneous profiles and sometimes result in physically unrealistic stress situations in the sliding soil mass.
The VARCON method seems to be the appropriate method to use when the landslide hazard of a slope with heterogenous material, either in bedding or by changes in the material strength has to be estimated.

The variability of strength parameters used in methods to assess landslide hazard on a local scale (chapter 3)

The variability of strength parameters plays an important role in the assessment of landslide hazard by means of probabilistic limit equilibrium methods.
The variability of the strength parameters, like cohesion and angle of internal friction were estimated on 131 core samples taken at plot 1, Riou Bourdou. The variances in the cohesion and the angle of internal friction are large, but well within the range of coefficients of variation upto 80%, as mentioned by Lee et al (1983).

The following conclusions can be drawn from the data:
- the absence of a spatial variation in the data on cohesion and angle of internal friction, implies that the mean of the total data set is the best estimate of these parameters;
- the pure nugget effect in the data shows that the strength of a soil sample is caused by processes and interactions on a scale much smaller than the sample size;
- the failure envelopes based on the direct shear tests are better approximated by a power model ($y = P_1 x^{P_2}$, where y = shear strength, x = normal stress), than by a straight line as prescribed by the Coulomb failure theory;
- the parameters cohesion and angle of internal friction are independent parameters, as shown by their correlation, r=-0.0578. Apparently, the assumption made in the derivation of the variance equation of a safety factor, is correct.
- the constants P_1 and P_2, are strongly correlated (r = -0.8035), suggesting that it is possible to describe the failure envelope by only one parameter. Despite the reduction by one parameter, the resulting probabilistic limit equilibrium models were far more complicated than the conventional methods based on a straight line approximation.
- for the core samples taken in the root zone and those from the rootfree subsoil, no significant difference in the mean of the strength parameters could be found. This is in agreement with the results of unconfined compression tests where no relation between the root content and the root reinforcement could be established. Apparently the roots do not contribute to the shear strength of the soil. However, literature indicates opposite results: e.g. Ziemer (1981) and O'Loughlin (1972), both using large direct shear boxes for testing on peak strength, found correlations between root content and shear strength with $r^2 = 0.79$ and $r^2 = 0.56$ respectively. Reported magnitudes of root reinforcement range between 2 and 25 kPa (Burroughs and Thomas, 1977; Ziemer, 1981; Riestenberg and Sovonick-Dunford, 1983).

The mechanical effects of roots on the variation in the shear strength of a soil (Chapter 4)

The processes causing the reinforcement of the soil by roots are not well understood. Experimental data are scarce, sometimes conflicting and not always conclusive.
A model for the reinforcement of the soil was derived and validated in this chapter. The model is based on the following concept of the processes involved. Due to a displacement along a shear zone, a root which crosses the shear zone, will elongate. This elongation generates a stress inside the root. This root stress gives rise to additional stresses in the shear zone. The root stress is transferred to the soil by a friction stress at the root-soil contact. The friction stress at the root-soil contact causes the anchorage of a root in the soil. The total force, that can be applied to a root is limited either by breaking of the root, or by slipping of the root through the soil.
The derivation of a model for reinforcement of a soil by roots, comprised the following steps: (1) estimation of the forces acting on the shear zone due to the presence of roots, (2) estimation of the root reinforcement of the soil assuming no restriction on the stresses applicable to roots, and (3) inclusion of limitations on the stresses applicable to roots.

The model is formulated by equation 4.19, 4.20 and 4.21 and needs as input variables: initial angle between the root and the shear zone, the displacement along the shear zone, the elastic modulus of roots, E_r, the rupture stress of the root, the friction stress at the root-soil contact and the cross sectional area of roots per cross sectional area of soil.
The model was validated against the well documented experiments of Waldron et al. (1983). It appeared, that averaged root reinforcement of the soil due to roots with different initial angles to the shear zone is in good agreement with the data of Waldron et al. (1983; see figure 4.6)
The following tentative conclusions and remarks result from model simulations:
- The average elongation of randomly oriented roots crossing a shear zone remains, to a shear strain of 0.4, approximately zero. This shows that roots are contributing to the shear strength of a soil only at shear strains larger than 0.4. At these shear strains most soils are already at their residual strength (Lee et al., 1983). Therefore, the mechanical effects of roots increase the residual strength of a soil, i.e. roots make a soil less brittle. Shear strains of beyond 0.4 are hardly reached on small samples. This explains why no relationship was found between root content and the peak strength characteristics of a soil (paragraph 3.3.3). Conventional direct shearing and unconfined compression shear tests are unsuitable in estimating the effects of roots on the peak strength.
- A limit equilibrium analysis is based on the assumption of static equilibrium, i.e. no movement takes place. Root reinforement of a soil only starts after displacements have taken place. Thus root reinforcement needs no consideration in a limit equilibrium analysis.
- The elongations of roots, with different initial angles to the shear zone, vary for a given displacement. The root stress is linearly related to the elongation of a root (eq 4.6). Therefore, the stresses inside a root will vary for roots with a different initial angle to the shear zone at the any displacement. The roots will not simultaneously reach the rupture stress, as is assumed by Wu et al. (1979) and Riestenberg and Sovonick-Dunford (1983).
- A realistic estimation of the friction stress between root and soil is still not feasible. The parameters describing stresses and strength characteristics at the root-soil contact, are difficult to quantify. Two proposed mechanisms, however, related to roots exerting stress on a soil, explain the high experimental values of the friction stress, as mentioned in literature.
- Root slippage rather than breakage of roots may be the prevailing process, limiting root reinforcement.
- The following concept of the development of a landslide and the influence of the roots on the strength of the soil may be outlined: at maximum groundwater levels, in early spring, a slope may fail for the first time. This initial failure of a slope happens as the soil is at peak strength. After failure and sufficient displacement have taken place (shear strains > 0.4), the soil is at its residual strength and the root reinforcement of a soil increases. This may enlarge the total shear strength (root reinforcement, plus the residual strength of the soil) and may cause the landslide to stop sliding. It may even be possible that the total strength rises to a level above the peak strength of the soil material alone. The influence of the root reinforcement on

the total strength of the soil will be most obvious with soil materials, which do not exhibit a clear difference between peak and residual strength. After the landslide stops, the root stress and therefore the root reinforcement may decrease, due to processes like root growth or deformations at the root-soil contact.

Examples of landslide hazard analysis on a local scale (chapter 5)

The presence of morainic material on top of impervious marls (terres noires) in combination with relief and hydrological factors induce a large number of mass movements in the basin of Barcelonnette. Many of these mass movements were (re-) activated during the 18th and 19th century, due to abandoning of agricultural land and the logging of large forested areas.
The landslide hazard of three typical slopes in the study area were assessed. The analysis uses the VARCON method. Two slopes are on plot 1, Riou Bourdou. One represents the stable locations, while the other illustrates a landslide typical for colluvium. The last profile is from plot 2, the landslide next to "la Maison Forestiere Le Treou". This landslide is one of the few that partly developed in coarse morainic material. Both plots are described in paragraph 1.4.
Some tentative conclusions regarding the landslide hazard on a local scale in the study area may be drawn:
- The landslides have a failure probability of 50% in early spring, when groundwater levels are close to the ground surface (about 0.2 till 0.5 metres below the surface). This decreases to a probability of 30 %, when the groundwater levels drop to more than 3 metres below the surface.
- The stable areas have under field conditions of peak strength and a groundwater level of 3 metres below the surface, a landslide hazard, that is slightly lower than that of a landslide, with a groundwater level at 0.3 metres below the surface and peak strength.
- The distribution of the probability of failure along the failure surface indicates landslides, consisting of several 'blocks' of material with a comparable probability, separated by stretches of lower probability of failure.
- The influence of water pressure at the failure surface on the probability of failure is higher under peak strength conditions than under residual conditions. This shows, that changes in the hydrology of a slope have a larger influence on initial failure than on the continuation of movement of an already failed soil mass.
- The overburden of vegetation hardly affects the probability of failure of a slope. Removal of the vegetation may increase the landslide hazard, due to their effect on the hydrology of the slope: the removal may reduce the water losses through interception and evaporation, thus increasing the amount of infiltrating water. This may result in groundwater levels closer to the surface. This condition increases the landslide hazard.

Assessment of landslide hazard on a regional scale (Chapter 6)

On regional scale, usually statistical methods are applied for assessment of landslide hazard. In chapter 6 a soil mechanical approach is proposed to assess the landslide hazard on a regional scale. Both the statistical and soil mechanical approach are applied to the study area.
In a statistical approach, the landslide hazard may be assessed by a statistical (multivariate) analysis. The factors contributing to the landslide hazard, are weighted quantitatively, according to their statistical significance. A standard technique is discriminant analysis. This analysis can be used to select the critical terrain parameters and to assess their relative contribution to the landslide hazard. A standardized form was used to gather the data on terrain parameters. They covers aspects of geomorphology, geology, hydrology, vegetation and morphometry of the mass movements in an area.
The use of discriminant analysis for landslide hazard zonation in the Ubaye river valley is questionable. The reasons are:
- The high percentage of incorrect classified sites due to methodological errors. This large methodological error is caused by the uniformity in the study area of several of the terrain parameters.
- The low unbiased percentage of correctly classified sites. This indicates a low reliability of the predictive power of the discriminant function.
Some tentative conclusions may be drawn:
- The analysis gives no indication of the relative contribution of the various terrain parameters to the landslide hazard, because the parameters are correlated. The most important parameters of the discriminant function were: the presence of steps-/terracettes, maximum rooting depth, ground area of meso relief, type of material, maximum slope angle, thickness of litter layer, and basal area of trees.
- The analysis indicates a frequent association between forests and the landslides in the study area. This is probably due to the planting of trees at the turn of the century in areas, which suffered most from erosion, including mass movement. Apparently these mass movements are still active.
A more laborious way of quantitative hazard analysis is the use of soil mechanical models, in order to determine the probability of failure within a certain land unit. The case study here presented, used the infinite slope model. It showed that the use of sensitivity analysis enables the selection of the most important factors. A very sensitive factor proved to be the slope angle. Therefore, it was proposed to distinguish hazard zones, according to the slope angle. For all other parameters, a randomized value was introduced. It is assumed that this randomized value is drawn from a probability distribution, which is valid for the whole area under investigation. This probability distribution can be assessed with little effort.
Given the probability distributions of these parameters, the probability of a safety factor, less than one, can be calculated using Monte Carlo simulations. This probability is considered to be a measure for landslide hazard within a land unit.
The results show that a reliable estimate of maximum groundwater levels can lead to a more precise assessment of the landslide hazard. The soil mechanical approach also shows that different scenarios can be developed to study the effect of human activity

on landslide hazard. In this case the effect of deforestation and changes in groundwater level on the landslide hazard was analyzed. It showed a relatively weak influence of the mechanical effect of a forest cover on the landslide hazard, while changes in the groundwater level did considerably change the landslide hazard. Groundwater levels close to the surface are assoiciate with high probabilities of failure.
A combination of the qualitative and quantitative assessment of the landslide hazard, on basis of detailed geomorphological mapping and soil mechanical analyses may lead to a more valuable hazard assessment of landslides on regional scale.

SAMENVATTING

Aardverschuivingen zijn het belangrijkste denudatieve proces in bergachtige gebieden. Veldwaarnemingen geven aan dat menselijke activiteit het optreden en de frequentie van aardverschuivingen beïnvloedt. Aan de andere kant wordt de menselijke activiteit beïnvloed door aardverschuivingen. Het zal duidelijk zijn dat er behoefte is aan methoden die het gevaar van het optreden van aardverschuivingen kunnen taxeren en evalueren bij de planning van menselijke activiteiten.
In dit proefschrift wordt de nadruk gelegd op de taxatie van het gevaar voor het optreden van aardverschuivingen op lokale en regionale schaal. In het bijzonder wordt gekeken naar aardverschuivingen waarvan het glijvlak duidelijk gedefinieerd is.
Het gevaar voor aardverschuivingen wordt door Varnes (1984) gedefinieerd als de kans van het optreden van aardverschuivingen in een bepaalde periode (temporeel gevaar) en binnen een bepaald gebied (ruimtelijk gevaar).
De taxatie van het aardverschuivingsgevaar houdt het gebruik in van analytische of numerieke methoden. Deze methoden worden gewoonlijk gebaseerd op de aanname van een beperkt evenwicht. De analysemethode van een beperkt evenwicht veronderstelt dat wanneer een helling bezwijkt, een starre moot grond begint te glijden over een glijvlak. De basale aanname is dat de gehele helling en elk gedeelte ervan in een statisch evenwicht zijn op het moment van bezwijken. Dit type analyse houdt expliciet rekening met de primaire factoren, volumegewicht, cohesie, hoek van interne wrijving, hellingshoek en waterdrukken en is gebaseerd op de veiligheidsfactor (vergelijking 1.1).
Het deterministische veiligheidsfactorconcept is beperkt in zijn gebruik om het aardverschuivingsgevaar te taxeren. De beperkingen zijn als volgt samen te vatten:
- de omzetting van een veiligheidsfactor in een aardverschuivingsgevaar is niet gemakkelijk. In het deterministische veiligheidsfactorconcept wordt de taxatie gedaan aan de hand van ervaringen met hellingen met een vergelijkbare veiligheidsfactor. Deze manier van omzetten kan worden bekritiseerd: De keuze van het aardverschuivingsgevaar hangt af van persoonlijk inzicht en is daardoor subjectief en vaak willekeurig. Verder geldt dat de omzetting van de veiligheidsfactor voor geen van de kritisch evenwicht situatie methoden lineair is.
- de aanname van een constante veiligheidsfactor voor alle individuele hellinggedeelten is niet geldig. Talrijke spanning-deformatiestudies op basis van de eindige elementenmethode hebben aan getoond dat de veiligheidsfactor duidelijk kan variëren.
- de vegetatie-, bodem- en rotseigenschappen zijn variabel. Hiermee houdt het deterministisch veiligheidsfactorconcept geen rekening.
Een alternatief voor het deterministisch veiligheidsfactorconcept is het probabilistisch veiligheidsfactorconcept, hierbij wordt het aardverschuivingsgevaar uitgedrukt in termen van de kans dat een veiligheidsfactor kleiner dan 1 wordt. De kans van bezwijken kan worden bepaald wanneer naast een gemiddelde waarde van de veiligheidsfactor, de variantie van de veiligheidsfactor bekend is. De variantie of spreiding van de veiligheidsfactor kan berekend worden met behulp van de kritisch evenwicht situatie methoden, wanneer er gebruik gemaakt wordt van de spreiding in de waarden van parameters die in deze methoden gebruikt worden.

Het probabilistisch veiligheidsfactorconcept is nog steeds subjectief, omdat er een waarschijnlijkheids-verdeling voor de veiligheidsfactor aangenomen moet worden. Maar de omzetting van een veiligheidsfactor naar een kans voor het optreden van aardverschuivingen is gestandaardiseerd.

Grondmechanische methoden voor de taxatie van het aardverschuivingsgevaar op lokale schaal. (hoofdstuk 2)

In een conventionele analyse wordt een constante veiligheidsfactor aangenomen langs het glijvlak. Twee conventionele analyses zijn uitgebreid met een variantievergelijking, (1) GLEA, een methode die aan alle evenwichtcondities voldoet en niet overbepaald is en (2) de Fellenius methode.
Het probabilistisch veiligheidsfactorconcept schept de mogelijkheid om alternatieven voor de constante veiligheidsfactor langs het glijvlak te geven. Twee alternatieve methoden zijn afgeleid:
(1) een methode gebaseerd op de aanname van een constante kans van bezwijken langs het glijvlak (PROBCON).
(2) een methode gebaseerd op de aanname van een constante variantie van de veiligheidsfactor langs het glijvlak (VARCON).
De methoden gebaseerd op het probabilistisch veiligheidsfactorconcept kunnen meer details geven over de spanningssituatie in een aardverschuiving. Uit een vergelijking van de probabilistische methoden blijkt dat er grote verschillen in de uitkomsten van de verdeling van de veiligheidsfactoren, variantie in de veiligheidsfactor en de ratio tussen de horizontale en verticale interlaminaire krachten zijn. Dit geeft aan dat alle vier methoden een andere spanningsverdeling langs het glijvlak impliceren. Dit betekent dat waarschijnlijk geen van de methoden de werkelijke spanningssituatie beschrijft. Bij de interpretatie moet dan ook enige voorzichtigheid in acht worden genomen.
De variantie van de veiligheidsfactor lijkt voornamelijk beïnvloed te worden door de normaalspanning op het glijvlak. De normaalspanning is een functie van de ligging van het glijvlak, de interne krachten en het volumegewicht. Verder blijkt dat de variantie bepaald met de VARCON methode bijna onafhankelijk te zijn van de condities van de helling.
De resultaten van de Fellenius methode zijn volkomen verschillend van die van de andere probabilistische methoden. Dit betekent dat de manier waarop de interne krachten in de methoden verdisconteerd zijn de resultaten beïnvloeden.
De aannamen van een constante kans van bezwijken of een constante veiligheidsfactor langs het glijvlak zijn discutabel in het geval van heterogene profielen en resulteren soms in fysisch onmogelijke spanningssituaties in de afglijdende moot grond.
De VARCON methode lijkt de aangewezen methode te zijn om het gevaar voor aardverschuivingen te bepalen van hellingen bestaande uit heterogene materialen.

De variabiliteit van sterkteparameters, die gebruikt worden in methoden voor de taxatie van aardverschuivingen op lokale schaal (hoofdstuk 3)

De variabiliteit van de sterkteparameters speelt een belangrijke rol in de taxatie van het aardverschuivingsgevaar door middel van probabilistische methoden.
De variabiliteit van de sterkteparameters, als cohesie en hoek van interne wrijving zijn bepaald met behulp van 131 monsters verkregen op plot 1, Riou Bourdou.
De variantie in cohesie en hoek van interne wrijving is groot, maar binnen de range van waarden die er voor gegeven wordt in Lee et al. (1983).
De volgende conclusies kunnen worden getrokken:
- De afwezigheid van een ruimtelijk afhankelijke variatie van de cohesie en de hoek van interne wrijving, betekent dat het gemiddelde van de totale verzameling gegevens de beste schatting is van deze parameters;
- Het bestaan van een puur 'nugget' effect in de gegevens toont aan dat de sterkte van een bodemmonster bepaald wordt door processen en interacties op een schaal die veel kleiner is dan de monster grootte;
- de 'failure envelope' gebaseerd op metingen van 'direct shear' experimenten wordt beter beschreven door een vergelijking in de vorm van $y=P_1x^{P2}$, waarin y, de schuifsterkte en x, de normaal spanning is en P_1 en P_2 regressieconstanten zijn, dan door de rechte lijn, zoals wordt voorgeschreven door de Coulomb bezwijktheorie;
- de parameters cohesie en hoek van interne wrijving zijn onafhankelijk, zoals wordt aangetoond door hun correlatiecoëfficiënt van r=-0.0578. Dit is blijkbaar terecht aangenomen in de afleiding van de variantievergelijking van de veiligheidsfactor;
- de parameters P_1 an P_2 zijn sterk gecorreleerd (r=-0.8035). Dit suggereert dat het mogelijk is de 'failure envelope' te beschrijven met behulp van 1 parameter. Ondanks de reductie met 1 parameter zijn de resulterende kritisch evenwicht situatie methoden veel gecompliceerder dan wanneer de conventionele rechte lijn beschrijving van de 'failure envelope' wordt gebruikt;
- tussen de monsters, genomen in de wortelzone en die van de wortelvrije ondergrond kan geen verschil in het gemiddelde van de sterkteparameters worden vastgesteld. Dit komt overeen met de resultaten van 'unconfined compression tests' waarmee geen relatie tussen het wortelgehalte en de pieksterkte van de grond kan worden vastgesteld. Blijkbaar dragen de wortels niet bij aan de sterkte van de grond. Dit is in sterke tegenstelling tot hetgeen vaak in de literatuur wordt aangetroffen, waarin bijdragen van de wortels in de sterkte van de bodem worden genoemd van 2-25 kPa.

De mechanische effecten van wortels op de variatie in schuifsterkte van een grond (hoofdstuk 4)

De werking van de processen, die de versterking van de grond door wortels veroorzaken is niet duidelijk. Experimentele gegevens zijn schaars, soms tegenstrijdig en niet altijd afdoende. In dit hoofdstuk wordt een theoretisch model voor de versterking van de grond door wortels afgeleid en gevalideerd. Het model is op het volgende concept van de betrokken processen gebaseerd: door een verplaatsing langs een schuifzone wordt een wortel die deze schuifzone passeert, verlengd. Deze verlenging

wekt een spanning op in de wortel. Deze wortelspanning is de oorzaak van additionele spanningen in de schuifzone. De wortelspanning wordt op de grond overgebracht door wrijving aan het wortel-grond contact. De wrijvingsspanning aan het wortel-grond contact veroorzaakt de verankering van een wortel in de grond. De totale kracht die kan worden toegediend aan een wortel wordt beperkt doordat de wortel breekt of doordat de wortel door de grond gaat slepen.
De afleiding van het model omvat de volgende stappen: (1) de schatting van de krachten die werken in de schuifzone bij de aanwezigheid van wortels, (2) de schatting van de versterking van de grond bij de aanname dat er geen beperking is aan de spanningen die kunnen worden toegediend aan wortels, en (3) het meenemen van beperkingen op de spanningen die toegediend kunnen worden aan wortels.
Het model is weergegeven met de vergelijkingen 4.19, 4.20 en 4.21 en heeft als invoer gegevens nodig: de initiële hoek van de wortels naar de schuifzone, de verplaatsing langs het glijvlak, de elasticiteitsmodulus van de wortels, de spanning nodig om een wortel te breken, de wrijvingsspanning aan het wortel-grond contact en het oppervlak aan wortel per doorsnede van de bodem.
Het model werd gevalideerd met behulp van de uitvoerig beschreven experimenten van Waldron et al. (1983). Het lijkt, dat het middelen van de versterking van de bodem door wortels met een verschillende initiele hoek naar de schuifzone, leidt tot een schatting van de versterking van de grond door wortels die goed overeenkomt met de door Waldron et al. gemeten versterking.
De volgende voorzichtige conclusies en opmerkingen resulteren uit de model simulaties:
- De gemiddelde verlenging van de wortels is tot bij vervorming van het glijvlak van 0.4 praktisch nog gelijk aan nul. Dit geeft aan dat wortels pas aan de schuifsterkte van een grond bijdragen wanneer de vervorming van het glijvlak meer is dan 0.4. Bij deze vervormingen zijn de meeste gronden op hun reststerkte (Lee et al., 1983). De mechanische effecten van wortels doen de reststerkte van de grond toenemen. De vervorming van het glijvlak van 0.4 wordt zelden gehaald in de kleine monsters. Daarom wordt er ook een geen relatie tussen de sterkteparameters en het wortelgehalte gevonden. De monsters die gebruikt worden in 'unconfined compression tests' en 'direct shear tests' zijn te klein om voldoende vervorming te bereiken;
- Een kritisch evenwicht situatie analyse methode is gebaseerd op de aanname van statisch evenwicht. Dit betekent dat er geen beweging plaatsvindt. Versterking van grond door wortels vindt pas plaats wanneer er verplaatsingen zijn opgetreden. Dus versterking van de grond door wortels hoeft niet beschouwd te worden in een kritisch evenwichtssituatie analyse;
- De verlenging van de wortels met verschillende initiële hoek naar de schuifzone is verschillend voor een bepaalde verplaatsing. De wortelspanning is lineair gerelateerd aan de uitrekking van de wortel. Daardoor is de spanning in de wortels met een verschillende initiele hoek naar het glijvlak eveneens verschillend bij een bepaalde verplaatsing. De wortels zullen nooit allemaal tegelijkertijd breken.
- Een realistische schatting van de wrijvingsspanning tussen de wortel en de grond is nog niet mogelijk. De parameters die de spanningen en de sterkteeigenschappen aan het wortel-grond contact beschrijven zijn moeilijk te kwantificeren. Twee voorgestelde mechanismen, waarbij wordt aangenomen dat de wortel een kracht uitoefent op de

grond, verklaren de hoge experimentele waarden van de wrijvingsspanningen die in de literatuur worden gevonden;
- Het slippen van wortels door de bodem is meer nog dan het breken van wortels de beperkende omstandigheid voor de versterking van de grond door wortels.
- Het volgende concept van de ontwikkeling van een aardverschuiving en de invloed van wortels op de sterkteeigenschappen van de grond kan worden geschetst:
Onder de maximale grondwaterstanden in het voorjaar kan een helling voor de eerste keer bezwijken, wanneer de pieksterkte van de grond wordt overschreden. Na bezwijken en voldoende verplaatsing (vervormingen van het glijvlak > 0.4) is de grond op zijn reststerkte en zal de versterking van de grond door wortels toenemen. Dit kan de totale sterkte van de grond (=versterking als gevolg van wortels plus de reststerkte van de grond) vergroten en de aardverschuiving doen stoppen met bewegen. Het is zelfs mogelijk dat de totale sterkte toeneemt tot een niveau dat boven de pieksterkte van de grond alleen ligt. De invloed van de versterking door wortels zal het meest prominent aanwezig zijn bij gronden die geen duidelijk verschil hebben tussen de rest- en pieksterkte. Nadat de aardverschuiving is gestopt, kan de wortelspanning afnemen als gevolg van processen als wortelgroei of vervormingen aan het wortel-grondoppervlak.

Voorbeelden van analyses van het gevaar voor aardverschuivingen op lokale schaal (hoofdstuk 5)

De aanwezigheid van morenemateriaal bovenop ondoorlatende mergels (terres noires) in combinatie met het reliëf en hydrologische factoren hebben geleid tot een groot aantal aardverschuivingen in het gebied van het bekken van Barcelonnette. Veel van deze aardverschuivingen zijn geactiveerd gedurende de 18de en 19de eeuw, toen landbouwgebieden verlaten en grote bosgebieden gekapt werden.
Van drie profielen, die typisch voor het onderzoeksgebied zijn, is het aardverschuivingsgevaar getaxeerd. De analyses maken gebruik van de VARCON methode. Twee profielen komen van plot 1, Riou Bourdou. Een vertegenwoordigt de stabiele omstandigheden, terwijl de andere een typisch voorbeeld is van een aardverschuiving ontwikkeld in kolluvium. Het derde en laatste profiel is van plot 2, de aardverschuiving naast het boshuis 'Le Treou'. Deze aardverschuiving is een van de weinige die gedeeltelijk is ontwikkeld in grof morenemateriaal.
Een paar voorzichtige conclusies kunnen getrokken worden betreffende het gevaar voor aardverschuivingen op lokale schaal in het studiegebied:
- de aardverschuivingen hebben een bezwijkkans van 50 % in het vroege voorjaar wanneer de grondwaterstanden het dichtst (0.2-0.5 m) onder het maaiveld staan. Deze kans neemt af tot 30 % wanneer het grondwater naar meer dan 3 meter onder het maaiveld zakt.
- de stabiele gebieden hebben een iets kleinere kans om te bezwijken dan een aardverschuiving, wanneer beiden uit materiaal van pieksterkte bestaan, en het grondwater 3 m onder het maaiveld staat in het stabiele gebied en 0.3 m bij de aardverschuiving.

- de verdeling van de kans van bezwijken langs het glijvlak geeft aan dat de aardverschuivingen uit een aantal blokken materiaal bestaan met een gelijke kans gescheiden door stukken met een lagere kans van bezwijken.
- de invloed van de waterdrukken aan het glijvlak op de kans van bezwijken is hoger onder pieksterkte dan onder reststerkte condities. Dit geeft aan dat veranderingen in de hydrologie van een helling een grotere invloed hebben op initieel bezwijken, dan op de continuatie van de beweging van een reeds bezweken moot grond.
- het gewicht van de vegetatie beïnvloedt nauwelijks de kans van het bezwijken van een helling. Verwijdering van de vegetatie kan het gevaar voor aardverschuivingen doen toenemen, vanwege haar potentiele effecten op de hydrologie van de helling. Na verwijdering van de vegetatie nemen de verliezen als gevolg van interceptie en evapotranspiratie af. Er kan meer water infiltreren. Dit kan resulteren in grondwaterniveaus dichter bij het maaiveld. Deze omstandigheid kan het aardverschuivingsgevaar doen toenemen.

Taxatie van het aardverschuivingsgevaar op regionale schaal (hoofdstuk 6)

Op een regionale schaal worden voor de taxatie van het aardverschuivingsgevaar meestal statistische methoden gebruikt. In hoofdstuk 6 wordt een grondmechanische benadering voorgesteld om het gevaar voor aardverschuivingen op regionale schaal te schatten. Zowel de statistische als de grondmechanische benadering zijn toegepast op het onderzoeksgebied.
In een statistische benadering kan het aardverschuivingsgevaar getaxeerd worden door statistische (multivariate) analyses. De meest significante factoren, die bijdragen aan het gevaar, worden kwantitatief gewogen op basis van hun statistische significantie. Een standaard techniek is de discriminant analyse. De analyse kan worden gebruikt voor de selectie van de meest kritische terreinparameters en hun relatieve invloed op het aardverschuivingsgevaar. Een gestandaardiseerd formulier is gebruikt voor de verzameling van gegevens betreffende terreinparameters. Het formulier beslaat aspecten van de geomorfologie, geologie, vegetatie and morfometrie van de aardverschuivingen in het gebied.
Het gebruik van de discriminant analyse is twijfelachtig door:
- het hoge percentage fout geclassificeerde terreinen als gevolg van methodologische fouten, veroorzaakt door uniforme eigenschappen van het studiegebied voor een aantal van de terreinparameters.
- het lage niet-beïnvloede percentage van goed geclassificeerde terreinen geeft aan dat de ontwikkelde discriminantfunctie een geringe voorspellende kracht heeft.
Een paar voorzichtige conclusies zijn:
- de analyse geeft geen indicatie voor de relatieve bijdrage van de verschillende terreinparameters aan het aardverschuivingsgevaar, omdat een aantal van de parameters aan elkaar gecorreleerd zijn. Belangrijke factoren zijn: het voorkomen van terracettes, maximum bewortelingsdiepte, dikte van de organisch laag, oppervlakte van het mesoreliëf, type materiaal, maximum hellingshoek, en het stam oppervlak van de bomen.

- de analyse geeft aan dat er een samenhang bestaat tussen het voorkomen van bossen en aardverschuivingen in het studiegebied. Dit is waarschijnlijk het gevolg van het planten van bomen rond de eeuwwisseling in het studie gebied op die terreinen die het meest hadden te lijden van erosie, waaronder aardverschuivingen. Blijkbaar zijn deze aardverschuivingen nog steeds actief.

Een meer arbeidsintensieve manier om het aardverschuivingsgevaar te analyseren is het gebruik van grondmechanische modellen. Het voorbeeld dat hier gepresenteerd wordt maakt gebruik van het oneindige hellingmodel en toont aan dat een gevoeligheid analyse de mogelijkheid biedt om de belangrijkste parameters te bepalen. Een erg gevoelige parameter is de hellingshoek. Er wordt dan ook voorgesteld om gevaren zones te onderscheiden aan de hand van de hellingshoek. Voor alle andere parameters is een toevalsgetal geïntroduceerd. Aangenomen wordt dat de waarschijnlijkheidsverdeling van dit toevalsgetal geldig is voor het gehele onderzoeksgebied. De waarschijnlijkheidsverdeling kan met weinig moeite bepaald worden.

Wanneer de waarschijnlijkheidsverdelingen bekend zijn van de verschillende parameters dan kan de kans op een veiligheidsfactor kleiner dan 1 berekend worden door middel van Monte Carlo simulaties.

De resultaten van die simulaties laten zien dat een betere bepaling van de hoogste grondwaterstanden kan leiden tot een meer precieze taxatie van het aardverschuivingsgevaar. De grondmechanische benadering laat verder zien dat verschillende draaiboeken ontwikkeld kunnen worden om de invloed van menselijk handelen op het aardverschuivingsgevaar te bepalen.

In de voorbeeld studie zijn de effecten van ontbossing en veranderingen in de grondwaterstand op het aardverschuivingsgevaar bekeken. Het blijkt dat het mechanische effect van bossen een geringe invloed op het gevaar heeft, terwijl veranderingen in de grondwaterstanden een duidelijk invloed hebben op het gevaar. Een grondwaterstand dichter bij het maaiveld resulteert in een groter gevaar voor aardverschuivingen. Een combinatie van kwantitatieve en kwalitatieve taxatie van het aardverschuivingsgevaar, op basis van een gedetailleerde geomorfologische kartering en een grondmechanische analyse kan leiden tot een waardevollere gevarenanalyse voor aardverschuivingen op een regionale schaal dan het gebruik van statistische analyse.

REFERENCES

A-Grivas, D., and R.N. Chowdhury, (1988), Two- and three-dimensional progressive failure of slopes: Model development and implementation, 643-648. In: Landslides Proceedings of the fifth Intern. Symposium on landslides, Lausanne 10-15 july 1988, Editor C. Bonnard.

A-Grivas, D., and Reagan, (1988), An expert system for evaluation and treatment of earth slope instability, 649-654. In: Landslides Proceedings of the fifth International Symposium on landslides, Lausanne 10-15 july 1988, Editor C. Bonnard.

Anderson, M.G., and R. G. Pope (1984), The incorporation of soil water physics models into geotechnical studies of landslide behavior. Proc. 4th International Symposium on Landslides, Vol 1, 349-353.

Aniya, M., (1985), Landslide-susceptibility mapping in the Amahata river basin, Japan. In: Annals of the Association of American Geographers, 75(1), pp 102-114.

Antoine, P., (1977), Reflexion sur la cartographie ZERMOS et bilan des experiences en cours. Bulletin de Bureau de Reserche Geologique et Miniere, Sec III, No 1-2, 9-20.

Antoine, P., D. Faber, A. Giraud, M. Al Hayari, (1988), Proprietes geotechnique de quelques ensembles Geologique propices aux glissements de terrain. 1301-1306. In: Landslides Proceedings of the fifth Intern. Symposium on landslides, Lausanne 10-15 july 1988, Editor C. Bonnard.

Benjamin, J.R. and C.A. Cornell, (1970), Probability, statistics and decision for civil engineers. New York McGraw-Hill.

Braam, R.R., E.E.J. Weiss and P. A. Burrough, (1987), Spatial and temporal analysis of mass movement using dendrochronology. Catena Vol 14, 573-584.

Brombacher, P. and M. Hartman, (1989), Invloed van wortels op hellingstabiliteit. (in dutch), Msc thesis. Department of Physical Geography University of Utrecht.

Burroughs, E. R., and B.R. Thomas (1977), Declining Root strength in Douglas- Fir after felling as a factor in slope stability. Research Paper INT-190, Intermountain Forest and Range Experiment Station, US Forest Service, Ogden, Utah, USA, 27pp.

Burrough, P.A., (1986), Principles of Geographical Information Systems for Land Resources Assessment. Oxford, Clarendon Press.

Carrara, A., (1983), Geomathematical assessment of regional landslide hazard, pp 9-20. Proceedings of the 4th Int. Conf. on the applications of statistics and probability in soil and structural engineering.

Carrara, A., and L. Merenda, (1976), Landslide inventory in Northern Calabria, Southern Italy. Bulletin of the Geological Society of America, Vol 87, No 1, 1153-1162.

Carrara, A., Puglies Carratelli, E. , Merenda, L, (1977), Computer-based data bank and statistical analysis of slope instability phenomena. In: Zeitschrift fur die Geomorphologie NF, vol 21, pp 187-222.

Chowdhury, R.N., and D. A-Grivas, (1982) Probabilistic model for progressive failure of slopes, Journal of Geotechnical Engineering Division, ASCE, Vol. 108, GT6, 803-822.

Chowdhury, R.N., (1988), Special Lecture: Analysis methods for assessing landslide risk - Recent developments, 515-524. In: Landslides Proceedings of the fifth Intern. Symposium on landslides, Lausanne 10-15 july 1988, Editor C. Bonnard.

Craig, R.F., (1987), Soil Mechanics. Van Nostrand Reinhold (UK) Co. Ltd, 410pp.

De Willigen, P., and M. van Noordwijk, (1987), Roots, plant production and nutrient use efficiency. PhD thesis University of Wageningen. pp282.

De Josselin de Jong, G., (1988), Application of the calculus of variations to the vertical cut off in cohesive frictionless soil. Geotechnique 30, No. 1, 1-16.

De Josselin de Jong, G., (1981), A variational fallacy. Technical note Geotechnique no31. 289-290.

Dexter, A.R. and J.S. Hewitt, (1978), The deflection of plant roots, Journal of Agricultural Engineering Resources Vol 23, 17-22.

Fredlund, D.G., and J. Krahn (1977), Comparison of slope stability methods of analysis. Canadian Geotech. Journalvol 14, 429-439.

Fredlund, D.G. (1987). Slope stability analysis incorporating the effect of soil suction, 113-144. In: Slope Stability eds: Anderson, M.G. and K.S. Richards. Chechester: Wiley and sons.

Freitag, D.R., (1986), Soil Randomly Reinforced with Fibers, Journal of Geotechnical Engineering, Vol 112, No. 8, 823-826.

Gray, D.H., and W.F. Megahan, (1981), Forest vegetation removal and slope stability in the Idaho Batholith. Research Paper INT-271, Intermountain Forest and Range Experiment Station, US Forest Service, Ogden, Utah, USA, 23pp.
Gray, D.H., and A.J. Leisner, (1980), Biotechnical slope protection and erosion control. Van Nostrand Reinhold, New York, 271pp.
Gray, D.H., and H. Ohashi (1983), Mechanics of fiber reinforcement in sand, J.Geotechn. Eng. Div. ,ASCE, vol 109, No. 3, 335-353.
Greco, V.R., and G. Gulla, (1988), Slope stability charts for slip surfaces of general shape, 637-642. In: Landslides Proceedings of the fifth International Symposium on landslides, Lausanne 10-15 july 1988, Editor C. Bonnard.
Greenway, D.R., (1987), Vegetation and slope stability, 187-230. In: Slope Stability eds: Anderson, M.G. and K.S. Richards. Chichester: Wiley and sons.
Grimmett, G.R., and D.R. Stirzaker, (1982), Probability and random processes. Oxford Science Publications, Clarendon Press, Oxford.
Haigh, M.J., Rawat, J.S., Bartarya, S., (1988), Environmental correlations of landslide frequency along new highways in the Himalaya: Preliminary results. In: Catena, vol 15, pp 539-553.
Harr, M.E, (1977), Mechanics of particular media. New York McGraw-Hill.
Harrop-Williams, K., (1986), Probability distribution of strength parameters in uniform soils, Journalof Engineering Mechanics Vol 112, 345-350.
Hathaway, R.L., and D. Penny, (1975), Root strength in some Populus and Salix clones. New Zealand . Botany, Vol 13, 333-344.
Hawkins, A.B., (1988), Stability of inland soil slopes: Some geotechnical considerations., 181-186. In: Landslides Proceedings of the fifth International Symposium on landslides, Lausanne 10-15 july 1988, Editor C. Bonnard.
Hazeu, G.W., (1988), Grondmechanische proeven op morene-materiaal. (in dutch), Msc thesis. Department of Physical Geography University of Utrecht.
Janbu, N., (1954), Application of composite slip surfaces for stability analysis, Eur. Conf. Stability Earth slopes, Stockholm, Vol 3, 43-49.
Jones, C.J.F.P., (1985), Earth Reinforcement and soil structures. Butterworths advanced series in geotechnical engineering. London: Butterworths. pp192.
Journal, A.J. and Ch.J. Huybregts, (1978), Mining Geostatistics. London: Academic Press.
Kenney, T.C., (1984), Properties and behavior of soils relevant to slope instability. In: Slope Instability, Eds: Brunsden, D., and D.B. Prior, Wiley, Chichester.
Kienholz, H., (1978), Maps of geomorphology and natural hazards of Grindwald, Switzerland, Scale 1: 10.000. Arctic and Alpine Research, Vol 10, No 2, 169-184.
Lambe, T.W., and R.V. Whitman, (1969), Soil Mechanics. New York: Wiley.
Lee, I.K., W White, O.G. Ingles (1983), Geotechnical engineering. Boston: Pitman.
Lee, I.W.Y., (1985), A review of vegetative slope stabilization. Hong Kong Engineer, Vol 13, No 7, 9-21.
Lumb, P., (1966), The variability of natural soils. Canadian Geotechnical Journal, Vol 3, No. 2, 74-97.
Lumb, P., (1970), Safety Factors and probability distributions of soil strength. Canadian Geotechnical Journal, Vol 17, No. 3, 225-242.
Lyford, W.H., (1975), Rhizography of non-woody roots of tress in the forest floor. 270-305. In: the development and function of roots, Eds J.G. Torrey and D.T. Clarkson.
McBratney, A.B., and R. Webster, (1983), How many observations are needed for regional estimation of soil properties ?, Soil Science vol 135, 177-183.
McGuffy, V., J.Iori, Z. Kyfor, D. A-Grivas, (1981), Statistical geotechnical properties of Lockport clays, Annual meeting of the Transportation Research board, Washington, DC.
McKyes, E., (1985), Soil Cutting and Tillage. Developments in Agricultural Engineering 7. Amsterdam Elsevier.
Meriam, J.L. and L.G. Kraige, (1987), Engineering Mechanics Statics Vol 1. New York: Wiley. pp453.
Milligan, G.W.E., and E.P., Palmeira, (1987), Prediction of the bond between soil and reinforcement. In Prediction and Performance in Geotechnical engineering/ Galgary/ 17-19 june 1987. Eds: Joshi, R.C. and F.J. Griffiths.

Mood, A.M., F.A. Graybill, D.C. Boes, (1974), Introduction to the theory of statistics. McGraw-Hill series in probability and statistics. Auckland.
Morgenstern, N.R. and V.E. Price, (1965), The analysis of the stability of generalized surfaces. Geotechnique, vol 15, 79-93.
Mulder H.F.H.M. and T.W.J. van Asch, (1987), Quantitative approaches in landslide hazard zonation, In Geomorphologie et risques naturels, Travaux de L'Institute de Geographie de Reims. No 69-72 pp 43-53
Mulder H.F.H.M., T.W.J. van Asch and E.E.J. Weiss (1987), The influence of forest on landslide activity. Proceedings of the symposium on erosion and sedimentation in the Pacific steep rimlands, 2-7 july 1987, Corevallis, Oregon USA. pp 288-290.
Mulder H.F.H.M. and T.W.J. van Asch, (1988), Risicokartering van massabewegingen in Alpine Bosgebieden; een kwantitatieve aanpak. In: Nieuwe Karterings Methoden in de Fysische Geografie. Blz 125-136. Nederlandse Geografische Studies No 63. H.J.A. Breendsen and H. van Steijn (eds).
Mulder H.F.H.M. and T.W.J. van Asch, (1988), Het gebruik van discriminant analyse ten behoeve van een evaluatie van hellingstabiliteit. In: Nieuwe Karterings Methoden in de Fysische Geografie. Blz 137-149. Nederlandse Geografische Studies No 63. H.J.A. Breendsen and H. van Steijn (eds).
Mulder H.F.H.M and T.W.J. van Asch, (1988), On the nature and the magnitude of the variance of important geotechnical parameters, with special reference to a forest area in the French Alps. In: Landslides Proceedings of the fifth International Symposium on landslides, Lausanne 10-15 july 1988, Editor C. Bonnard. pp 239-244.
Mulder H.F.H.M. and T.W.J. van Asch, (1988), A stochastical approach to landslide hazard determination in a forested area. In: Landslides Proceedings of the fifth International Symposium on landslides, Lausanne 10-15 july 1988, Editor C. Bonnard. pp 239-244.
Narayan C.G.P., V.P. Bhatkar and T. Ramamurthy, (1982), Nonlocal variational method in stability analysis, Journal of Geotechnical Engineering Division, ASCE, Vol 108 No. GT11.
Nash, D., (1987), A comparative Review of limit equilibrium methods of stability analysis. 11-75. In: Slope Stability eds: Anderson, M.G. and K.S. Richards. Chichester: Wiley and sons.
Neuland, H., (1976). A predictive model of landslips. Catena No 3, 215-230.
Nie, N.H, C.H. Hull, J.G. Jenkens, K. Steinbrenner and D.M. Bent, (1981), Statistical package for the social science Supplement 2. McGraw-Hill New York.
Nielsen, D.R., J.W. Biggar and K.T. Erh, (1973), Spatial variability of field-measured soil-water properties. Hilgardia Vol 42, No. 7, 216-259.
Nieuwenhuis, J.D., (1983), Stabiliteit van Grondmassieven, Department of Physical Geography, University of Utrecht, 118pp.
Norusis, M.J., (1985), Advanced statistics guide SPSS-x, New York McGraw-Hill.
Oboni, F. and P.L. Bourdeau, (1983), Determination of the critical slip surface in stability problems. Proceedings of the 4th International Conference on the applications of statistics and probability in soil and structural engineering. Vol 2, pp 1413-1424.
Oliver, M.A. and R. Webster, (1986), Combining nested and linear sampling for determining the scale and form of spatial variation of regionalized variables. Geographical analysis No 18, 227-242.
Oosterweegel, J.L.V. and E.W.H. van Veen, (1988), Grondwaterstromingen op instabiele hellingen, Msc thesis Department of Physical Geography University of Utrecht. 160pp.
Press, W.H., B.P. Flannery, S.A. Teukolsky and W.T. Vetterling, (1986), Numerical Recipes, Cambridge University Press. 830pp.
Read, J.R.L. and M.E. Harr, (1988), Slope stability analyses using the principle of maximum entropy, 749-755. In: Landslides Proceedings of the fifth International Symposium on landslides, Lausanne 10-15 july 1988, Editor C. Bonnard.
Reger, L.P., (1979), Discriminant analysis as a possible tool in landslide investigation. Earth surface processes, No 4, 267-273.
Rendu, J-M., (1981), An introduction to geotechnical methods of mineral evaluation. South African Institute of Mining and Metallurgy, Johannesburg South Africa.
Riestenberg, M.M. and S. Sovonick-Dunford, (1983), The role of woody vegetation on stabilizing slopes in the Cincinnati area. Geol. Society Bullutin, 94, pp 506-518.

Russo, D. and E. Bresler, (1980), Scaling soil hydraulic properties of a heterogeneous field. Soil Science. Society American Journal, 44 pp 681-684.
Sarma, S.K., (1979), Stability analysis of embankments and slopes. Journal Geotechnical Engineering Division, ASCE, vol 105, 1511-1524.
Schiechtl, H.M., (1973), Sicherungsarbeiten im landschaftsbau. Calway.
Schiechtl, H.M., (1980), Bioengineering for landreclamation and conservation. University of Alberta Press, Edmonton Canada, 404pp.
Schultz, E., (1957), Large scale shear tests. Fourth International conference on soil mechanics and foundation engineering, London, 193-199.
Scott, R.F., (1963), Principles of soil mechanics. Addison-Wesley Publ. Company, Inc, Reading Massachusetts.
Sidle, R.C., A.J. Pearce and C.L. O'Loughlin, (1985), Hillslope stability and land use. American Geophysical Union, Water Resources Monograph 11, 140pp.
Spencer, E., (1967), A method of analysis of the stability of embankments assuming parallel interslice forces. Geotechnique, Vol 17, 11-26.
Stolzy, L.H. and K.P. Barley, (1968), Mechanical resistance encountered by roots entering compact soils. Soil Science Vol 105, 297-301.
Swanston, D.N., (1969), Timber harvesting, mass erosion, and steepland geomorphology in the Pacific northwest. In: D.R. Coates (ed.) Geomorphology and engineering. Dowden, Hutchinson and Ross, Inc, Stroudsburg, 119-211.
Terwilliger, V.J. and L.J. Waldron, (1990), Assessing the contribution of roots to the strength of undisturbed, slip prone soils. Catena Vol 17, 151-162.
Terzaghi, K. and R.B. Peck, (1968), Soil Mechanics in Engineering Practice. New York: Wiley
Tsukamoto, Y, and H. Minematsu, (1987), Evaluation of the effect of deforestation on slope stability and its application to watershed management. Proceedings of the symposium on front hydrology and watershed management at XIX GG General Assembly, Vancouver, 1987.
Turmanina, V.I., (1965), The magnitude of the reinforcing role of tree roots. Moscow University Herald, Science. Journal, series V, 78-80.
van Asch, T.W.J., (1986), Massabewegingen. Department of Physical Geography, University of Utrecht.
van Asch, T.W.J., M.S. Deimel, W.J.C. Haak and J. Simon, (1989), The viscous creep component in shallow clayey soil and the influence of tree load on creep rates. Earth surface and processes and landforms, Vol 14 557-564.
VanMarcke, E.H., (1977), Reliability of earth slopes. Journal of Geotechnical engineering Division, ASCE, vol 103, no GT11, 1247-1265.
Varnes, D.J., (1984), Landslide hazard zonation: a review of principles and practice. Paris, Unesco.
Vidal, H. (1969), La terre armee. Annales Institute Technique Batim, Paris, No 223-229, July-August, 888-939.
Waldron, L.J. and S. Dakessian, (1981), Soil reinforcement by roots: calculations of increased soil shear resistance from root properties. Soil Science. Vol 132, No 6, 427-435.
Waldron, L.J., S. Dakessian, J.A. Nemson, (1983), Shear resistance enhancement of 1.22 meter diameter soil cross sections by Pine and Alfalfa roots. Soil Science Society American Journal Vol 47, 9-14.
Waldron, L.J., (1977), The shear resistance of root-permeated homogenous and stratified soil. Soil Science Society American JournalVol 41, 427-435.
Ward, T.J., R-M Li and D.B. Simons, (1982), Use of a mathematical model for estimating potential landslide sites in steep forested drainage basins. 21-41. In : Erosion and Sediment Transport in the Pacific Rim Steeplands. IAHS publ. No 32. Eds T.R.H. Davies and A.J. Pearce.
Whiteley, G.M. and A.R. Dexter, (1981), Elastic response of the roots of field Crops. Physiol. Plant. Vol 51, 407-417
Whitman, R.V., and W.A. Baily, (1967), Use of computers for slope stability analysis. JournalSoil Mech Fndtn Div, ASCE, Vol 93, No. SM4, 475-498.
Wu, T.H., W.P. McKinnell III, and D.N. Swanston, (1979), Strength of tree roots and landslides on Prince of Wales Island, Alaska. Canadian Geotechnical Journal, Vol 16, 19-33.
Wu, T.H., (1976), Investigation of landslides on Prince of Wales Island. Geotechnical Engineering Reports, Civil Engineering Department Ohio State University, Columbus, Ohio, USA, 94pp.

Wu, T.H., (1984), Effect of vegetation on slope stability. Transportation Research record 965, Transportation Research Board, Washington, DC, 37-46.
Wu, T.H. and L.M. Kraft, (1969), The probability of foundation safety. Journal soil mechanic Foundations Division Vol 93, No 5, 213-231.
Ziemer, R.R., (1978), An apparatus to measure the cross-cut shearing strength of roots. Canadian Journal of Forestry Resources, Vol 8, 142-144.
Ziemer, R.R, (1981), Roots and the stability of forested slopes. 343-361. In : Erosion and Sediment Transport in the Pacific Rim Steeplands. IAHS publ. No 32. Eds T.R.H. Davies and A.J. Pearce.
Ziemer, R.R. and D.N. Swanston, (1977), Root strength changes after logging in Southeast Alaska. Research note PNW-306, Pacific Northwest Forest and Range Experiment Station, US Forest Service, Portland, Oregon, USA, 9p.

NEDERLANDSE GEOGRAFISCHE STUDIES / NETHERLANDS GEOGRAPHICAL STUDIES

1 G MIK & J H STIKKELBROEK, Verkiezingen in Rotterdam; een geografische verkenning van de verkiezingsuitslagen 1970-1982 en een nadere analyse van de ruimtelijke structuur der Tweede Kamerverkiezingen van 1982 -- Amsterdam/Rotterdam 1985: Knag/Economisch-Geografisch Instituut Erasmus Universiteit Rotterdam. 130 pp, 51 figs, 8 tabs. ISBN 90-6809-009-7 Dfl 17,50

2 S MUSTERD, Verschillende structuren en ontwikkelingen van woongebieden in Tilburg -- Amsterdam 1985: Knag/Geografisch en Planologisch Instituut van de Vrije Universiteit Amsterdam. 292 pp, 104 figs, 44 tabs. ISBN 90-6809-010-0 Dfl 27,75

3 M J TITUS, Urbanisatie, integratie en demografische respons in Jakarta; een empirisch onderzoek naar de stedelijke moderniseringsrol in de periode 1961-1976 -- Amsterdam/Utrecht 1985: Knag/Geografisch Instituut Rijksuniversiteit Utrecht. 380 pp, 14 figs, 202 tabs. ISBN 90-6809-012-7 Dfl 39,50

4 H SCHENK, Views on Alleppey; Socio-historical and socio-spatial perspectives on an Industrial port town in Kerala, South India -- Amsterdam 1986: Knag/Instituut voor Sociale Geografie Universiteit van Amsterdam. 246 pp, 41 figs, 36 tabs. ISBN 90-6809-011-9 Dfl 29,50

5 P J BOELHOUWER & F M DIELEMAN (Red), Wonen in de stad; samenvatting van sociaal-geografisch onderzoek in de Domstad -- Amsterdam/Utrecht 1986: Knag/Geografisch Instituut Rijksuniversiteit Utrecht. 138 pp, 41 figs, 32 tabs. ISBN 90-6809-013-5 Dfl 19,50

6 P LUKKES & J H M VAN ROODEN, De makelaardij in onroerende goederen in Nederland; een regiologisch-geografische analyse -- Amsterdam/Groningen 1986: Knag/Geografisch Instituut Rijksuniversiteit Groningen. 102 pp, 9 figs, 28 tabs. ISBN 90-6809-015-1 Dfl 25,00

7 P P P HUIGEN, Binnen of buiten bereik? Een sociaal-geografisch onderzoek in Zuidwest-Friesland -- Amsterdam/Utrecht 1986: Knag/Geografisch Instituut Rijksuniversiteit Utrecht. 276 pp, 58 figs, 72 tabs. ISBN 90-6809-014-3 Dfl 34,00

8 V M VAN DALEN & L VAN DER LAAN (Red), Werken aan de kust; verslag van het Knag-symposium over de plannen tot uitbreiding van de Nederlandse kust gehouden op 3 oktober 1985 in het Provinciehuis te Den Haag -- Amsterdam 1986: Koninklijk Nederlands Aardrijkskundig Genootschap. 78 pp, 8 figs, 2 tabs. ISBN 90-6809-016-X Dfl 14,00

9 H KNIPPENBERG, Deelname aan het lager onderwijs in Nederland gedurende de negentiende eeuw; een analyse van de landelijke ontwikkeling en van de regionale verschillen -- Amsterdam 1986: Knag/Instituut voor Sociale Geografie Universiteit van Amsterdam. 268 pp, 29 figs, 81 tabs. ISBN 90-6809-017-8 Dfl 29,00

10 H J A BERENDSEN (Red), Het landschap van de Bommelerwaard -- Amsterdam/Utrecht 1986: Knag/Geografisch Instituut Rijksuniversiteit Utrecht. 186 pp, 71 figs, 2 maps. ISBN 90-6809-019-4 Dfl 34,50

11 M DE SMIDT (Red), Regionale statistiek: organisatie en onderzoek; bijdragen voor drs J Schmitz bij zijn afscheid van het CBS -- Amsterdam/Utrecht 1986: Knag/Geografisch Instituut Rijksuniversiteit Utrecht. 86 pp, 17 figs, 9 tabs. ISBN 90-6809-020-8 Dfl 14,95

12 J M VAN MOURIK, Pollen profiles of slope deposits in the Galician area (NW Spain) -- Amsterdam 1986: Knag/Fysisch-Geografisch en Bodemkundig Laboratorium Universiteit van Amsterdam. 174 pp, 55 figs, 4 tabs. ISBN 90-6809-018-6 Dfl 29,00

13 J J HARTS & L HINGSTMAN, Verhuizingen op een rij; een analyse van individuele verhuisgeschiedenissen -- Amsterdam/Utrecht 1986: Knag/Geografisch Instituut Rijksuniversiteit Utrecht. 312 pp, 54 figs, 108 tabs. ISBN 90-6809-022-4 Dfl 38,50

14 A VAN SCHAIK, Colonial control and peasant resources in Java; agricultural involution reconsidered -- Amsterdam 1986: Knag/Instituut voor Sociale Geografie Universiteit van Amsterdam. 214 pp, 14 figs, 31 tabs. ISBN 90-6809-021-6 Dfl 27,00

15 L L J M DIRRIX, T K GRIMMIUS & P VAN DER VEEN, The functioning of periodic markets in the Bombay Metropolitan Region -- Amsterdam/Groningen 1986: Knag/Geografisch Instituut Rijksuniversiteit Groningen. 200 pp, 38 figs, 47 tabs. ISBN 90-6809-030-5 Dfl 25,00

16 J G BORCHERT, L S BOURNE & R SINCLAIR (Eds), Urban Systems in Transition -- Amsterdam/Utrecht 1986: Knag/Geografisch Instituut Rijksuniverseit Utrecht. 248 pp, 41 figs, 48 tabs. ISBN 90-6809-028-3 Dfl 24,90

17 P W BLAUW, Suburbanisatie en sociale contacten -- Amsterdam/Rotterdam 1986: Knag/Faculteit der Economische Wetenschappen Erasmus Universiteit Rotterdam. 168 pp, 68 tabs. ISBN 90-6809-024-0 Dfl 25,00

18 H J SCHOLTEN, R J VAN DE VELDE & P PADDING, Doorstroming op de Nederlandse woningmarkt; geanalyseerd en gemodelleerd -- Amsterdam/Utrecht 1986: Knag/Geografisch Instituut Rijksuniversiteit Utrecht. 116 pp, 38 figs, 22 tabs. ISBN 90-6809-025-9 Dfl 13,00

19 F M DIELEMAN, A W P JANSEN & M DE SMIDT (Red), Metamorfose van de stad; recente tendenzen van wonen en werken in Nederlandse steden -- Amsterdam/Utrecht 1986: Knag/Geografisch Instituut Rijksuniversiteit Utrecht. 134 pp, 31 figs, 22 tabs. ISBN 90-6809-026-7 Out of print

20 E VOS, M NIEUWENHUIS, M HOOGENDOORN & A SENDERS, Vele handen ...; vrouw en werk in Latijns Amerika -- Amsterdam 1986: Knag/Geografisch en Planologisch Instituut van de Vrije Universiteit. 210 pp, 9 figs, 7 tabs. ISBN 90-6809-027-5 Dfl 30,00

21 J H J VAN DINTEREN & H W TER HART (Red.), Geografie en kantoren 1985; verslag van een congres gehouden te Nijmegen op 29 november 1985 -- Amsterdam/Nijmegen 1986: Knag/Geografisch en Planologisch Instituut Katholieke Universiteit Nijmegen. 144 pp, 15 figs, 15 tabs. ISBN 90-6809-029-1 Dfl 17,00

22 J VIJGEN & R v ENGELSDORP GASTELAARS, Stedelijke bevolkingskategorieen in opkomst; stijlen en strategieën in het alledaags bestaan -- Amsterdam 1986: Knag/Instituut voor Sociale Geografie Universiteit van Amsterdam. 122 pp, 3 figs, 40 tabs. ISBN 90-6809-031-3 Dfl 15,00

23 H J MÜCHER, Aspects of loess and loess-derived slope deposits; an experimental and micromorphological approach -- Amsterdam 1986: Knag/Fysisch-Geografisch en Bodemkundig Laboratorium Universiteit van Amsterdam. 268 pp, 42 figs, 9 tabs. ISBN 90-6809-032-1 Dfl 25,00

24 P HENDRIKS, De relationele definitie van begrippen; een relationeel realistische visie op het operationaliseren en representeren van begrippen -- Amsterdam/Nijmegen 1986: Knag/Geografisch en Planologisch Instituut Katholieke Universiteit Nijmegen. 282 pp, 28 figs, 7 tabs. ISBN 90-6809-033-X Dfl 30,00

25 J M G KLEINPENNING (ed), Competition for rural and urban space in Latin America; its consequences for low income groups. Contributions to a symposium organized at the 45th International Congress of Americanists, Bogota, 1-7 July 1985 -- Amsterdam/Nijmegen 1986: Knag/Geografisch en Planologisch Instituut Katholieke Universiteit Nijmegen. 178 pp, 36 figs, 11 tabs. ISBN 90-6809-034-8 Dfl 22,50

26 J BUURSINK & E WEVER (red), Regio en ontwikkeling; aspecten van regionaal-economische ontwikkelingen in Nederland -- Amsterdam/Nijmegen 1986: Knag/Geografisch en Planologisch Instituut Katholieke Universiteit Nijmegen. 160 pp, 41 figs, 50 tabs. ISBN 90-6809-035-6 Dfl 20,00

27 G CLARK, P DOSTAL & F THISSEN (eds), Rural research and planning: the Netherlands and Great Britain. Report of the Second British-Dutch Symposium on Rural Geography and Planning, 5 September 1986 -- Amsterdam 1987: Knag/Instituut voor Sociale Geografie Universiteit van Amsterdam. 88 pp, 6 figs, 4 tabs. ISBN 90-6809-037-2 Dfl 10,00

28 W M KARREMAN & M de SMIDT (red), Redevoeringen en kleine geschriften van Prof A C de Vooys; verzameling van niet eerder uitgegeven werk ter gelegenheid van zijn tachtigste verjaardag, 22 jan. 1987 -- Amsterdam/Utrecht 1987: Knag/Geografisch Instituut Rijksuniversiteit Utrecht. 156 pp, 8 figs, 5 tabs. ISBN 90-6809-036-4 Dfl 21,70

29 G PEPERKAMP (red), Mens en milieu in de derde wereld; bijdragen aan de Nederlandse Geografendagen te Utrecht, 2-4 april 1986 -- Amsterdam/Nijmegen 1987: Knag/Geografisch en Planologisch Instituut Katholieke Universiteit Nijmegen. 146 pp, 17 figs, 11 tabs. ISBN 90-6809-038-0 Dfl 20,00

30 A R WOLTERS & A PIERSMA, Beschermde reservaten? Een milieugeografische benadering -- Amsterdam/Groningen 1987: Knag/Geografisch Instituut Rijksuniversiteit Groningen. 184 pp, 47 figs, 4 tabs. ISBN 90-6809-039-9 Out of print

31 W J v d BREMEN & P H PELLENBARG (red), Het geografisch plechtanker: eenheid in verscheidenheid. Liber amicorum Rob Tamsma -- Amsterdam/Groningen 1987: Knag/Geografisch Instituut Rijksuniversiteit Groningen. 336 pp, 58 figs, 22 tabs. ISBN 90-6809-040-2 Dfl 35,00

32 G MIK, Segregatie in het grootstedelijk milieu; theorie en Rotterdamse werkelijkheid -- Amsterdam/Rotterdam 1987: Knag/Economisch-Geografisch Instituut Erasmus Universiteit Rotterdam. 252 pp, 48 figs, 45 tabs. ISBN 90-6809-041-0 Dfl 25,00

33 H J M GOVERDE, Macht over de Markerruimte -- Amsterdam/Nijmegen 1987: Knag/Geografisch en Planologisch Instituut Katholieke Universiteit Nijmegen. 480 pp, 26 figs, 22 tabs. ISBN 90-6809-042-9 Dfl 57,50

34 P P GROENEWEGEN, J P MACKENBACH & M H STIJNENBOSCH (red), Geografie van gezondheid en gezondheidszorg -- Amsterdam/Utrecht 1987: Knag/Geografisch Instituut Rijksuniversiteit Utrecht. 132 pp, 25 figs, 19 tabs. ISBN 90-6809-043-7 Dfl 19,70

35 R ter BRUGGE & E WEVER (red), Energiebeleid; het Nederlandse energiebeleid in ruimtelijk perspectief. Verslag van een Knag-symposium -- Amsterdam/Groningen/Nijmegen 1987: Knag/Geografisch Instituut Rijksuniversiteit Groningen/Geografisch en Planologisch Instituut Katholieke Universiteit Nijmegen. 132 pp, 21 figs, 18 tabs. ISBN 90-6809-044-5 Dfl 18,00

36 J A v d SCHEE, Kijk op kaarten; een empirisch onderzoek naar het gebruik van geografische denkvaardigheden bij het analyseren van kaarten door leerlingen uit het vierde leerjaar van het VWO -- Amsterdam 1987: Knag/Geografisch en Planologisch Instituut van de Vrije Universiteit Amsterdam. 312 pp, 42 figs, 58 tabs. ISBN 90-6809-045-3 Dfl 39,50

37 O VERKOREN & J v WEESEP (eds), Spatial mobility and urban change -- Amsterdam/Utrecht 1987: Knag/Geografisch Instituut Rijksuniversiteit Utrecht. 180 pp, 17 figs, 45 tabs. ISBN 90-6809-051-8 Dfl 24,75

38 M W de JONG, New economic activities and regional dynamics -- Amsterdam 1987: Knag/Economisch-Geografisch Instituut Universiteit van Amsterdam. 200 pp, 26 figs, 27 tabs. ISBN 90-6809-046-1 Dfl 29,00

39 A C M JANSEN, Bier in Nederland en België; een geografie van de smaak -- Amsterdam 1987: Knag/Economisch-Geografisch Instituut Universiteit van Amsterdam. 282 pp, 14 figs, 7 tabs. ISBN 90-6809-047-X Dfl 37,50

40 Y C J BROUWERS, M C DEURLOO & L de KLERK, Selectieve verhuisbewegingen en segregatie; de invloed van de etnische samenstelling van de woonomgeving op verhuisgedrag -- Amsterdam 1987: Knag/Instituut voor Sociale Geografie Universiteit van Amsterdam. 112 pp, 9 figs, 22 tabs. ISBN 90-6809-048-8 Dfl 16,00

41 R J SCHOUW & F M DIELEMAN, Echtscheiding en woningmarkt; een voorstudie naar de complexe relatie tussen echtscheiding en woningmarkt -- Amsterdam/Utrecht 1987: Knag/Geografisch Instituut Rijksuniversiteit Utrecht. 98 pp, 8 figs, 21 tabs. ISBN 90-6809-049-6 Dfl 14,95

42 J G GROENENDIJK, De positie van dorpen in het beleid van Nederlandse plattelandsgemeenten; een politiekgeografisch onderzoek naar de verdeling van woningbouwlokaties tijdens een fase van omvangrijke groei -- Amsterdam 1987: Knag/Instituut voor Sociale Geografie Universiteit van Amsterdam. 314 pp, 22 figs, 55 tabs. ISBN 90-6809-050-X Dfl 31,50

43 J G BORCHERT & J BUURSINK (red), Citymarketing en geografie -- Amsterdam/Nijmegen 1987: Knag/Geografisch en Planologisch Instituut Katholieke Universiteit Nijmegen. 172 pp, 32 figs, 14 tabs. ISBN 90-6809-052-6 Dfl 20,00

44 J J M ANGENENT & A BONGENAAR (eds), Planning without a passport: the future of European spatial planning -- Amsterdam 1987: Knag/Stichting Interuniversitair Instituut voor Sociaal-Wetenschappelijk Onderzoek. 184 pp, 26 figs, 7 tabs. ISBN 90-6809-053-4 Out of print

45 R C v d MARK, A H PERRELS & J J REYNDERS, Kansen voor het Noorden; een beleidsstrategisch onderzoek naar nieuwe technologie -- Amsterdam/Utrecht 1987: Knag/Geografisch Instituut Rijksuniversiteit Utrecht/Economische Faculteit Vrije Universiteit Amsterdam. 168 pp, 54 figs, 41 tabs. ISBN 90-6809-054-2 Dfl 22,50

46 J J STERKENBURG, Rural development and rural development policies: cases from Africa and Asia -- Amsterdam/Utrecht 1987: Knag/Geografisch Instituut Rijksuniversiteit Utrecht. 196 pp, 13 figs, 14 tabs. ISBN 90-6809-055-0 Dfl 26,50

47 C CORTIE, Alkmaar, van streekcentrum naar groeikern; een onderzoek naar migratie en forensisme tijdens de transformatie van een stedelijk systeem -- Amsterdam 1987: Knag/Instituut voor Sociale Geografie Universiteit van Amsterdam. 204 pp, 28 figs, 39 tabs. ISBN 90-6809-056-9 Dfl 25,00

48 J A A M KOK & P H PELLENBARG (red), Buitenlandse bedrijven in Nederland; werving in Europees perspectief -- Amsterdam/Groningen 1987: Knag/Geografisch Instituut Rijksuniversiteit Groningen. 112 pp, 17 figs, 30 tabs. ISBN 90-6809-059-3 Out of print

49 T DIETZ, Pastoralists in Dire Straits; survival strategies and external interventions in a semi-arid region at the Kenya/Uganda border: Western Pokot, 1900-1986 -- Amsterdam 1987: Knag/Instituut voor Sociale Geografie Universiteit van Amsterdam. 332 pp, 34 figs, 66 tabs. ISBN 90-6809-057-7 Dfl 43,00

50 F J J H v HOORN, Onder anderen; effekten van de vestiging van Mediterranen in naoorlogse wijken Amsterdam/Utrecht 1987: Knag/Geografisch Instituut Rijksuniversiteit Utrecht. 226 pp, 36 figs, 55 tabs. ISBN 90-6809-060-7 Dfl 29,70

51 M J DIJST & C CORTIE, Universiteit en revitalisering -- Amsterdam 1987: Knag/Instituut voor Sociale Geografie Universiteit van Amsterdam. 140 pp, 6 figs, 13 tabs. ISBN 90-6809-058-5 Dfl 17,00

52 Planologie als kleurbepaling; de rol van toonaangevende instellingen en bedrijven op de ontwikkeling van de Amsterdamse Museum- en Concertgebouwbuurt -- Amsterdam 1987: Knag/Centrum Beleidsadviserend Onderzoek. 164 pp, 2 figs, 23 tabs. ISBN 90-6809-061-5 Dfl 25,00

53 J VERHORST & M H STIJNENBOSCH, Bedrijvigheid en stadsvernieuwing; analyse van de bedrijvigheidsontwikkeling in enkele stadsvernieuwingsgebieden in Utrecht en Den Haag in de periode 1973/1974 - 1983/1984 -- Amsterdam/Utrecht 1987: Knag/Geografisch Instituut Rijksuniversiteit Utrecht. 112 pp, 47 figs, 25 tabs. ISBN 90-6809-063-1 Dfl 15,70

54 B G J DRIESSEN, R VERHOEF & J G P ter WELLE-HEETHUIS, Overheid en bevolkingsontwikkelingen; een onderzoek naar autonome en niet-autonome bevolkingsontwikkelingen in de stadsgewesten Arnhem en Utrecht -- Amsterdam/Utrecht 1987: Knag/Geografisch Instituut Rijksuniversiteit Utrecht. 166 pp, 53 figs, 42 tabs. ISBN 90-6809-064-X Dfl 23,30

55 O A L C ATZEMA, P P P HUIGEN, A G A de VOCHT & C R VOLKERS, De bereikbaarheid van voorzieningen in Noord Nederland -- Amsterdam/Utrecht 1987: Knag/Geografisch Instituut Rijksuniversiteit Utrecht. 220 pp, 49 figs, 122 tabs. ISBN 90-6809-065-8 Dfl 24,00

56 P C BEUKENKAMP, G A HOEKVELD & A MUDDE (red), Geografie en onderwijstelevisie -- Amsterdam/Utrecht 1987: Knag/Geografisch Instituut Rijksuniversiteit Utrecht. 222 pp, 29 figs, 6 tabs. ISBN 90-6809-066-6 Dfl 26,50

57 G CARDOL, Ruimte voor agribusiness-complexen; structuur, positie en dynamiek van het Noordlimburgse tuinbouwcomplex vanuit functioneel, geografisch en regionaal perspectief -- Amsterdam/Nijmegen 1988: Knag/Geografisch en Planologisch Instituut Katholieke Universiteit Nijmegen. 312 pp, 34 figs, 57 tabs. ISBN 90-6809-067-4 Dfl 30,00

58 M JANSEN-VERBEKE, Leisure, recreation and tourism in inner cities; an explorative study -- Amsterdam/Nijmegen 1988: Knag/Geografisch en Planologisch Instituut Katholieke Universiteit Nijmegen. 316 pp, 61 figs, 51 tabs. ISBN 90-6809-068-2 Dfl 32,00

59 A H H M KEMPERS-WARMERDAM, Vergrijzen in het groen; het bereik van ouderen en de bereikbaarheid van voorzieningen in landelijke gebieden -- Amsterdam/Utrecht 1988: Knag/Geografisch Instituut Rijksuniversiteit Utrecht. 236 pp, 47 figs, 70 tabs. ISBN 90-6809-069-0 Dfl 29,50

60 P J BOELHOUWER, De verkoop van woningwetwoningen; de overdracht van woningwetwoningen aan bewoners en de gevolgen voor de volkshuisvesting -- Amsterdam/Utrecht 1988: Knag/Geografisch Instituut Rijksuniversiteit Utrecht. 208 pp, 49 figs, 122 tabs. ISBN 90-6809-070-4 Dfl 29,30

61 A G J DIETVORST & M C JANSEN-VERBEKE, De binnenstad: kader van een sociaal perpetuum mobile; een literatuurstudie naar tijdsbesteding en binnenstadsgebruik -- Amsterdam/Nijmegen 1988: Knag/Geografisch en Planologisch Instituut Katholieke Universiteit Nijmegen. 240 pp, 10 tabs. ISBN 90-6809-071-2 Dfl 30,00

62 H SCHRETTENBRUNNER & J v WESTRHENEN, Empirische Forschung und Computer im Geographie-unterricht; Niederländisch-deutsches Symposium Amsterdam 1987 -- Amsterdam 1988: Knag/Centrum voor Educatieve Geografie Vrije Universiteit. 120 pp, 27 figs. ISBN 90-6809-072-0 Dfl 15,00

63 H J A BERENDSEN & H v STEIJN (red), Nieuwe karteringsmethoden in de fysische geografie -- Amsterdam/Utrecht 1988: Knag/Geografisch Instituut Rijksuniversiteit Utrecht. 176 pp, 56 figs, 24 tabs. ISBN 90-6809-073-9 Dfl 22,50

64 A G J DIETVORST & J P M KWAAD (eds), Geographical research in the Netherlands 1978-1987 -- Amsterdam 1988: Knag/International Geographical Union Netherlands. 262 pp, 7 figs, 2 tabs. ISBN 90-6809-074-7 Dfl 33,00

65 J v WEESEP, Appartementsrechten; het gebruik van het splitsingregime -- Amsterdam/Utrecht 1988: Knag/Geografisch Instituut Rijksuniversiteit Utrecht. 94 pp, 4 figs, 16 tabs. ISBN 90-6809-075-5 Dfl 14,50

66 T W A EPPINK, Choice of mathematical models in geographic research considering alternatives -- Amsterdam/Nijmegen 1988: Knag/Geografisch en Planologisch Instituut Katholieke Universiteit Nijmegen. 244 pp, 74 figs, 49 tabs. ISBN 90-6809-076-3 Dfl 30,00

67 J HINDERINK & E SZULC-DABROWIECKA (eds), Successful rural development in Third World Countries -- Amsterdam/Utrecht 1988: Knag/Geografisch Instituut Rijksuniversiteit Utrecht. 256 pp, 14 figs, 20 tabs. ISBN 90-6809-077-1 Dfl 31,50

68 S BARENDS, J D H HARTEN, J RENES, J VERHORST & K E v d WIELEN (red), Planning in het verleden -- Amsterdam/Utrecht 1988: Knag/Geografisch Instituut Rijksuniversiteit Utrecht. 192 pp, 71 figs. ISBN 90-6809-078-X Dfl 26,00

69 J MANSVELT BECK, The rise of a subsidized periphery in Spain -- Amsterdam 1988: Knag/Instituut voor Sociale Geografie Universiteit van Amsterdam. 286 pp, 15 figs, 28 tabs. ISBN 90-6809-079-8 Dfl 37,50

70 S SMITH, Kleinschalige industrie in Latijns Amerika; een studie van de ontwikkelingsmogelijkheden van de 'informele' kleding- en textielnijverheid in Aguascalientes, Mexico -- Amsterdam/Nijmegen 1988: Knag/Geografisch en Planologisch Instituut Katholieke Universiteit Nijmegen. 422 pp, 4 figs, 16 tabs. ISBN 90-6809-080-1 Dfl 42,50

71 W DWARKASING, D HANEMAAYER, M de SMIDT & P P TORDOIR, Ruimte voor hoogwaardige kantoren; onderzoek naar toplocaties voor de commerciële kantorensector gezien vanuit de optiek van de gebruikers -- Amsterdam/Utrecht/Leiden/Delft 1988: Knag/Geografisch Instituut Rijksuniversiteit Utrecht/Research voor Beleid/Inro-tno. 112 pp, 7 figs, 44 tabs. ISBN 90-6809-081-X Out of print

72 P J KORTEWEG, Dynamiek en immobiliteit in naoorlogse wijken; het funktioneren van woonwijken in Alkmaar, Haarlem en Purmerend -- Amsterdam/Utrecht 1988: Knag/Geografisch Instituut Rijksuniversiteit Utrecht. 144 pp, 21 figs, 34 tabs. ISBN 90-6809-082-8 Dfl 20,90

73 P J WIJERS, Land prices in Tokyo; causes and effects, government policies and implications for the real estate industry -- Amsterdam 1988: Knag/Economisch-Geografisch Instituut Universiteit van Amsterdam. 84 pp, 12 figs, 8 tabs. ISBN 90-6809-084-4 Dfl 47,50

74 J v MOURIK (red), Landschap in beweging; ontwikkeling en bewoning van een stuifzandgebied in de Kempen -- Amsterdam 1988: Knag/Faculteit Ruimtelijke Wetenschappen Universiteit van Amsterdam. 197 pp, 95 figs, 1 tab. ISBN 90-6809-083-6 Dfl 30,00

75 W J M OSTENDORF, Het sociaal profiel van de gemeente; woonmilieudifferentiatie en de vorming van het stadsgewest Amsterdam: het ruimtelijk beleid van een achttal gemeenten na de tweede wereldoorlog -- Amsterdam 1988: Knag/Instituut voor Sociale Geografie Universiteit van Amsterdam. 192 pp, 12 figs, 26 tabs. ISBN 90-6809-085-2 Dfl 23,00

76 J de BRUIN & J A KOETSIER (red), De kracht van de regio; sociaal-economische ontwikkelingsmogelijkheden van de regio -- Amsterdam 1988: Knag/Instituut voor Sociale Geografie Universiteit van Amsterdam. 104 pp, 12 figs, 6 tabs. ISBN 90-6809-086-0 Dfl 15,00

77 A G M v d SMAGT & P H J HENDRIKS (red), Methoden op een keerpunt; opstellen aangeboden aan prof drs P J W Kouwe bij zijn afscheid als hoogleraar aan de Katholieke Universiteit Nijmegen -- Amsterdam/Nijmegen 1988: Knag/Geografisch en Planologisch Instituut Katholieke Universiteit Nijmegen. 170 pp, 20 figs, 30 tabs. ISBN 90-6809-087-9 Dfl 25,00

78 C v d POST, Migrants and migrant-labour absorption in large and small centres in Swaziland; a comparative study of the towns Manzini and Nhlangano -- Amsterdam/Utrecht 1988: Knag/Geografisch Instituut Rijksuniversiteit Utrecht. 310 pp, 32 figs, 84 tabs. ISBN 90-6809-088-7 Dfl 35,00

79 L J de HAAN, Overheid en regionale integratie van de savanne in Togo 1885-1985 -- Amsterdam 1988: Knag/Instituut voor Sociale Geografie Universiteit van Amsterdam. 304 pp, 31 figs, 65 tabs. ISBN 90-6809-089-5 Dfl 33,00

80 L H v WIJNGAARDEN-BAKKER & J J M v d MEER (eds), Spatial sciences, research in progress: Proceedings of the symposium "Spatial sciences, research in progress", 14 April 1988 Amsterdam -- Amsterdam 1988: Knag/Faculteit Ruimtelijke Wetenschappen Universiteit van Amsterdam. 112 pp, 16 figs, 2 tabs. ISBN 90-6809-091-7 Dfl 24,00

81 F M H M DRIESSEN & J H v HOUWELINGEN, Vrije tijd en korte verblijfsrecreatie -- Amsterdam/Utrecht 1988: Knag/Bureau Driessen. 256 pp, 25 figs, 146 tabs. ISBN 90-6809-095-X Dfl 15,00

82 G HOEKVELD-MEIJER & G J SCHUTTE, Aardrijkskunde gebiedenderwijs; tekst en uitleg bij het schrijven, lezen, denken en leren over gebieden en verschijnselen in gebieden -- Amsterdam 1988: Knag/Centrum voor Educatieve Geografie Vrije Universiteit Amsterdam. 252 pp, 76 figs, 12 tabs. ISBN 90-6809-090-9 Dfl 39,00

83 P K DOORN, Social structure and spatial mobility: composition and dynamics of the Dutch labour force -- Amsterdam/Utrecht 1989: Knag/Geografisch Instituut Rijksuniversiteit Utrecht. 262 pp, 72 figs, 41 tabs. ISBN 90-6809-092-5 Dfl 31,50

84 A LOEVE, Buitenlandse ondernemingen in regionaal perspectief; vestigingsstrategieën en regionale effecten van buitenlandse bedrijven in Nederland -- Amsterdam/Utrecht 1989: Knag/Geografisch Instituut Rijksuniversiteit Utrecht. 272 pp, 49 figs, 78 tabs. ISBN 90-6809-093-3 Dfl 32,00

85 D H de BAKKER, Ruraal nederzettingenpatroon en beleid; ontwikkelingen in Zuidwest-Friesland -- Amsterdam/Utrecht 1989: Knag/Geografisch Instituut Rijksuniversiteit Utrecht. 230 pp, 32 figs, 68 tabs. ISBN 90-6809-094-1 Dfl 29,00

86 L J PAUL (ed), Post-war development of regional geography; with special attention to the United Kingdom, Belgium, and the Netherlands -- Amsterdam/Utrecht 1989: Knag/Geografisch Instituut Rijksuniversiteit Utrecht. 88 pp, 15 figs, 5 tabs. ISBN 90-6809-096-8 Dfl 14,00

87 P HOEKSTRA, River outflow, depositional processes and coastal morphodynamics in a monsoon-dominated deltaic environment, East Java, Indonesia -- Amsterdam/Utrecht 1989: Knag/Geografisch Instituut Rijksuniversiteit Utrecht. 220 pp, 77 figs, 24 tabs. ISBN 90-6809-097-6 Dfl 28,50

88 E LENSINK, Intermediaire diensten in landelijke gebieden; een economisch-geografisch onderzoek in een rurale omgeving -- Amsterdam/Nijmegen 1989: Knag/Faculteit Beleidswetenschappen Katholieke Universiteit Nijmegen. 246 pp, 21 figs, 65 tabs. ISBN 90-6809-098-4 Dfl 30,00

89 P P P HUIGEN & M C H M v d VELDEN (red), De achterkant van verstedelijkt Nederland; de positie en funktie van landelijke gebieden in de Nederlandse samenleving -- Amsterdam/Utrecht 1989: Knag/Geografisch Instituut Rijksuniversiteit Utrecht. 181 pp, 25 figs, 46 tabs. ISBN 90-6809-100-X Dfl 25,00

90 J H J VAN DINTEREN, Zakelijke diensten en middelgrote steden, een vergelijkend onderzoek naar de vestigingsplaatskeuze en het functioneren van zakelijke dienstverleningsbedrijven in Noord-Brabant, Gelderland en Overijssel -- Amsterdam/Nijmegen 1989: Knag/Faculteit der Beleidswetenschappen Katholieke Universiteit Nijmegen. 312 pp, 28 figs, 84 tabs. ISBN 90-6809-099-2 Dfl 40,00

91 L VAN DER LAAN, H SCHOLTEN & G A VAN DER KNAAP, Het regionaal arbeidsaanbod in Nederland; structuur en ontwikkeling -- Amsterdam/Rotterdam 1989: Knag/Economisch-Geografisch Instituut Erasmus Universiteit Rotterdam. 128 pp, 27 figs, 28 tabs. ISBN 90-6809-101-8 Dfl 17,50

92 C CLARK, P HUIGEN & F THISSEN (eds), Planning and the future of the countryside: Great Britain and the Netherlands; proceedings of the second British-Dutch Symposium on Rural Geography, 6-8 september 1986 Amsterdam -- Amsterdam 1989: Knag/Instituut voor Sociale Geografie Universiteit van Amsterdam. 240 pp, 25 figs, 43 tabs. ISBN 90-6809-102-6 Dfl 35,00

93 J A VAN DEN BERG, Variability of parameters for modelling soil moisture conditions; studies on loamy to silty soils on marly bedrock in the Ardèche drainage basin, France -- Amsterdam/Utrecht 1989: Knag/Geografisch Instituut Rijksuniversiteit Utrecht. 214 pp, 76 figs, 16 tabs. ISBN 90-6809-103-4 Dfl 28,50

94 O VERKOREN, Huizen op de hoogvlakte; een residentieel-geografische verkenning van La Paz, Bolivia -- Amsterdam/Utrecht 1989: Knag/Geografisch Instituut Rijksuniversiteit Utrecht. 210 pp, 29 figs, 16 tabs. ISBN 90-6809-104-2 Dfl 32,00

95 G MIK (red), Herstructurering in Rotterdam; modernisering en internationalisering en de Kop van Zuid -- Amsterdam/Rotterdam 1989: Knag/Economisch Geografisch Instituut Erasmus Universiteit Rotterdam. 324 pp. 86 figs, 54 tabs. ISBN 90-6809-105-0 Dfl 30,00

96 P BEEKMAN, P VAN LINDERT, J POST & W PRINS, Huisvestingsbeleid en informele bouw in de derde wereld; tussen idee en realiteit -- Amsterdam 1989: Knag/Instituut voor Sociale Geografie Universiteit van Amsterdam. 174 pp, 9 figs, 25 tabs. ISBN 90-6809-106-9 Dfl 30,00

97 J G L PALTE, Upland farming on Java, Indonesia; a socio-economic study of upland agriculture and subsistence under population pressure -- Amsterdam/Utrecht 1989: Knag/Geografisch Instituut Rijksuniversiteit Utrecht. 256 pp, 15 figs, 38 tabs. ISBN 90-6809-107-7 Dfl 34,50

98 P VAN GENUCHTEN, Movement mechanisms and slide velocity variations of landslides in varved clays in the French Alps -- Amsterdam/Utrecht 1989: Knag/Geografisch Instituut Rijksuniversiteit Utrecht. 160 pp, 70 figs, 17 tabs. ISBN 90-6809-108-5 Dfl 25,00

99 M DE SMIDT & E WEVER (eds), Regional and local economic policies and technology -- Amsterdam/Utrecht/Nijmegen 1989: Knag/Geografisch Instituut Rijksuniversiteit Utrecht/Geografisch en Planologisch Instituut Katholieke Universiteit Nijmegen. 156 pp, 53 figs, 36 tabs. ISBN 90-6809-109-3 Dfl 24,00

100 P J H RIEMENS, On the foreign operations of third world firms -- Amsterdam 1989: Knag/Instituut voor Sociale Geografie Universiteit van Amsterdam. 148 pp, 20 tabs. ISBN 90-6809-110-7 Dfl 30,00

101 G B M PEDROLI, The nature of landscape; a contribution to landscape ecology and ecohydrology with examples from the Strijper Aa landscape, Eastern Brabant, the Netherlands -- Amsterdam 1989: Knag/Fysisch-Geografisch en Bodemkundig Laboratorium Universiteit van Amsterdam. ca. 144 pp. ISBN 90-6809-111-5 Dfl 25,00

102 H LEENAERS, The dispersal of metal mining wastes in the catchment of the river Geul, Belgium-the Netherlands -- Amsterdam/Utrecht 1989: Knag/Geografisch Instituut Rijksuniversiteit Utrecht. ca. 208 pp. ISBN 90-6809-112-3 Dfl 30,00

103 G A HOEKVELD, G SCHOENMAKER & J VAN WESTRHENEN, Wijkende grenzen -- Amsterdam 1989: Knag/Centrum voor Educatieve Geografie Vrije Universiteit Amsterdam. 216 pp, 38 figs, 24 tabs. ISBN 90-6809-113-1 Dfl 27,50

104 P C J DRUIJVEN, Mandenvlechters en Mexcalstokers in Mexico -- Amsterdam 1990: Knag/Instituut voor Sociale Geografie Universiteit van Amsterdam. 294 pp, 21 figs, 55 tabs. ISBN 90-6809-114-X Dfl 38,50

105 W BLEUTEN, De verwatering van meststoffen; analyse en modellering van de relaties tussen landgebruik en waterkwaliteit in het stroomgebied van de Langbroeker Wetering -- Amsterdam/Utrecht 1990: Knag/Geografisch Instituut Rijksuniversiteit Utrecht. 262 pp, 80 figs, 31 tabs. ISBN 90-6809-115-8 Dfl 37,00

106 J VAN WEESEP & P KORCELLI (eds), Residential mobility and social change; studies from Poland and the Netherlands -- Amsterdam/Utrecht 1990: Knag/Geografisch Instituut Rijksuniversiteit Utrecht. 182 pp. 46 figs, 34 tabs. ISBN 90-6809-116-6 Dfl 29,50

107 M VAN HERWIJNEN, R JANSSEN & P RIETVELD, Herbestemming van landbouwgrond; een multicriteria benadering -- Amsterdam 1990: Knag/Instituut voor Milieuvraagstukken Vrije Universiteit. 106 pp, 32 figs, 5 tabs. ISBN 90-6809-117-4 Dfl 25,00

108 D H DRENTH, De informatica-sector in Nederland tussen rijp en groen; een ruimtelijk-economische analyse. Amsterdam/Nijmegen 1990: Knag/Faculteit der Beleidswetenschappen Katholieke Universiteit Nijmegen. 268 pp, 24 figs, 87 tabs. ISBN 90-6809-118-2 Dfl 37,50

109 H KNOL & W MANSHANDEN, Functionele samenhang in de noordvleugel van de Randstad -- Amsterdam/Utrecht 1990: Knag/Economisch-Geografisch Instituut Universiteit van Amsterdam/Geografisch Instituut Rijksuniversiteit Utrecht. 112 pp, 26 figs, 27 tabs. ISBN 90-6809-119-0 Dfl 19,50

110 C D EYSBERG, The Californian wine economy: natural opportunities and socio-cultural constraints - a regional geographic analysis of its origins and perspectives -- Amsterdam/Utrecht 1990: Knag/Geografisch Instituut Rijksuniversiteit Utrecht. 272 pp, 64 figs, 26 tabs. ISBN 90-6809-121-2 Dfl 29,75

111 J W A DIJKMANS, Aspects of geomorphology and thermoluminescence dating of cold climate eolian sands -- Amsterdam/Utrecht 1990: Knag/Geografisch Instituut Rijksuniversiteit Utrecht. 256 pp, 119 figs, 19 tabs. ISBN 90-6809-120-4 Dfl 36,50

112 H TER HEIDE (ed), Technological change and spatial policy -- Amsterdam/Utrecht 1990: Knag/Geografisch Instituut Rijksuniversiteit Utrecht. 218 pp, 9 figs, 31 tabs. ISBN 90-6809-122-0 Dfl 29,00

113 I L M VAN HEES, De ontwikkeling van een woningmarktmodel en zijn toepassing op Italië; The building of a housing-market model and its application to Italy -- Amsterdam/Nijmegen 1990: Knag/Faculteit der Beleidswetenschappen Katholieke Universiteit Nijmegen. 196 pp, 12 figs, 26 tabs. ISBN 90-6809-123-9 Dfl 35,00

114 M R HENDRIKS, Regionalisation of hydrological data: Effects of lithology and land use on storm runoff in east Luxembourg -- Amsterdam/Utrecht 1990: Knag/Geografisch Instituut Rijksuniversiteit Utrecht. 174 pp, 23 figs, 50 tabs. ISBN 90-6809-124-7 Dfl 26,00

115 P H RENOOY, The informal economy: meaning, measurement and social significance -- Amsterdam 1990: Knag/Regioplan. 204 pp, 12 figs, 21 tabs. ISBN 90-6809-125-5 Dfl 35,00

116 J H T KRAMER, Luchthavens en hun uitstraling; een onderzoek naar de economische en ruimtelijke uitstralingseffecten van luchthavens -- Amsterdam/Nijmegen 1990: Knag/Faculteit der Beleidswetenschappen Katholieke Universiteit Nijmegen. 356 pp. ISBN 90-6809-126-3 Dfl 55,00

117 M DE KWAASTENIET, Denomination and primary education in the Netherlands (1870-1984): a spatial diffusion perspective -- Amsterdam/Florence 1990: Knag/Instituut voor Sociale Geografie Universiteit van Amsterdam/European University Institute Florence. 268 pp, 28 figs, 39 tabs. ISBN 90-6809-127-1 Dfl 36,00

118 W P M F IVENS, Atmospheric deposition onto forests: An analysis of the deposition variability by means of throughfall measurements -- Amsterdam/Utrecht 1990: Knag/Geografisch Instituut Rijksuniversiteit Utrecht. 156 pp, 53 figs, 36 tabs. ISBN 90-6809-128-X Dfl 25,00

119 R HASSINK, Herstructurering en innovatiebevordering in het Ruhrgebied; een onderzoek naar de beleids- en bedrijfsreacties op de herstructureringsproblematiek -- Amsterdam/Utrecht 1990: Knag/Geografisch Instituut Rijksuniversiteit Utrecht. 122 pp, 20 figs, 18 tabs. ISBN 90-6809-120-8 Dfl 24,00

120 P P SCHOT, Solute transport by groundwater flow to wetland ecosystems; The environmental impact of human activities -- Amsterdam/Utrecht 1991: Knag/Geografisch Instituut Rijksuniversiteit Utrecht. 136 pp, 27 figs, 9 tabs. ISBN 90-6809-130-1 Dfl 25,00

121 S DEN HENGST & B DE PATER (Red), Externe relaties en regionale ontwikkeling: voorbeelden uit Spanje en Portugal -- Amsterdam/Utrecht 1991: Knag/Geografisch Instituut Rijksuniversiteit Utrecht. 198 pp, 31 figs, 27 tabs. ISBN 90-6809-131-X Dfl 29,50

122 J KROES, Onvolledige opstrek op de Nederlandse zandgronden; een onderzoek naar de verspreiding en de achtergronden van overgangsvormen tussen opstrek en andere occupatievormen -- Amsterdam/Utrecht 1991: Knag/Geografisch Instituut Rijksuniversiteit Utrecht. 256 pp, 65 figs. ISBN 90-6809-132-8 Dfl 35,00

123 H S VERDUIN-MULLER, Serving the knowledge-based society: research on knowledge products -- Amsterdan/Utrecht 1991: Knag/Geografisch Instituut Rijksuniversiteit Utrecht. 100 pp. ISBN 90-6809-133-6 Dfl 24,00

124 F MULDER, Assessment of landslide hazard -- Amsterdan/Utrecht 1991: Knag/Geografisch Instituut Rijksuniversiteit Utrecht. 160 pp. ISBN 90-6809-134-4 Dfl 29,50

125 M VIS, Processes and patterns of erosion in natural and disturbed Andean forest ecosystems -- Amsterdam 1991: Knag/Fysisch Geografisch en Bodemkundig Laboratorium Universiteit van Amsterdam. ca 158 pp. ISBN 90-6809-136-0 Dfl 12,00

126 V EIFF, Beleid voor bedrijfsterreinen; een politiek-geografische studie naar betrekkingen in het openbaar bestuur bij het lokatiebeleid voor de bedrijfsvestiging in stadsgewesten -- Amsterdam 1991: Knag/Instituut voor Sociale Geografie Universiteit van Amsterdam. ca 250 pp. ISBN 90-6809-135-2 Dfl 37,50

127 O ATZEMA, Stad uit, stad in; residentiële suburbanisatie in Nederland in de jaren zeventig en tachtig -- Amsterdam/Utrecht 1991: Knag/Geografisch Instituut Rijksuniversiteit Utrecht. 288 pp. ISBN 90-6809-137-9 Dfl 37,50

128 M HULSHOF, Zatopec moves; networks and remittances of US-bound migrants from Oaxaca, Mexico -- Amsterdam 1991: Knag/Instituut voor Sociale Geografie Universiteit van Amsterdam. ca 80 pp. ISBN 90-6809-138-7 Dfl 18,50

129 J M J DOOMERNIK, Turkse moskeeën en maatschappelijke participatie; de institutionalisering van de Turkse Islam in Nederland en de Duitse Bondsrepubliek -- Amsterdam 1991: Knag/Instituut voor Sociale Geografie Universiteit van Amsterdam. ca 168 pp. ISBN 90-6809-139-5 Dfl 32,50

Publications of this series can be ordered from Netherlands Geographical Studies, Weteringschans 12, 1017 SG Amsterdam, The Netherlands.
Prices include packing and postage by surface mail. Orders should be prepaid, with cheques made payable to "Netherlands Geographical Studies". Please ensure that all banking charges are prepaid.
Alternatively, American Express, Eurocard, Access, MasterCard, BankAmericard and Visa credit cards are accepted (quote card number and expiry date with your signed order). Customers in the Netherlands are requested to order directly by a giro transfer to Postbank a/c 225837 of "Nederlandse Geografische Studies", Amsterdam.